Title
Sample Preparation of Biofluids Using Microscale Vortices

Author
Mach, Albert

Publication Date
2012

Peer reviewed|Thesis/dissertation

UNIVERSITY OF CALIFORNIA

Los Angeles

Sample Preparation of Biofluids Using Microscale Vortices

A dissertation submitted in partial satisfaction of the requirements

for the degree of Doctor of Philosophy

in Biomedical Engineering

by

Albert J. Mach

2012

ABSTRACT OF THE DISSERTATION

Sample Preparation of Biofluids Using Microscale Vortices

by

Albert J. Mach

Doctor in Philosophy in Biomedical Engineering

University of California, Los Angeles, 2012

Professor Dino Di Carlo, Chair

Analysis of cellular samples is widely used for medical diagnostics. While there has been significant progress made in developing cell detection and analysis technologies, the development of miniaturized and automated tools to prepare cellular specimens for sample analysis quietly lags behind. Sample preparation continues to be performed off-chip with macroscale instruments, like the bench top centrifuge, which limits the use of cell-based diagnostics in point-of-care settings, and increases the cost of tests through manually-performed steps. This dissertation reports the development of a miniaturized microfluidic device that recapitulates the high-throughput operations of enrichment and concentration of a standard

laboratory centrifuge. The “Centrifuge Chip” employs unique inertial fluid physics to selectively isolate larger cancer cells from bloody samples using laminar fluid microvortices. Specifically, cancer cells are captured in vortices while smaller leukocytes and erythrocytes are not stably trapped in vortices and are significantly reduced in the collected concentrated sample. This unique cell trapping mechanism was explored to systematically understand particle and cell behavior in microvortices and to design deterministic and predictable vortex trapping systems for biological and clinical applications. The design rules were employed to develop a tool for 1) isolating rare circulating tumor cells from blood of cancer patients and 2) harvesting large quantities of cancer and mesothelial cells from pleural and peritoneal effusions. By selectively enriching larger cells over a background of red and white blood cells, the miniaturized centrifuge replaces the traditional centrifugation step in the clinical lab while also potentially enabling more sensitive analysis of pure preparations originating from a larger volume. Ultimately, the Centrifuge Chip is an instrument that increases reproducibility of cell-based protocols, minimizes manual handling steps, reduces reagent costs via label free biomarker, and potentially revolutionizes traditional sample preparation procedures.

The dissertation of Albert J. Mach is approved.

Hsian-Rong Tseng

Aydogan Ozcan

Jeff Eldredge

Dino Di Carlo, Chair

University of California, Los Angeles

2012

To my Family with Love.

Table of Contents

Acknowledgements

"*If I have seen further it is by standing on the shoulders of Giants*," – Isaac Newton

I am deeply grateful for those who made the completion of my Ph.D. possible. And so I would like to tip my hat to those whose shoulder I stood upon during my Ph.D. tenure as they have guided me in the right direction. Here's my list of some, not all, of the Giants I learned from:

Professor Dino Di Carlo, who supervised my thesis research. As one of his first students, I have been fortunate enough to work with a young and talented professor who I consider as a model mentor. He taught me how to tackle problems with breadth and depth but above all, to seek simplicity in all things.

The Di Carlo Lab. In particular, I've benefited from interactions with: Danny Gossett (who traveled with me to foreign lands at conferences), Westbrook Weaver (who taught me biology and chemistry), Henry Tse (who taught me image processing), Hamed Amini, Claire Soojung Hur, Elodie Sollier, Wonhee Lee, Aram Chung, James Che, Mahdokht Masaeli, Oladunni Adeyiga, Coleman Murray, and Peter Tseng. To my undergraduate students who I have had the privilege to mentor over the years, where in many cases the teacher became the student.

The many individuals beyond the Di Carlo Lab who worked on experiments with me, who provided training and resources: Libo Zhao, Huijiang Ding, Kan Lui, and Hsian-Rong Tseng. Thanks to Jianyu Rao, Yong Ying, and the cytology laboratory team, including Sean O'Byrne and Chris Johnson.

The Department of Biomedical Engineering at UCLA. I cannot imagine a better place to undertake a Ph.D. I would like to express special thanks to Daniel Kamei, who served as one of my mentors and met with me regularly throughout my Ph.D. To the staff that routinely helped me, Apryll Chin, Stacey Tran, Lee Yang, Larry Nadeau, and Brian Lee.

My committee members: Hsian-Rong Tseng, Aydogan Ozcan, and Jeff Eldredge.

To my Friends: Alan Tran, John Waldeisen, Kevin Zhang, Benjamin Blackman, Kevin Lung, Apryll Chin, Kuan Chen, and Ricky Chiu for moral support. And to all my Berkeley and Los Angeles friends.

To my Family. My Mom and Dad for their unbridled support and for allowing me to do the things I love. Without their love, support and guidance, completing my Ph.D. would have been impossible. To my little brother, Kevin, who constantly reminds me to dream big. To my older brother, Edwin, who influenced my decisions to continue for a higher education. This dissertation is dedicated to my Family.

Thank you all for your generosity.

Vita

Education

B.S., Bioengineering, University of California, Berkeley 2008

M.S., Biomedical Engineering, University of California, Los Angeles, 2010

Ph.D., Biomedical Engineering, University of California, Los Angeles, 2012

Honors and Awards

2012 ’30 Under 30’ on Forbes List in Science and Innovation

2011 Bronze Medal Prize at National Collegiate Inventors Competition

2010 CHEMINAS Young Researcher Poster Award, MicroTAS Conference 2010, Netherlands

2009 CHEMINAS Young Researcher Poster Award, MicroTAS Conference 2009, Korea

Publications Patents and Proceedings

AJ Mach, JH Kim, A Arshi, SC Hur and D Di Carlo, Automated cellular sample preparation using a Centrifuge-on-a-Chip. *Lab Chip*, 2011, 11, 2827-2834.

SC Hur, **AJ Mach**, and D Di Carlo. High-throughput size-based rare cell enrichment using microscale vortices. *Biomicrofluidics*, 2011, 5, 022206.

AJ Mach and D Di Carlo. Continuous Scalable Blood Filtration Device Using Inertial Microfluidics. *Biotechnology and Bioengineering*. 2010 107 (2) 302-11.

D Di Carlo, SC Hur, and **AJ Mach**. Isolation of target cells from heterogeneous solution using microfluidic cancer cell trapping vortex. PCT International Patent application filed for UCLA Case 2010-283-2.

AJ Mach, JH Kim, A Arshi, and D Di Carlo. Centrifuge-on-a-Chip: Rapid and Automated Sample Preparation for Cell Suspensions. Lab Automation, Palm Springs, CA, USA. Poster Presentation. 2011

AJ Mach, JH Kim, and D Di Carlo Deterministic Particle Trapping in Laminar Microvortices. American Physical Society 63rd Annual Division of Fluid Dynamics Meeting, Long Beach, California, USA. Podium Presentation 2011.

DR Gossett, WM Weaver, and **AJ Mach**, SC Hur, HTK Tse, W Lee, H Amini, D Di Carlo. Label-free Cell Separation and Sorting in Microfluidic Systems. *Analytical and Bioanalytical Chemistry*. 2010, 397, 8, 3249-3267.

AJ Mach, JH Kim, SC Hur, and D Di Carlo. Size-Based Particle Trapping in Microvortices. Micro Total Analysis Systems (μTAS) Conference, 14th International Conference on Miniaturized Systems for Chemistry and Life Sciences, Groningen, Netherlands. Poster Presentation. 2010

AJ Mach, S Behrens, and D Di Carlo. High-Throughput Cell Separation using Differential Inertial Migration for Rapid Sepsis Therapy. Micro Total Analysis Systems (μTAS) Conference, 13th International Conference on Miniaturized Systems for Chemistry and Life Sciences, Jeju Island, Korea. Poster Presentation. 2009

AJ Mach, S Behrens, and D Di Carlo. High-Throughput Cell Separation using Differential Inertial Migration for Rapid Sepsis Therapy. Biomedical Engineering Society (BMES), Pittsburgh, PA. Poster Presentation. 2009.

Chapter 1

Microfluidic Sample Preparation for Diagnostic Cytopathology

1.1 Introduction

Analysis of cell samples is widely used for medical diagnostics. Some areas of use include (i) quantifying cellular components of blood like complete blood counts (CBC), (ii) reviewing tissue sections and liquid-based cellular solutions by pathology, and (iii) analysis and sorting of target cell populations with flow cytometry. Miniaturization of flow cytometry and differential blood cell counts have been a strong focus of the microfluidics community [1–4]. However, there has been less focus on analysis of tissue slices and cytology-based diagnostics, which often require a larger amount of sample preparation. While there has been significant progress made in developing cell detection and analysis technologies, the development of miniaturized and automated tools to prepare cellular specimens for sample analysis quietly lags behind. Sample preparation continues to be performed off-chip with macroscale instruments, like the bench top centrifuge, which limits the use of cell-based diagnostics in point-of-care settings, and increases the cost, and reduces consistency of tests through manually-performed steps [5]. Additionally, beyond the analysis of cells present in blood, processing and analyzing cells from other body

fluids can address important diagnostic needs. The preparation of other body fluid samples for the analysis of cells present has unique challenges towards miniaturization and automation.

Sample preparation of cells, for the purposes of cytology-based tests, traditionally is a multi-step process. Steps routinely require concentrating collected cells from solution, separating specific cell populations, chemically and biologically staining cells, washing cells with various solutions, and lysing cells in order to harvest nucleic acids or protein [6]. These steps usually involve multiple centrifugation and manual pipetting operations. Notably, some miniaturized sample preparation techniques have been realized and successfully integrated with sample analysis methods for complete diagnostic systems, creating useful point-of-care applications with self sustainable units [7][8]. While there has been success in device design where sample preparation and analysis have been integrated into one system, this has largely been achieved using exclusively low volume blood samples (e.g. a pinprick of blood). Therefore, expansion into the development of integrated devices for evaluation of larger volume samples, as well as samples consisting of other biofluids, is needed.

Such large volumes present a difficult handling challenge within the discipline of microfluidics, where most developed capabilities can handle sample small volumes in the microliter range. To address this challenge, there is a critical need for the development of sample preparation technologies that allow microscale manipulation of milliliter volumes and also perform on a level comparable to bench top machines, like centrifuges and flow sorters. This capability would enable the harvesting of large quantities of cells for cytopathology diagnostics, given that sampling large volumes would provide a means to gain improved statistical accuracy for measuring rare cellular events. For example, isolating rare circulating tumor cells and fetal cells from amongst a heterogeneous population in a complex fluid, like

blood, is of significant interest for non-invasive diagnosis and treatment monitoring. With the advent of these applications, there has been a paradigm shift, from only focusing on low sample volumes [9][10], toward creating high-throughput systems with clinically relevant processing times. Blood has been the major body fluid explored using higher throughput microfluidic technologies [11]. However, there are significant opportunities to address unique challenges in preparing other body fluids, like pleural fluids [12][13], saliva [14][15][16] and urine [17].

Here we review the assortment of biofluids clinically analyzed, along with their characteristics and diagnostic value. We investigate the conventional methods for cytological diagnosis and the challenges and opportunities in developing microfluidic devices for sample preparation of biofluids for cytodiagnostics. We then identify some initial efforts in the microfluidics community to prepare and analyze various biofluids with a focus outside of traditionally analyzed cells in blood [12]. We hope to convey the importance and help identify new research directions addressing the vast biological and clinical applications in preparing and analyzing the array of clinically-available biological fluids.

1.2 Standard Procedure for Liquid-Based Cytology

Examination of the cellular content of body fluids, cytology, is routinely performed for disease detection and diagnosis. As noted by the CDC, in 2007 over 7 billion laboratory tests were performed. Samples for cytological examination are first collected in a clinical setting, by a physician, nurse, or dedicated technician. These samples are transported to the cytology lab which is often present within major medical centers, but may be off site for smaller community hospitals or clinics. In the cytology laboratory various sample preparation steps are performed

prior to analysis including centrifugation to concentrate cells in dilute samples, followed by preparation and staining of slides, and examination under a light microscope (Figure 1.1).

1.2.1 Sample Collection

Sample collection is the first step in preparing a sample for analysis, in which the collection technique can often impact downstream cytodiagnostic assays that can be performed. Samples are obtained through collection techniques that vary in their level of invasiveness. Sample collection techniques include phlebotomy, fluid aspiration via needle or syringe, or saline washing of a mucosal surface with catheter assistance. First impressions like color, odor, and volume are noted by the physician to determine whether further testing is required. For example, red-colored urine may indicate the presence of red blood cells in the urine sample due to underlying pathology, including infection or cancer. To further elucidate the cause and make a proper diagnosis, additional tests may be ordered. Typically, this procedure is conducted in the clinical laboratory or an off-site location. Once the sample is obtained, it is sent to a cytopathology lab and stored at 4°C. Generally, samples can be refrigerated for several days while maintaining sample integrity [18]. In some cases, samples are treated with anti-clotting agents to preserve cell morphology. For example, blood is collected into a collection tube containing an anti-coagulant to prevent cell clumping, and fixing agents are added to urine due to fast degradation times.

1.2.2 Sample Preparation

Most laboratories use two or more methods of preparing liquid-based samples for further evaluation and analysis. From a sample, cell smears or cell blocks may be prepared for

microscopic review by cytopathologist using conventional or immunohistochemical stains, and then further analyzed with flow cytometry and cytogenetic analysis. To make a cell smear or cell block, an aliquot of the sample, typically 50 mL in pleural and peritoneal fluid specimens, is centrifuged with a bench top centrifuge. The supernatant is aspirated and the sediment is used for preparing direct cell smears or cell blocks. Direct smear is the conventional method whereby sedimented cells are manually transferred onto a glass slide for examiner review under the microscope. Alternatively, an automated instrument called the cytocentrifuge takes the cell sediment and evenly distributes the cells onto a designated circle on a glass slide in an automatic and reproducible fashion. Ultimately, a cell smear can take up to two centrifugation steps and multiple pipetting procedures, requiring as much as 10 minutes per sample. Additionally, the presence of blood cells can prevent the formation of a uniform cell layer, which may make the cell smear difficult to interpret under microscopy examination. Cell blocks are formed from cell sediments that are then embedded in paraffin and cut into histological sections. Following cell preparation, the slides are stained with colored dyes to help differentiate cells by label-specific features of cellular morphology described in the sample analysis section. The slides are alcohol-fixed or air-dried to remove water content, followed by a series of washes and stains like Papanicolaou (Pap) or Romanowsky to highlight nuclear and cytoplasmic features. In some cases, biofluid samples are prepared for flow cytometry where the cells are labeled with compatible fluorescent dyes in liquid solution rather than on a glass slide. The remaining fluid specimens are stored in the refrigerator for further and repeated testing if needed. Slide preparations for cytology review can take up to 45 minutes for a single sample [19]. Manual sample preparation of slides and blocks lead to increased costs and variation in quality from lab to lab.

1.2.3 Sample Analysis

Once samples are prepared, they are handed off to the cytopathologist for diagnosis. Cell smears and blocks are examined under light microscopy and described with various parameters including cell size, morphology, multi-nucleation, nuclear to cytoplasmic ratio, and cell aggregates. In the case of malignancy, chromatin is more unfolded and will often appear darker [20], [21]. The laboratory diagnosis may be typically reported with a heading such as 'positive for malignant cells', 'suspicious', or 'negative for malignant cells'. Oftentimes, further testing is requested by the cytopathologist especially in 'suspicious' and 'positive' cases. The biofluid specimens are also analyzed with flow cytometry, cytogenetic testing using fluorescence in-situ hybridization (FISH), or immunocytochemistry analysis, which provides a more sensitive and specific approach to determine malignancy using specific labels.. Use of flow cytometry and cytogenetic analysis are accurately predicting prognosis in certain disease states in a reproducible fashion. These studies have therefore become increasingly more important in defining disease characteristics, a theorem that is well illustrated in the diagnosis and treatment of particular hematologic malignancies [22]. Regarding immunohistochemistry for example, a sample from a patient with a history of lung cancer would require staining for biomarkers specific to the lung like EGFR, KRAS or TTF-1. Oftentimes, immunolabeling of existing colormetric slides are performed by washing out previous colorimetric labels and applying new labels with more specificity. Additionally, cytopathologists are interested in extracting nucleic acid sequence information from malignant cells within samples to identify mutations that are potential therapeutic targets, but this is still not routinely performed in the clinic. One method of collecting pure malignant cells is to use laser capture microdissection [23], [24], which uses a laser to cut out malignant cells from cell smears for molecular analysis [25].

1.3 Background and Applications of Biofluids

Human biofluids are liquid-based cellular solutions that originate from the human body. Examples include urine, blood, pleural fluid, peritoneal fluid, cerebrospinal fluid, and wound exudates (Figure 1.2, Table 1.1). Sample preparation and analysis of biofluids is an emerging application area that many microfluidic technologies may be able to address. Microfluidic research has in particular focused on the preparation and analysis of blood [11]. With already over 1,100 citations, much of the work thus far has related to the development of devices for cell and molecular analysis of blood samples [7], [26], [27][1][28]. While significant diagnostic information about the patient can be obtained from blood analysis, other biofluids may be as rich in terms of diagnostic information, with unique sample preparation and analysis challenges that microfluidic technologies are poised to address. Note that biofluids other than blood can contain elevated amounts of blood cells due to underlying pathology. Given that under these circumstances, the amount of blood cells present generally would not be equal to the amount present in whole blood, these biofluids can be treated as diluted blood for sample preparation purposes. In particular, regarding most biofluids, it is noteworthy that the cellular profile of the biofluid present as a result of a non-malignant versus a malignant process can be significantly different. Additionally, fine needle aspirations and core biopsies, while not included in this review due to their high cellular content, can potentially behave as biofluids when placed in liquid solution. Here, we highlight clinically relevant biofluids with a brief background, identify the diagnostic value and clinical applications for microfluidics, and discuss critical challenges with developing sample preparation tools for each biofluid. We categorize each biofluid with fluid volume (mL), cellularity (cells/mL), fluid viscosity, and its prevalence, and associated diseases. For some of these biofluids, researchers can gain access to remnant samples after all

diagnostic tests are performed with expedited IRB review, which can speed investigation into simple approaches to prepare and analyze these diagnostically important fluids beyond blood [29].

1.3.1 Blood

Background. Blood harbors vast information about the physiological and pathological conditions of the human body. The sampling and analysis of blood plays a significant role in medical diagnostics. One example of blood testing includes surveying the cellular constituents of blood with a complete blood count (CBC) that quantifies the number of red blood cells (erythrocytes), white blood cells (leukocytes), and platelets present in the sample analyzed. Full blood counts have largely been automated by hematology analyzers and flow cytometers, becoming the gold standard for CBC determination. Blood will continue to be the biofluid that is the dominant focus for engineering specimen handling and analysis technologies. It is easily accessible among researchers and has proven to be a valid proof-of-concept biofluid to be used in evaluating prototypes being developed for use with various other biofluids.

Diagnostic Value. A complete blood count (CBC) is routinely used as a laboratory test to determine health status. Typically a microliter of blood contains 5 million erythrocytes, 5,000-10,000 leukocytes, and 400,000 platelets [11]. Leukocytes are further classified into subpopulations of cells that have different physiological functions, including neutrophils, lymphocytes, monocytes, basophils, and eosinophils. An abnormal CBC is often indicative of underlying pathology, including infection or cancer. Noting the presence of abnormal numbers of specific populations of leukocytes [1], [30], [31] assists in diagnosing particular hematologic

conditions, monitoring response to therapy or disease progression. For example, the absolute number of CD4+ T cells (helper T-cells) is used to monitor HIV progression [32]. In another example, in patients with chronic myeloid leukemia, a gene translocation results in the presence of a constitutively active tyrosine kinase known as BCR-ABLthat is now a target for therapeutic intervention [33]. Preparation of a peripheral blood smear for review would be needed if cell counts appear to be low. Review of a peripheral blood smear is also in order if there is concern for certain infectious diseases, such as malaria or babesiosis. In the case of malaria, one can directly visualize the presence of the parasite in infected erythrocytes. The level of parasitemia (volume of blood occupied by the malaria parasite) can be estimated from review of the peripheral blood smear, which is important in terms of patient prognosis [34]. A current additional method for pathogen detection includes conventional blood culture, where an aliquot of blood is placed into blood culture media. If a microorganism is detected, further analysis is required for specific microorganism identification. This process usually takes 2-3 days, and can be suboptimal in terms of pathogen isolation [35].

Finally, although not clinically used as of yet, there has been much work in isolating and identifying rare cells from blood. For example, the fraction of circulating tumor cells (CTC) present in blood could be as minute as one circulating tumor cell per billion blood cells; the capture and analysis of circulating tumor cells could provide information about cancer relapse or mutational state [36]. Similarly, fetal cells are present in maternal peripheral blood in rare amounts, and can help determine health of the developing fetus (see Amniotic Fluid)[37]. Notably, a recent shift has emerged for developing sample preparation tools to process large mL volumes of blood as a method to gain additional access to rare cell populations in blood samples [38], [39]. It is highly anticipated that this paradigm shift will bring about a critical challenge for

the cell type-specific enrichment from large blood volumes in rapid fashion, allowing clinicians to incorporate this information in real time

Sample Preparation Challenges. Many sample preparation challenges have been highlighted in Toner and Irimia's review [11]. Briefly, challenges include the high cellularity of samples and the propensity of cellular components to aggregate. In this case, chemicals that prevent platelet activation can be used, ex. EDTA. While dilution may seem as a remedy, this translates to greater processing times for a 1 mL blood volume. Another alternative is to lyse red blood cells which can remove >95% of the cellular content leaving a population of platelets and leukocytes. However, chemical lysis buffers may affect the other blood cells and its properties. In microchannels, where there will be less particle interactions between blood cellular components, physical phenomena such as mechanical, electromagnetic, and fluidic forces can also be exploited in device design to encourage interaction of cells with surfaces, concentrate cell subpopulations, stain, wash, and focus cells for analysis. Under circumstances where large (milliliter) volumes of blood are to be processed, this requires additional technological advancements that can allow for processing of whole blood in a continuous and rapid fashion. Using massively parallel devices, some have demonstrated that processing at sample flow rates of 1 mL/min [40] to 1 mL/hr [41], [42] is achievable. A rapid blood culture test could be developed that would require specific separation and concentration of enough bacterial components from a sample of blood that would allow for rapid growth and analysis, perhaps shortening time from 2-3 days to 2-3 hours and significantly aiding clinical decision making.

1.3.2 Pleural and Peritoneal Fluid

Background. Both the lungs and inner thoracic cavity are lined with visceral and parietal pleura respectively, which slide against one another when the lungs contract and expand. Between the two pleura there is a small amount of fluid called pleural fluid that acts as a lubricant, enhancing lung movement during inspiration and expiration under normal circumstances. However, under pathologic conditions, a pleural effusion may develop, where excess amount of pleural fluid accumulates in the pleural cavity. At times, volumes of 1-2 L of pleural fluid may accumulate. During a procedure called a thoracentesis, the operator will choose a location along the patient's back, insert a needle through the chest wall into the pleural space, and withdraw the pleural fluid present. Once collected, the fluid is described in terms of its gross, or clinical, appearance. Biochemical analyses are performed; using Light's criteria (criteria correlating the ratio of various types of proteins within pleural fluid and serum to classes of disease states), results of these tests assist in determining if the pleural effusion has developed as the result of a transudative or exudative process [43]. Transudates result from an imbalance of hydrostatic pressure while exudates result from injury from infection or cancer. Additional laboratory tests include total cell counts with differential cell count values, cultures for various microorganisms, and cytology. A pleural effusion may develop as the result of an infection, an inflammatory process, or malignancy. In the normal state, pleural fluid is largely acellular. However, depending on the process causing the pleural effusion to develop, a pleural fluid sample contains cells ranging from leukocytes predominated by mononuclear or polymorphonuclear cells (1000-100,000 per uL), RBCs (1000-100,000 per uL), mesothelial cells that line the pleura cavity, cancer cells, and/or microorganisms such as bacteria or fungi. There has been considerable interest in extracting the malignant cell populations to study about the cancer as well as the effusion microenvironment [44]. Peritoneal fluid is similar to pleural fluids but found in the

pelvic cavity surrounding the abdominal organs. Accumulation of these fluids, described as ascites, produces abdominal distension, which may be reflective of up to several liters in volume of ascitic, or peritoneal fluid. Peritoneal fluid is collected through a procedure called paracentesis.

Diagnostic Value. Possible cytolological diagnoses include: positive for malignancy, suspicious for malignancy, and negative for malignancy. Patient samples diagnosed with negative fluid results oftentimes were diagnosed with acute inflammation - associated with an increased neutrophil population, chronic inflammation - associated with a larger fraction of lymphocytes and histiocytes, reactive mesothelial changes, and lymphocytosis – associated with the increase of lymphocytes. The manifestation of malignant effusions in the pleura and peritonea typically indicate poor prognosis. Malignant pleural effusions account for 10% of all pleural fluids. Of those, lung and breast tumors account for more than 50% of pleural effusions while intestinal and ovarian cancers make up a dominant portion of peritoneal effusions. Cytological examination of pleural fluids have reported positive findings ranging from 33% to 87% [45]. The accuracy of this cytopathology method relies on the experience of the technician as well as the cytopreparation method [46]. False negative findings may be a result of improper handling. Supplementary techniques have been used to improve sensitivity like immunocytochemistry. For example, biomarkers like carcinoembryonic antigen (CEA) are helpful for distinguishing malignant cells from reactive mesothelial cells. Additionally, these tests can give information about the malignant cells and whether specific gene mutations like EGFR or KRAS are present [47]. In cases with negative malignant effusions, specimens are analyzed for leukocyte prevalence.

Sample Preparation Challenges. These types of fluid samples may be highly cellular and full of proteinaceous debris in certain clinical situations. The difficulty, then, would lie in isolating particular cells from a background of more plentiful and less relevant cell populations, in terms, of clinical diagnosis. Harvesting malignant cells from pleural and peritoneal fluid is challenging, especially when malignant cells can easily be confused with mesothelial cells during microscopic review, even with the trained eye. Both cell types are generally larger than the blood cell population of cells that may co-exist in such a sample, but they may be similar in size. Interestingly, label-free biomarkers can be used to separate these cell populations such as size. In pleural fluids, measuring cell deformability using mesothelial and epithelial cells can be accomplished with AFM measurements [48]. Cell deformability can be used as a method of cell separation and may be a useful biomarker parameter that can be linked with clinical outcomes [49][12], [48]. After removal of bloody cells, this technique can be used as a way to remove cellular background when imaging cell smears and finding specific gene mutations with molecular analysis. Isolation of specific rare cell populations from a large sample volume can also be difficult. For example, during large volume paracentesis, as much as 9 L of fluid can be removed from the patient's abdomen; in this case it is also important to process a large volume of biofluid for analysis in a time efficient manner. These rare cell populations are important for molecular analysis of mutation status from purified malignant pleural effusions. One potential chip-based technology would automate the concentration and staining of these samples using microfluidic cell concentrators such as affinity or size-based capture methods and solution exchange systems.

1.3.3 Amniotic Fluid

Background. Amniotic fluid, the fluid in the amniotic sac that surrounds the developing fetus, contains a rich source of information for prenatal testing. It provides a safe and nourishing environment and a lubricated interface between the fetus and placenta. Approximately 300,000 pregnant women undergo an invasive procedure called amniocentesis, where amniotic fluid is sampled. A typical test requires harvesting 20 mL of amniotic fluid for the screening of genetic diseases. Amniocentesis is considered a risky procedure as it can cause induced abortion or maternal injury. Amniotic fluid is composed mostly of water giving a fluid viscosity comparable to water with traces of cells sloughed from the developing fetus.

Diagnostic Value. The isolation and genotyping of fetal cells (erythrocytes, leukocytes, trophoblasts) is important for prenatal diagnosis. Cytogenetic analyses include karyotyping and FISH to detect aneuploidy of all chromosomes and structural chromosomal abnormalities such as Down syndrome. The harvested amniotic fluid also contains multiple cell types that differentiate along adipogenic, osteogenic, myogenic, endothelial, neurogenic and hepatic pathways [50][51]. Although not addressing a clinical problem, microfluidic technologies have been used for the culturing and differentiation of amniotic stem cells [52][53].

Sample Preparation Challenges. A major challenge with sample preparation of amniotic fluid is distinguishing between cells of maternal or fetal origin. This becomes critical when wanting to perform molecular analysis on the fetal cells where maternal cells may interfere with results. Additionally, collecting sufficient numbers of fetal cells in high purity remains to be a challenge in order to initiate stem cell cultures and extract DNA for sequencing. Others have investigated

maternal blood as a less-invasive alternative to isolating embryonic cells. Fetal cells migrate into the maternal peripheral blood and then can be isolated [54], [55]. Recently, the detection of cell-free DNA in maternal blood has been demonstrated as a method for prenatal diagnosis[56]. Under these circumstances, a device that is able to process a large sample volume would be valuable.

1.3.4 Urine

Background. The genitorinary system includes the kidneys, ureters, urinary bladder and urethra. In the kidney, as blood is filtered and toxic metabolites are removed, urine is formed. Urine then flows along the genitourinary tract from the kidney, through the ureters, into the urinary bladder, where it collects until bladder emptying occurs. At that time, when urine is voided, it exits the body from the bladder through the urethra. Voided urine may be collected as it is eliminated from the body through the genitourinary system. Alternatively, a urine specimen may be obtained by inserting a catheter into the bladder via the urethra. During cystoscopy, a procedure where the interior surface of the bladder is visualized with a fiber optic camera inserted through the urethra, to collect a bladder washing specimen, an operator may introduce a saline solution into the bladder, and then aspirate this fluid. The contents of this fluid are then further analyzed to determine if underlying pathology is present, such as malignancy. In general, the human body forms a total of 1-2L a day of urine. As a biofluid, in comparison to blood, it is largely acellular, containing soluble metabolites and, at most, a small amount of protein[17]. However, particularly in circumstances where underlying pathology is present, one may find cells, casts of cells, and/or crystals. Routine testing of urine includes urinalysis and urine microscopy. The term urinalysis describes a collection of tests done to determine whether particular metabolites

and/or protein is present, and is performed usually as a group in order to screen for common diseases. In general, urinalysis will evaluate urine samples for the presence and level of particular metabolites and protein, whereas urine microscopy entails the microscopic examination of the sediment obtained from a centrifuged sample of urine.

Diagnostic Value. Upon collection, one notes the color and odor of the urine sample, which may indicate the presence of disease. For example, tea-color or frankly red urine may signify that red blood cells, or hematuria is present. Urine contains a variety of metabolites that are of diagnostic importance. For example, urine may be screened for whether glucose is present in excess, to determine if a patient has diabetes mellitus. Urine pregnancy tests evaluate urine for the presence of human chorionic gonadotrophin. Concern for infection would prompt a clinician to send urine samples for microbiologic evaluations, such as staining and culturing for microorganisms. In urinary tract infections, isolating bacteria is necessary to study the methods and consequences of biofilm formation and has significant implications in catheter development and understanding MRSA. Unlike epithelial cells, microorganisms can survive these harsh degrading and high shear environments and actually proliferate up the urinary tract. In the case of acute kidney injury, examination of urine sediment is a virtual requirement as part of the diagnostic evaluation. In this case, cell casts representing damaged renal epithelial cells, indicate that renal tubule epithelial cells have been damaged. Under other pathologic conditions, the presence of red or white blood cells in excess will assist in determining an appropriate diagnosis. Other findings that may be present during microscopic evaluation of urine include the presence of red or white blood cell casts and/or crystals. Urine cytology assists in diagnosing malignancy, especially those that arise from cells originating from the genitourinary system, ex.

bladder cancer. Urine cytology may also be important in determining the etiology of acute kidney injury in renal transplant patients. For example, investigators were able to distinguish renal transplant graft rejection from cyclosporine toxicity in renal allograft recipients [57]. Cytodiagnostic urinalysis is also useful in diagnosing kidney allograft, where allograft dysfunction may be due to allograft rejection, the presence of polyoma virus, or calcineurin inhibitor toxicity [58].

Sample Preparation Challenges. Sample preparation of urine is difficult due to its acellular nature, even with bloody samples that indicate microorganism infection or malignancy. In the latter case, small quantities of malignant cells are shed from the kidney, prostate or bladder and released into the urine. There is considerable interest in harvesting these cells but large milliliter volume assessment and repetitive testing are generally required. Analysis for the presence of microorganisms such as bacteria or fungi is currently performed by inoculating culture media with an aliquot of urine. Specific isolation of a species may take up to the 2-3 days, and currently done by exploiting the metabolic differences present between species as they consume the nutrients present in culture media. Isolation and identification of a specific organism at the time of urine sample collection (rather than 2-3 days later), would require the separation of single colony forming units, a difficult task when considering the typical volumes of urine that may be collected. Similarly, the separation of rare cells from urine may also be difficult. Urine may also contain debris such as red or white cell casts or crystals, further complicating the task of isolating specific cells for the purposes of cytology review. Additionally, high urea concentrations present in the urine degrade the cells rapidly; thus, samples should be prepared and processed quickly to increase the yield for cytologic review.

1.3.5 Bone Marrow Aspiration

Background. Bone marrow is located in the fatty core of cancellous bone (sternum, rib, and pelvis), and the long bones (femur, tibia, and humerus). Cells that give rise to the cellular components of blood are housed in bone marrow. Collecting a sample of bone marrow for further evaluation and testing would include obtaining a bone marrow aspiration or obtaining a bone marrow biopsy. During a bone marrow aspiration, a needle is inserted into the bone marrow space; a sample is then withdrawn though the needle into a syringe. Bone marrow tissue is spongy semisolid tissue, and typical bone marrow specimens are highly cellular. Further analysis of a bone marrow specimen is usually indicated if there is concern that a pathologic hematologic process is present. An example of such a process would be a hematologic cancer or a deficiency in one or more hematologic cell line.

Diagnostic Value. Cytology review of a bone marrow specimen is in order in many clinical scenarios. Bone marrow sampling is commonly performed in the evaluation of hematologic malignancies. Cytology review gives important information regarding the behavior of cells present in marrow. Particular abnormalities that can be appreciated during microscopic review of a prepared slide will allow for accurate diagnosis of a clinical condition. Research has progressed to the extent that specific cell surface markers that have been identified are known to correlate with the clinical behavior of particular malignancies. This makes the identification of specific cell surface markers important in making the diagnosis, determining appropriate therapies available to the patient, and in predicting the clinical course as well as prognosis for the patient. Usual testing performed on bone marrow biopsy specimens include glass slide

preparation, immunophenotypic, cytogenetic, molecular genetic studies such as fluorescence in siu hybridization, and flow cytometry analysis (Bain, 2001). Also, bone marrow specimens may be sent for microbiologic studies, including microscopic review, culture for microorganisms, and molecular testing.

Sample Preparation Challenges. Bone marrow samples are highly cellular and have a spongy semisolid consistency. This makes separation of specific cell populations more difficult. Typically, a volume of less than 500 microliters is harvested for analysis; a portion is sent for glass slide preparation for microscopic review, and the remaining sample is sent for further testing. Separation of specific cell populations is important for diagnostic reasons. Also, this is important in harvesting cells to be used for clinical treatment; for example, hematopoietic stem cells are used for engrafting in patients undergoing bone marrow transplantation. Given that low volumes are typically available for testing, the efficiency of a device to be used for the purposes of isolating specific cell populations should be high. As well, where there is a clinical condition causing a paucity of cells present in the bone marrow of a patient, the ability to isolate rare cells would provide a distinct advantage.

1.3.6 Cerebrospinal Fluid

Background. Cerebrospinal fluid (CSF) is formed by the choroid plexus, which is located within the ventricular system, and surrounds the structures that comprise the central nervous system (CNS), which includes the cerebrum and the spinal cord [59]. It protects the CNS, providing shock absorbency, and also allows for the elimination of chemical waste. Approximately 150 mL of CSF surrounds the adult brain. A sample of CSF, when sampled, should have less than 2

leukocytes per microliter, and no red cells; an abundance of red cells may be present, however, if inadvertently red cells and introduced into the sample during the collection process. The most common procedure performed to collect a sample of CSF for analysis is lumbar puncture. A needle introduced into space surrounding the lumbar spinal cord, which is occupied by CSF (as is the entire spinal cord). A sample is then taken and sent for biochemical, cytologic, and microbial studies. Under normal conditions, CSF is a clear, thin, watery fluid.

Diagnostic Value. Sampling of CSF is indicated in the evaluation of a patient with disease involving the central nervous system. Routine testing of CSF includes biochemical, microbiologic, and cytologic analysis. Additional tests that may be performed, if clinically indicated, would be molecular genetic, cytogenetic, or immunophenotypic analysis, as well as flow cytometry [60]. For example, consider a clinical scenario where there is concern that meningitis may be present. In addition to microscopic review of a glass slide for the presence of microorganisms, the number of cells present in the sample is quantified. Also, the specific population of cells present is determined; i.e., the number and type of white blood cells, and the number of red blood cells. This determination is also important where there is concern for central nervous system lymphoma.

Sample Preparation Challenges. In particular regarding CSF, the isolation of rare cells from a fluid sample is a dilemma. Where a sample contains a large amount of red blood cells because of trauma related to the procedure, removal of red blood cells before cytologic analysis is important. Also, given the number of tests that may be requested for a finite volume of collected sample, one can anticipate that only a small volume of fluid will be available for each test

requested. An advantage, then, would be for any given device to have the ability of isolating cells in an efficient manner while working with a small volume of fluid.

1.3.7 Bronchoalveolar Lavage Fluid

Background. Since the introduction of the fiberoptic bronchoscope in the early 1970's, bronchoalveolar lavage has been used as an investigative tool in the study and evaluate of acute and chronic pulmonary disorders [61][62]. In the lungs, gas exchange between inspired air and blood occurs. Upon inhalation, air is carried through the respiratory tree, a structure that begins with the trachea and progressively branches into small airways until it reaches the blind ends of the respiratory passages, termed the alveolar sac [59]. The walls of alveolar sacs are lined with alveoli, the site where gas exchange occurs [59]. As the respiratory tree further branches and subdivides, the population and identity of cells that make up the mucosal lining changes, as there are regional distinctions [63]. Examples of the cells found along respiratory mucosa include pseudostratified, tall, columnar, ciliated epithelial cells and mucus secreting goblet cells. Alveolar macrophages and recruited neutrophils are among the cells that protect against inhaled debris and invading pathogens. During bronchoalveolar lavage, after a bronchoscope is introduced into respiratory tree, aliquots of normal saline are introduced into the respiratory airways; this fluid is then aspirated for analysis.

Diagnostic Value. Bronchoalveolar lavage is indicated in patients with abnormalities of unclear etiology seen on chest imaging [64]. Recovered aliquots of bronchial alveolar lavage fluid are analyzed for the presence of microorganisms, the profile of cells present, and the type of soluble biochemical factors present. Upon collection, one notes the volume and gross appearance of

uncentrifuged fluid. A portion of fresh sample may be sent to the microbiology laboratory for quantitative bacterial culture. The supernatant and cell pellet in a portion of sample that is centrifuged sample is further analyzed. The type and amount of soluble factors present in the supernatant can be determined with biochemical methods. The resuspended cell pellet may be sent for additional tests, including flow cytometry, nucleic acid analysis, glass slide preparation for microscopic review, and further microbiologic studies. A complete profile of cells present in the sample is determined, and accuracy is enhanced by analyzing 400-500 cells [65]. There are reports available in the literature regarding the expected amounts and profiles of cells found in BAL fluid analysis [63]. Identification of the population of cells present, as well as the determination of cell phenotypes is used to assist in the evaluation of patients with lung pathology, including those with an acute respiratory infection, interstitial lung disease, or malignancy. In addition, regular long term monitoring of BAL fluid profiles with lung tissue sampling is performed in patients who have undergone lung transplantation to assess for acute and chronic long term graft and host interactions [63].

Sample Preparation Challenges. BAL fluid should be processed promptly if cells are collected in a nutrient poor media, such as normal saline [65]. In addition, note that mucus production increases the viscosity of respiratory secretions, and may interfere with BAL fluid specimen preparation; care should be taken as samples are collected to minimize this. Often, collected fluid is strained though material such as cotton gauze, to remove debris and allow for more adequate sample preparation. Isolation of specific cell populations is important for diagnostic purposes, so that the determination can been made whether the presence of these cells correlates with particular lung pathology. On average, 100 to 250 mL of collected fluid is available for

analysis. The number of cells present may vary from a sparse amount to a highly cellular specimen. While the majority of cells present may be neutrophils, lymphocytes present in smaller numbers may be more difficult isolate and further analyze.

1.3.8 Synovial Fluid

Background. Synovial fluid is the biofluid that lines the cavitated space in synovial joints. Examples of synovial joints include the elbow and knee. The synovial membrane is the boundary layer of this space, and consists of synoviocytes. Synoviocytes secrete hyaluronic acid and proteins, as well as synovial fluid, which functions as a lubricant, a shock absorbent, and provides nutrition for articular hyaline cartilage. Synovial fluid is a clear fluid that is a filtrate of plasma; it is viscous, containing hyaluronic acid, proteins, and few cells. Normal synovial fluid has fewer than 180 leukocytes per microliter. The abundance of these cells should be mononuclear cells. In particular disease states, this number of leukocytes can increase; as well as the percentage profile of subpopulations of leukocytes present may change, for example, granulocytes (polymorphonuclear cells) instead of mononuclear cells. In addition, the presence of crystals may be noted. The characteristics and profile of synovial fluid may be determined by obtaining a sample of fluid during arthrocentesis. During arthrocentesis, a sample of synovial fluid is aspirated through a needle that is inserted into the joint space. This procedure may be performed by a physician in the hospital at the bedside or in the office [66].

Diagnostic Value. Under normal circumstances synovial fluid is clear; cloudy or bloody fluid may be present in conditions where an inflammatory, infectious, or traumatic process has affected the joint from which the fluid was aspirated. The appearance of the fluid is noted at the

time of initial collection. Consider conditions causing joint inflammation, or arthritis: in the case of osteoarthritis, aspirated synovial fluid may appear clear; however, in the case of gout, where monourate crystals within the joint space elicit an inflammatory response, aspirated synovial fluid may appear cloudy, but translucent. To assist in accurately diagnosing the cause of arthritis, a sample of synovial fluid is obtained with arthrocentesis. In general, a 1-2 mL aspirate of fluid is adequate for routine diagnostic testing. Metabolites that are routinely quantified include glucose, total protein, and lactate dehyodrogenase levels [67]. Additionally, the total number of leukocytes and specific leukocyte subpopulations present is quantified. Further testing include performing a wet mount, or glass slide preparation, for review under normal light and compensated polarized light microscopy. Microscopy allows for the identification of crystals that may be responsible for the joint inflammation causing patient symptoms. If there is concern for infection, a sample of fluid is sent for Gram stain and microbial culture, to determine if any microorganisms are present. Further cytology studies are also appropriate, as cancer may affect the synovium as a primary tumor or as the result of tumor metastasis [68]. It has also been reported that the proportion of synovial fluid mesenchymal stem cells present in freshly collected joint aspirates inversely correlates with disease severity in osteoarthritis [69].

Sample Preparation Challenges. Typically, arthrocentesis may yield 1-5 mL of fluid for analysis, leaving one with a small volume to work with. This collected volume may be highly cellular, or acellular, depending on what process is present in the joint that prompts the patient to seek medical attention. Also, depending on the underlying pathology present, if any, aspirated fluid may be have high viscosity, requiring high pressure to allow for fluid flow through the intended device. As noted above, crystals may also be present, which should be considered in

the preparation of a sample where cells are to be further characterized and analyzed. The isolation of specific cell populations is important for diagnostic and prognostication purposes.

1.4 Critical Challenges in Microfluidic Sample Preparation

Retrieving target cell populations in solution with minimal perturbation is a complex sample preparation task. Most microfluidic approaches to sample preparation are scaled down versions of techniques derived from biologists or chemists using well-plates, centrifugation, and pipetting. For example, cells can be isolated in a conical tube by incubating with immunomagnetic beads followed by placing a large magnet lateral to the tube and performing multiple rinse steps. Microscale technologies followed suit by integrating with on-chip and off-chip magnets for separating cancer cells, bacteria, fungi from blood [70]. Other concepts were borrowed from chemistry discipline, like affinity and size-based chromatography, translating to microscale techniques using unique cell biomarkers like size or surface markers. Our survey of various diagnostically-important biofluids has revealed several classes of sample preparation challenges which microfluidic technologies are poised to address: 1) concentrating rare cells from large volumes of biofluids, 2) efficiently preparing small volume samples, 3) preparing samples with high cellularity, 4) automating multi-step sample preparation, and 5) obtaining high purity for molecular assays.

1.4.1 Concentrating Rare Cells from Large Volumes of Biofluids

Biofluid analysis may require large sampling volumes in the range of mL volumes, especially for rare cell applications. Oftentimes, a sample with a low cellularity combined with inadequate sampling and the rare presence of malignant cells within the total number of cells leads to

unsatisfactory results, prompting further diagnostic testing. Therefore, large volumes in the mL-L scale must be processed to harvest sufficient rare cellular materials for molecular analysis. In order to achieve large volume processing, potential devices need to process samples at flow rates in the mL/min scale to achieve the quick turnover that is similar to that of the flow cytometer. One challenge in a device using high flow rates is that this may lead to high shear stress in the microchannels which may damage cells in the process. Careful mathematical calculations and experimental testing is required to be sure that cell viability and integrity are maintained. Scaling up of flow rates is possible by creating massive parallel arrays or increasing the channel dimensions of the device enabling more volume throughput. Notably, only a few microfluidic technologies are able to expand in a parallel fashion and still retain the fundamental mechanics [71][72][73]. A valid metric to measure sample processing power can be defined as the number of cells processed over time (cells/s) or the amount of liquid processed over time (mL/min). Relevant biofluids where one would envision large volume analysis include blood, urine, pleural, peritoneal, and BAL fluid samples. For example, 50 mL of pleural fluid is adequate to gather enough material for a cell smear in malignant pleural fluid analysis [74]. In another case, the presence of >5 cancer cells circulating in the bloodstream was shown to be an independent predictor of overall patient survival in metastatic breast cancer [36]

1.4.2 Efficiently Preparing Small Volume Samples for Multiple Assays

There are circumstances where the sample volume available for testing is limited. For example, typically 300 microliters of bone marrow is collected during a single bone marrow aspiration. Also, in particularly diagnostically challenging cases, clinicians may require multiple tests to aid

in determining the final diagnosis present. In both examples, it is very important that the volume of sample available for testing is efficiently prepared so that an optimal number of investigations can be completed. Factors that may reduce the sample volume available for further analysis include dead volume, mishandling of collected samples, or even that the amount of sample originally collected was already minuscule. In developing microfluidic systems, regarding dead volume, apparatus such as tubing and syringes incorporated into devices for the purposes of sample flow will lead to a reduction in the effective volume of sample available for analysis. One potential solution is to enable repeated processing of the same sample to increase the overall yield for further downstream tests.

1.4.3 Preparing Samples That Have High Cellularity

Biofluids that have high cellularity, like blood or bone marrow aspirates, will contain very diverse and large populations of cells. This can be challenging because of the likelihood that cells will aggregate, making the accurate quantification of total and subpopulations of cells present within a sample difficult. In analyzing blood, targeted populations such as leukocytes, erythrocytes, and platelets are separately identified and quantified; the accuracy of this process is decreased when a clinical sample has a high number. Within the population of leukocytes, further identification of neutrophils, lymphocytes, monocytes, eosinophils, and basophils is clinically useful. Specific enumeration of leukocyte subpopulations is performed routinely in the clinical setting, and, in this study, the ratio of total neutrophil to total lymphocytes present per microliter of blood was a predictor of increased cardiovascular risk [75]. It is also important to isolate single cells with particular genetic variance from within a purified target population. To do this, one can consider using droplet generators [76][77], and other technologies described in

the literature[78][38]. Single cell isolation and analysis is important, as bulk measurements may confound the analysis of single cell outliers that may harbor important specific genetic mutations—gene mutations which may explain the underlying cause of the disease [79]. To address this issue, it is important to identify and gather quantitative and qualitative measurements using single cells. With large enough sampling, one can create cellular profiles and generate unique metrics. These quantitative measurements may complement pathological information obtained by a cytopathologists during microscopic examination of cell smears or cell blocks. These may include cell morphology like size or deformability, nuclear to cytoplasmic ratio, and presence of specific markers. These metrics can be quantified through downstream image processing technology like flow cytometers [80][2][12], which emphasizes the importance of upstream sample preparation techniques.

1.4.4 Automating Multi-Step Sample Preparation

Automated handling of samples is needed for standardizing the sample preparation process. This includes centrifugation, pipetting, and cell staining, all operations manually performed by the cytology team. When working with large liquid volumes, cytologists must aliquot, centrifuge and manually pipette the supernatant of the sample to make cell smears. However, mishandling and user error in processing such as neglecting a decanting step may lead to misleading results. And thus a standardized fluid plumbing system through the device would address this issue by removing user input; it can also allow for processing large liquid volumes. In the microfluidic laboratory, the common syringe pump or lesser-known pressure system introduces fluid into the device from a syringe or bottle. While these systems are valid in the research setting, clinical translation of these technologies requires computer controlled systems. Additionally, cell

staining techniques can be automated in microfluidic platforms to enable efficient uniform labeling using traditional and immunocytochemical stains as well as to enhance the performance of cytogenetic analysis ex. FISH. Automation of these steps to minimize sample handling will preserve sample integrity and leading to less error overall, leading to cost reduction and increase in the quality of prepared samples.

1.4.5 Achieving High Purity Cell Populations

Achieving high purity of specific cell populations from heterogeneous solutions presents a critical challenge in biofluids. The removal of particulates and non-relevant cells becomes significant in cytology exploration. This can aid in visualization purposes, given that in the review of standard cytology slides, target cells are difficult to examine where there is a high cellular background. Additionally, the removal of bloody components and the concentration of target cells in small field of view may expedite and increase accuracy on cytology examinations [38] [73], [81]. Also note that in bloody specimens, leukocytes can contaminate molecular analysis results when attempting to detect gene mutations or sequencing in the target cell population [82]. Thus, the purity of sample outputs, defined as the amount of target cells over the total number of cells, is regarded as a valuable metric to characterize cell separation and isolation techniques. Purity is generally characterized by the imaging and analysis of cells that have been chemically treated and stained cells. However, after these processing steps, the cells cannot be used for further applications, for example, cell culture or genetic sequencing. While a few example microfluidic approaches address this conflicting situation and describe methods that have been successful in recovering specific cells from a general population [73], [83], others lack the ability to make cells readily available in solution after sample preparation for integration with

existing cell-based analysis tools like flow cytometry and imaging based techniques. Microfluidic technologies that may potentially address this need use label-free separation methods [84] that take advantage of cell size, deformability [49], [85], shape using various approaches (physical phenomena) like magnetic, acoustic, electrokinetic, dielectrophoretic, and hydrodynamic forces.

1.5 Future Directions

Sample preparation of biofluids has significant implications to the microfluidic and clinical community. As we design new technologies to address current deficiencies, we need to consider all stakeholders involved, including clinicians, clinical lab professionals, regulatory agencies, such as the FDA in the US, and insurance companies. Most importantly, we must consider the very patients who stand to benefit from new advances in the field. It is important to involve stakeholders as early as possible in development process. In this way, a multidisciplinary approach would yield fruitful innovative ideas rooted in a desire to address the real problems currently present. Also, it can also provide motivation for more vigorous investigation of cutting edge applications. Understanding the requirement of the regulatory agencies present in a particular region of interest should then prompt designers to incorporate these ideas during prototype development and testing. Also, knowledge of reimbursement policies may guide the approach to be undertaken in terms of diagnostic development. Indeed reduced sample preparation time should lead to quicker turnover regarding clinical results, and ultimately, improved patient outcomes. In addition, standardization of sample preparation should improve sample quality while also reducing cost.

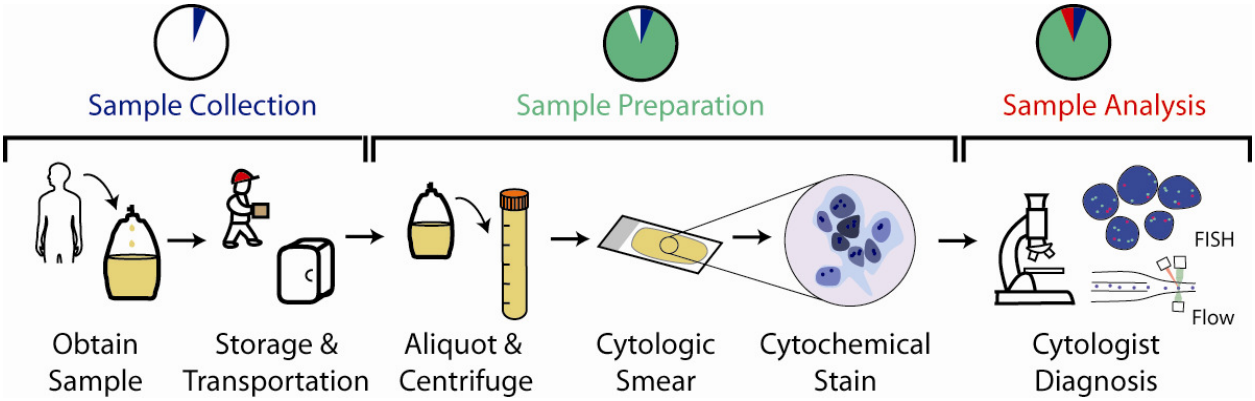

Figure 1.1 Standard procedure in collecting, preparing and analyzing biofluid samples for cytodiagnostics. Biofluid specimens are collected from the patient and transported to a cytopathology laboratory. Freshly collected samples are prepared with multiple centrifugation and manual handling steps including cell fixing, washing, and cytochemical staining. These are necessary steps for preparing cell-based assays including cell smears, cell blocks and cell solutions. Prepared samples are handed to cytologists for microscopic examination, flow cytometry, and cytogenetic analysis. From the initial collection of biofluid samples until final analysis is complete, the time spent during the sample preparation portion has the longest duration, relative to sample collection and sample analysis.

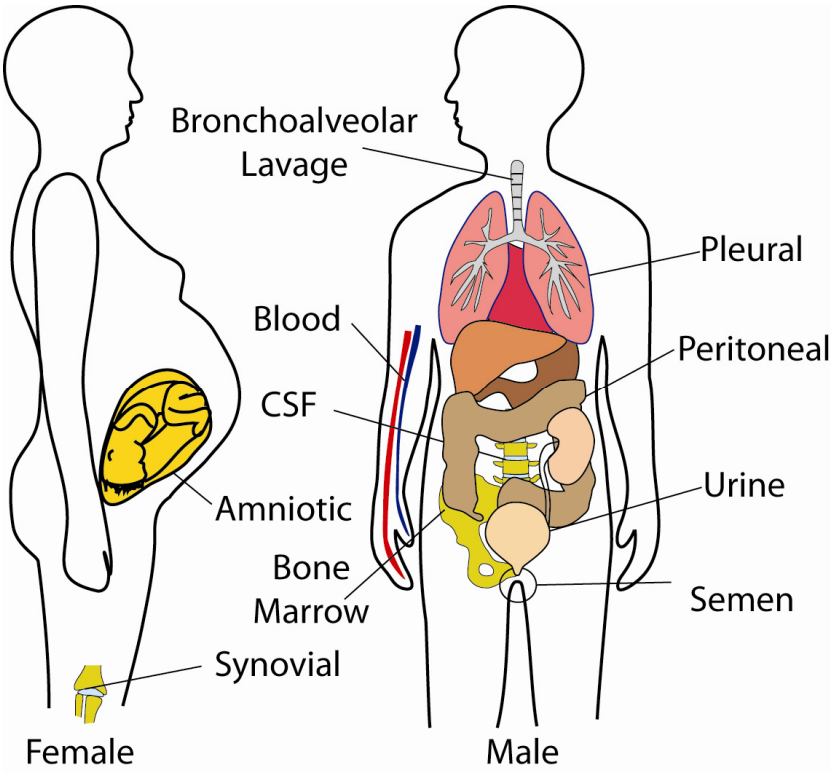

Figure 1.2 The human system produces biofluids to complete bodily functions. The constant secretion, absorption, and circulation of fluid in the body and the rich source of cellular material make it a valuable medium for liquid-based cytology. This presents vast opportunities in bridging medical and clinical applications with microfluidic technologies for sample preparation and analysis.

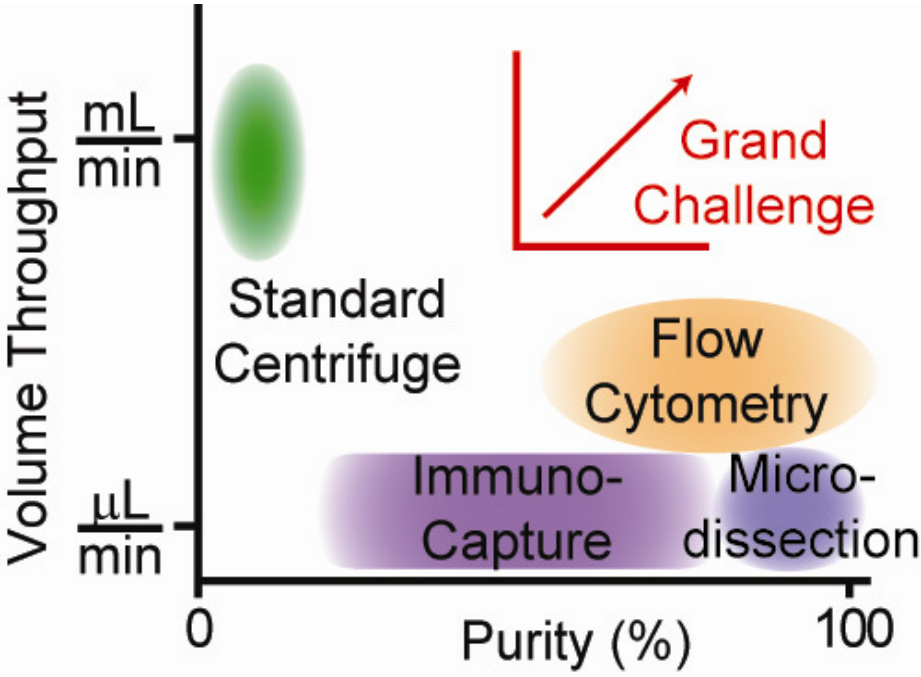

Figure 1.3 Sample Preparation of Biofluids Requires a Balance of Throughput and Purity. Macroscale instruments like the centrifuge specialize in throughput while microscale technologies emphasize on purity. Both high throughput and purity are useful alone, but for some samples it will be clinically useful to have technologies that can process fluids at high throughputs and with high purity.

Table 1.1 Body Fluids used for Cytodiagnostics

Body Fluid	Location	Procedure Required (Risk 0-3)	Volume per Test	Viscosity (mPa·s)	Diagnostics, Diseases or Applications	US Incidence (Cases/year)	Cell Type & Number (cells/mL)	Microfluidic Technologies
Blood	Veins	Venipuncture[1]	1-7.5 mL [86]	1.7-3.2 [87]	CBC	12 M [88]	RBCs (5 B) WBCs (5-10M) Platelets (400 M)	[11]
					HIV, HematologicMalignancies	48 K [89]	Lymphocyte subsets CD4+ (1.5 K)	[30], [1]
					Sepsis, Biofilm Investigation	0.75 K [90]	Bacteria Fungi	[70]
					Metastastic Cancer	*	CTCs (5) [36]	[39]
					Prenatal Diagnosis	*	Fetal Cells (NA)	[55][54]
Urine, Bladder Washings	Urethra	Voided[0]	8-50 mL [91]	1.2 [92]	Urothelial Carcinoma	9 M [88]	Epithelial Cells RBCs (>13 K) [93] WBCs	NA
					Infection	8.2 M [94]	Bacteria (>10^5 cfu)	NA
	Bladder	Catheterization[2]	100 mL[95]	1			Epithelial Cells	NA
Semen	Seminal vesicles	PESA[3]	>2 mL		In-Vitro Fertilizations	13 M [96]	Spermatozoa (20M)	[97]
Pleural	Pleura	Thoracentesis[3]	50 mL	1.25-1.68 [98]	Mesothelioma Malignancy Leukemia Infection Inflammation	1.5 M [99]	Mesothelial cells RBCs WBCs Cancer cells	[12], [48]
Peritoneal	Peritoneum	Paracentesis[3]	50 mL	1.425 [100]				NA
Pericardial	Pericardium	Pericardiocentesis[3]	250 mL					NA
Cerebrospinal Fluid	Subarachnoid space	Lumbar puncture [3]	15 mL	1.26-1.39 [101]	Meningitis CNS Lymphoma Multiple Sclerosis	0.4 M [102]	WBCs (0-5)	NA
Nasorespiratory Fluid	Respiratory Tree	Bronchoalveolar Lavage – bronchoscopy[3]	100-300 mL [103]		Infection Malignancy Inflammation	0.5 M [104]	WBCs, [63]RBCs Dendritic cells Eosinophils	[105]
Amniotic Fluid	Amniotic Sac	Amniocentesis[3]	20 mL	1.006-1.008	Prenatal Diagnosis	124,000 (NCHS)	Differentiated Cells, Trophoblast [106]	[52]
Synovial Fluid	Joints	Arthorcentesis[2]	1-2 mL	6 [107]	Joint pain Inflammation		Inflammatory Cells	NA
Bone Marrow Aspiration	Pelvis Bone	Bone marrow aspiration[3]	300 µL	37.5 [108]	Leukemia, Multiple Myeloma, Lymphoma		RBCs,WBCs ,CTCs Progenitor Cells	NA

Footnote: NCHS = National Center for Health Statistics, NA = Data not available, * = currently under investigation, cfu = colony forming units
Risk Level (rated 0-3): 0 indicates least invasive or procedurally difficult, 3 indicates very invasive and potential risk of harm to patient.

1.6 Acknowledgements

This chapter is a version of work in preparation for publication. Authors include Oladunni Adeyiga and Dino Di Carlo.

1.7 References

[1] D. Holmes, D. Pettigrew, C. H. Reccius, J. D. Gwyer, C. van Berkel, J. Holloway, D. E. Davies, and H. Morgan, "Leukocyte analysis and differentiation using high speed microfluidic single cell impedance cytometry," *Lab on a Chip*, vol. 9, no. 20, p. 2881, 2009.
[2] S. C. Hur, H. T. K. Tse, and D. Di Carlo, "Sheathless inertial cell ordering for extreme throughput flow cytometry," *Lab Chip*, vol. 10, no. 3, pp. 274–280, 2010.
[3] K. Cheung, S. Gawad, and P. Renaud, "Impedance spectroscopy flow cytometry: On-chip label-free cell differentiation," *Cytometry Part A*, vol. 65A, no. 2, pp. 124–132, 2005.
[4] J. P. Golden, J. S. Kim, J. S. Erickson, L. R. Hilliard, P. B. Howell, G. P. Anderson, M. Nasir, and F. S. Ligler, "Multi-wavelength microflow cytometer using groove-generated sheath flow," *Lab on a Chip*, vol. 9, no. 13, p. 1942, 2009.
[5] C. Rivet, H. Lee, A. Hirsch, S. Hamilton, and H. Lu, "Microfluidics for medical diagnostics and biosensors," *Chemical Engineering Science*, vol. 66, no. 7, pp. 1490–1507, Apr. 2011.
[6] J. Kim, M. Johnson, P. Hill, and B. K. Gale, "Microfluidic sample preparation: cell lysis and nucleic acid purification," *Integrative Biology*, vol. 1, no. 10, p. 574, 2009.
[7] I. K. Dimov, L. Basabe-Desmonts, J. L. Garcia-Cordero, B. M. Ross, A. J. Ricco, and L. P. Lee, "Stand-alone self-powered integrated microfluidic blood analysis system (SIMBAS)," *Lab on a Chip*, vol. 11, no. 5, p. 845, 2011.
[8] L. Gervais, N. de Rooij, and E. Delamarche, "Microfluidic Chips for Point-of-Care Immunodiagnostics," *Advanced Materials*, vol. 23, no. 24, pp. H151–H176, Jun. 2011.
[9] G. M. Whitesides, "The origins and the future of microfluidics," *Nature*, vol. 442, no. 7101, pp. 368–373, Jul. 2006.
[10] P. Yager, T. Edwards, E. Fu, K. Helton, K. Nelson, M. R. Tam, and B. H. Weigl, "Microfluidic diagnostic technologies for global public health," *Nature*, vol. 442, no. 7101, pp. 412–418, Jul. 2006.
[11] Mehmet Toner and Daniel Irimia, "Blood-On-A-Chip," 08-Jul-2005.
[12] D. R. Gossett, H. T. K. Tse, S. A. Lee, Y. Ying, A. G. Lindgren, O. O. Yang, J. Rao, A. T. Clark, and D. Di Carlo, "Hydrodynamic Stretching of Single Cells for Large Population Mechanical Phenotyping," *PNAS*, Apr. 2012.
[13] A.-E. Saliba, L. Saias, E. Psychari, N. Minc, D. Simon, F.-C. Bidard, C. Mathiot, J.-Y. Pierga, V. Fraisier, J. Salamero, V. Saada, F. Farace, P. Vielh, L. Malaquin, and J.-L. Viovy, "Microfluidic sorting and multimodal typing of cancer cells in self-assembled magnetic arrays," *PNAS*, vol. 107, no. 33, pp. 14524–14529, Aug. 2010.

[14] A. E. Herr, A. V. Hatch, D. J. Throckmorton, H. M. Tran, J. S. Brennan, W. V. Giannobile, and A. K. Singh, "Microfluidic Immunoassays as Rapid Saliva-Based Clinical Diagnostics," *PNAS*, vol. 104, no. 13, pp. 5268–5273, Mar. 2007.
[15] A. E. Herr, A. V. Hatch, W. V. Giannobile, D. J. Throckmorton, H. M. Tran, J. S. Brennan, and A. K. Singh, "Integrated Microfluidic Platform for Oral Diagnostics," *Annals of the New York Academy of Sciences*, vol. 1098, no. 1, pp. 362–374, Apr. 2007.
[16] C. F. Streckfus and L. R. Bigler, "Saliva as a diagnostic fluid," *Oral Diseases*, vol. 8, no. 2, pp. 69–76, Mar. 2002.
[17] C.-C. Lin, C.-C. Tseng, T.-K. Chuang, D.-S. Lee, and G.-B. Lee, "Urine analysis in microfluidic devices," *Analyst*, vol. 136, no. 13, pp. 2669–2688, Jun. 2011.
[18] L. Antonangelo, F. S. Vargas, M. M. P. Acencio, A. P. Corá, L. R. Teixeira, E. H. Genofre, and R. K. B. Sales, "Effect of temperature and storage time on cellular analysis of fresh pleural fluid samples," *Cytopathology*, vol. 23, no. 2, pp. 103–107, Apr. 2012.
[19] S. Natu, J. Hoffman, M. Siddiqui, C. Hobday, J. Shrimankar, and R. Harrison, "The role of endobronchial ultrasound guided transbronchial needle aspiration cytology in the investigation of mediastinal lymphadenopathy and masses, the North Tees experience," *Journal of Clinical Pathology*, vol. 63, no. 5, pp. 445 –451, May 2010.
[20] E. S. Cibas and B. S. Ducatman, *Cytology: Diagnostics Principles and Clinical Correlates*. Saunders, 2003.
[21] G.-K. Nguyen, *Essentials of Fluid Cytology*. Library and Archives Canada, 2010.
[22] T. Zenz, D. Mertens, H. Döhner, and S. Stilgenbauer, "Molecular diagnostics in chronic lymphocytic leukemia - pathogenetic and clinical implications," *Leuk. Lymphoma*, vol. 49, no. 5, pp. 864–873, May 2008.
[23] R. F. Bonner, M. Emmert-Buck, K. Cole, T. Pohida, R. Chuaqui, S. Goldstein, and L. A. Liotta, "Laser Capture Microdissection: Molecular Analysis of Tissue," *Science*, vol. 278, no. 5342, pp. 1481–1483, Nov. 1997.
[24] M. R. Emmert-Buck, R. F. Bonner, P. D. Smith, R. F. Chuaqui, Z. Zhuang, S. R. Goldstein, R. A. Weiss, and L. A. Liotta, "Laser Capture Microdissection," *Science*, vol. 274, no. 5289, pp. 998–1001, Nov. 1996.
[25] S. R. Chowdhuri, L. Xi, T. H.-T. Pham, J. Hanson, J. Rodriguez-Canales, A. Berman, A. Rajan, G. Giaccone, M. Emmert-Buck, M. Raffeld, and A. C. Filie, "EGFR and KRAS mutation analysis in cytologic samples of lung adenocarcinoma enabled by laser capture microdissection," *Modern Pathology*, vol. 25, no. 4, pp. 548–555, Dec. 2011.
[26] S. Seo, S. O. Isikman, I. Sencan, O. Mudanyali, T.-W. Su, W. Bishara, A. Erlinger, and A. Ozcan, "High-Throughput Lens-Free Blood Analysis on a Chip," *Anal. Chem.*, vol. 82, no. 11, pp. 4621–4627, 2010.
[27] R. Fan, O. Vermesh, A. Srivastava, B. K. H. Yen, L. Qin, H. Ahmad, G. A. Kwong, C.-C. Liu, J. Gould, L. Hood, and J. R. Heath, "Integrated barcode chips for rapid, multiplexed analysis of proteins in microliter quantities of blood," *Nature Biotechnology*, vol. 26, no. 12, pp. 1373–1378, 2008.
[28] N. Varadarajan, D. S. Kwon, K. M. Law, A. O. Ogunniyi, M. N. Anahtar, J. M. Richter, B. D. Walker, and J. C. Love, "Rapid, efficient functional characterization and recovery of HIV-specific human CD8+ T cells using microengraving," *PNAS*, Feb. 2012.
[29] F. W. Grannis, "Use of discard pleural fluid in molecular research," *Nature Reviews Clinical Oncology*, vol. 9, no. 1, pp. 64–64, Dec. 2011.

[30] D. W. Inglis, M. Lord, and R. E. Nordon, "Scaling deterministic lateral displacement arrays for high throughput and dilution-free enrichment of leukocytes," *Journal of Micromechanics and Microengineering*, vol. 21, no. 5, p. 054024, May 2011.
[31] S. S. Shevkoplyas, T. Yoshida, L. L. Munn, and M. W. Bitensky, "Biomimetic autoseparation of leukocytes from whole blood in a microfluidic device," *Anal. Chem*, vol. 77, no. 3, pp. 933–937, Feb. 2005.
[32] D. S. Stein, J. A. Korvick, and S. H. Vermund, "CD4+ Lymphocyte Cell Enumeration for Prediction of Clinical Course of Human Immunodeficiency Virus Disease: A Review," *J Infect Dis.*, vol. 165, no. 2, pp. 352–363, Feb. 1992.
[33] H. Kantarjian, N. P. Shah, A. Hochhaus, J. Cortes, S. Shah, M. Ayala, B. Moiraghi, Z. Shen, J. Mayer, R. Pasquini, H. Nakamae, F. Huguet, C. Boqué, C. Chuah, E. Bleickardt, M. B. Bradley-Garelik, C. Zhu, T. Szatrowski, D. Shapiro, and M. Baccarani, "Dasatinib versus Imatinib in Newly Diagnosed Chronic-Phase Chronic Myeloid Leukemia," *New England Journal of Medicine*, vol. 362, no. 24, pp. 2260–2270, Jun. 2010.
[34] N. White, "The Treatment of Malaria," *N Engl J Med*, vol. 335, pp. 800–806, 1996.
[35] G. L. Mandell, *Mandell, Douglas, and Bennett's Principles and Practice of Infectious Diseases: Expert Consult Premium Edition - Enhanced Online Features and Print*, 7th ed. Churchill Livingstone, 2009.
[36] M. Cristofanilli, G. T. Budd, M. J. Ellis, A. Stopeck, J. Matera, M. C. Miller, J. M. Reuben, G. V. Doyle, W. J. Allard, L. W. M. M. Terstappen, and D. F. Hayes, "Circulating Tumor Cells, Disease Progression, and Survival in Metastatic Breast Cancer," *N Engl J Med*, vol. 351, no. 8, pp. 781–791, Aug. 2004.
[37] S. Hahn, R. Sant, and W. Holzgreve, "Fetal Cells in Maternal Blood: Current and Future Perspectives.," *Mol. Hum. Reprod.*, vol. 4, no. 6, pp. 515–521, Jun. 1998.
[38] U. Dharmasiri, M. A. Witek, A. A. Adams, and S. A. Soper, "Microsystems for the Capture of Low-Abundance Cells," *Annual Review of Analytical Chemistry*, vol. 3, no. 1, pp. 409–431, Jun. 2010.
[39] J. Chen, J. Li, and Y. Sun, "Microfluidic approaches for cancer cell detection, characterization, and separation," *Lab on a Chip*, vol. 12, no. 10, p. 1753, 2012.
[40] S. Zheng, H. Lin, J.-Q. Liu, M. Balic, R. Datar, R. J. Cote, and Y.-C. Tai, "Membrane microfilter device for selective capture, electrolysis and genomic analysis of human circulating tumor cells," *Journal of Chromatography A*, vol. 1162, no. 2, pp. 154–161, Aug. 2007.
[41] S. Wang, K. Liu, J. Liu, Z. T.-F. Yu, X. Xu, L. Zhao, T. Lee, E. K. Lee, J. Reiss, Y.-K. Lee, L. W. K. Chung, J. Huang, M. Rettig, D. Seligson, K. N. Duraiswamy, C. K.-F. Shen, and H.-R. Tseng, "Highly Efficient Capture of Circulating Tumor Cells by Using Nanostructured Silicon Substrates with Integrated Chaotic Micromixers," *Angew. Chem. Int. Ed.*, vol. 50, no. 13, pp. 3084–3088, Mar. 2011.
[42] S. L. Stott, C.-H. Hsu, D. I. Tsukrov, M. Yu, D. T. Miyamoto, B. A. Waltman, S. M. Rothenberg, A. M. Shah, M. E. Smas, G. K. Korir, F. P. Floyd, A. J. Gilman, J. B. Lord, D. Winokur, S. Springer, D. Irimia, S. Nagrath, L. V. Sequist, R. J. Lee, K. J. Isselbacher, S. Maheswaran, D. A. Haber, and M. Toner, "Isolation of circulating tumor cells using a microvortex-generating herringbone-chip," *Proceedings of the National Academy of Sciences*, vol. 107, no. 43, pp. 18392 –18397, Oct. 2010.

[43] R. W. Light, M. I. Macgregor, P. C. Luchsinger, and W. C. Ball Jr, “Pleural effusions: the diagnostic separation of transudates and exudates,” *Ann. Intern. Med.*, vol. 77, no. 4, pp. 507–513, Oct. 1972.
[44] J. Kassis, J. Klominek, and E. C. Kohn, “Tumor microenvironment: what can effusions teach us?,” *Diagn. Cytopathol.*, vol. 33, no. 5, pp. 316–319, Nov. 2005.
[45] R. W. Light, Y. S. Erozan, and W. C. Ball, “Cells in Pleural Fluid Their Value in Differential Diagnosis,” *Arch Intern Med*, vol. 132, no. 6, pp. 854–860, Dec. 1973.
[46] U. Malapelle, C. Bellevicine, P. Zeppa, L. Palombini, and G. Troncone, “Cytology-based gene mutation tests to predict response to anti-epidermal growth factor receptor therapy: a review,” *Diagn. Cytopathol.*, vol. 39, no. 9, pp. 703–710, Sep. 2011.
[47] U. Malapelle, N. de Rosa, D. Rocco, C. Bellevicine, C. Crispino, A. Illiano, F. V. Piantedosi, O. Nappi, and G. Troncone, “EGFR and KRAS mutations detection on lung cancer liquid-based cytology: a pilot study,” *Journal of Clinical Pathology*, 2011.
[48] S. E. Cross, Y.-S. Jin, J. Rao, and J. K. Gimzewski, “Applicability of AFM in cancer detection,” *Nature Nanotechnology*, vol. 4, no. 2, pp. 72–73, Feb. 2009.
[49] S. C. Hur, N. K. Henderson-MacLennan, E. R. B. McCabe, and D. Di Carlo, “Deformability-based cell classification and enrichment using inertial microfluidics,” *Lab Chip*, 2011.
[50] P. D. Coppi, G. Bartsch, M. M. Siddiqui, T. Xu, C. C. Santos, L. Perin, G. Mostoslavsky, A. C. Serre, E. Y. Snyder, J. J. Yoo, M. E. Furth, S. Soker, and A. Atala, “Isolation of amniotic stem cell lines with potential for therapy,” *Nature Biotechnology*, vol. 25, no. 1, pp. 100–106, Jan. 2007.
[51] R. E. Priest, K. M. Marimuthu, and J. H. Priest, “Origin of cells in human amniotic fluid cultures: ultrastructural features,” *Lab. Invest.*, vol. 39, no. 2, pp. 106–109, Aug. 1978.
[52] H.-W. Wu, X.-Z. Lin, S.-M. Hwang, and G.-B. Lee, “A microfluidic device for separation of amniotic fluid mesenchymal stem cells utilizing louver-array structures,” *Biomedical Microdevices*, vol. 11, no. 6, pp. 1297–1307, 2009.
[53] H.-W. Wu, X.-Z. Lin, S.-M. Hwang, and G.-B. Lee, “The culture and differentiation of amniotic stem cells using a microfluidic system,” *Biomedical Microdevices*, vol. 11, no. 4, pp. 869–881, 2009.
[54] R. Huang, T. A. Barber, M. A. Schmidt, R. G. Tompkins, M. Toner, D. W. Bianchi, R. Kapur, and W. L. Flejter, “A microfluidics approach for the isolation of nucleated red blood cells (NRBCs) from the peripheral blood of pregnant women,” *Prenatal Diagnosis*, vol. 28, no. 10, pp. 892–899, 2008.
[55] H. Mohamed, J. N. Turner, and M. Caggana, “Biochip for separating fetal cells from maternal circulation,” *Journal of Chromatography A*, vol. 1162, no. 2, pp. 187–192, Aug. 2007.
[56] J. O. Kitzman, M. W. Snyder, M. Ventura, A. P. Lewis, R. Qiu, L. E. Simmons, H. S. Gammill, C. E. Rubens, D. A. Santillan, J. C. Murray, H. K. Tabor, M. J. Bamshad, E. E. Eichler, and J. Shendure, “Noninvasive Whole-Genome Sequencing of a Human Fetus,” *Sci Transl Med*, vol. 4, no. 137, pp. 137ra76–137ra76, Jun. 2012.
[57] M. Kyo, M. J. Mihatsch, F. Gudat, P. Dalquen, B. Huser, and G. Thiel, “Renal graft rejection or cyclosporin toxicity? Early diagnosis by a combination of Papanicolaou and immunocytochemical staining of urinary cytology specimens,” *Transpl. Int.*, vol. 5, no. 2, pp. 71–76, May 1992.

[58] T. Mehta, M. Sanaei-Ardekani, A. Farooqi, S. Khan, A. Shammas, M. Boonyapredee, C. Allston, J. Wu, H. Nsouli, and M. Pehlivanova, "The utility of cytodiagnostic urinalysis as a tool to diagnose kidney allograft dysfunction in the era lymphocyte-depleting induction therapy," *Transplant. Proc.*, vol. 43, no. 10, pp. 3679–3685, Dec. 2011.
[59] V. Kumar, A. K. Abbas, N. Fausto, and R. Mitchell, *Robbins Basic Pathology, Eighth Edition*, 8th ed. Saunders/Elsevier, 2007.
[60] D. A. Hafler, D. A. Fox, M. E. Manning, S. F. Schlossman, E. L. Reinherz, and H. L. Weiner, "In vivo activated T lymphocytes in the peripheral blood and cerebrospinal fluid of patients with multiple sclerosis," *N. Engl. J. Med.*, vol. 312, no. 22, pp. 1405–1411, May 1985.
[61] R. P. Daniele, J. A. Elias, P. E. Epstein, and M. D. Rossman, "Bronchoalveolar Lavage: Role in the Pathogenesis, Diagnosis, and Management of Interstitial Lung Disease," *Ann Intern Med*, vol. 102, no. 1, pp. 93–108, Jan. 1985.
[62] M. A. Sackner, A. Wanner, and J. Landa, "Applications of Bronchofiberoscopy," *CHEST*, vol. 62, no. 5_Supplement, p. 70S–78S, Nov. 1972.
[63] H. Reynolds, "Bronchoalveolar Lavage and Other Methods to Define the Human Respiratory Tract Milieu in Health and Disease," *Lung*, vol. 189, no. 2, pp. 87–99, 2011.
[64] N. A. Cobben, J. A. Jacobs, M. P. van Dieijen-Visser, P. G. Mulder, E. F. Wouters, and M. Drent, "Diagnostic value of BAL fluid cellular profile and enzymes in infectious pulmonary disorders," *Eur. Respir. J.*, vol. 14, no. 3, pp. 496–502, Sep. 1999.
[65] K. C. Meyer, "Bronchoalveolar lavage as a diagnostic tool," *Semin Respir Crit Care Med*, vol. 28, no. 5, pp. 546–560, Oct. 2007.
[66] D. G. Baker and H. R. Schumacher Jr., "Acute Monoarthritis," *N Engl J Med*, vol. 329, no. 14, pp. 1013–1020, 1993.
[67] R. H. Shmerling, T. L. Delbanco, A. N. Tosteson, and D. E. Trentham, "Synovial fluid tests. What should be ordered?," *JAMA*, vol. 264, no. 8, pp. 1009–1014, Aug. 1990.
[68] M. F. Marengo, M. E. Suarez-Almazor, and H. Lu, "Neoplastic and paraneoplastic synovitis," *Rheum. Dis. Clin. North Am.*, vol. 37, no. 4, pp. 551–572, Nov. 2011.
[69] D.-H. Lee, C. H. Sonn, S.-B. Han, Y. Oh, K.-M. Lee, and S.-H. Lee, "Synovial fluid $CD34^-$ $CD44^+$ $CD90^+$ mesenchymal stem cell levels are associated with the severity of primary knee osteoarthritis," *Osteoarthr. Cartil.*, vol. 20, no. 2, pp. 106–109, Feb. 2012.
[70] C. W. Yung, J. Fiering, A. J. Mueller, and D. E. Ingber, "Micromagnetic-microfluidic blood cleansing device," *Lab Chip*, vol. 9, no. 9, pp. 1171–1177, 2009.
[71] J. A. Davis, D. W. Inglis, K. J. Morton, D. A. Lawrence, L. R. Huang, S. Y. Chou, J. C. Sturm, and R. H. Austin, "Deterministic hydrodynamics: Taking blood apart," *Proceedings of the National Academy of Sciences*, vol. 103, no. 40, pp. 14779–14784, Oct. 2006.
[72] D. Di Carlo, "Inertial microfluidics," *Lab Chip*, vol. 9, no. 21, pp. 3038–3046, 2009.
[73] A. J. Mach, J. H. Kim, A. Arshi, S. C. Hur, and D. Di Carlo, "Automated cellular sample preparation using a Centrifuge-on-a-Chip," *Lab on a Chip*, vol. 11, p. 2827, 2011.
[74] W. Abouzgheib, T. Bartter, H. Dagher, M. Pratter, and W. Klump, "A Prospective Study of the Volume of Pleural Fluid Required for Accurate Diagnosis of Malignant Pleural Effusion," *Chest*, vol. 135, no. 4, pp. 999–1001, Apr. 2009.
[75] B. D. Horne, J. L. Anderson, J. M. John, A. Weaver, T. L. Bair, K. R. Jensen, D. G. Renlund, and J. B. Muhlestein, "Which white blood cell subtypes predict increased cardiovascular risk?," *J. Am. Coll. Cardiol.*, vol. 45, no. 10, pp. 1638–1643, May 2005.

[76] M. Chabert and J.-L. Viovy, “Microfluidic high-throughput encapsulation and hydrodynamic self-sorting of single cells,” *PNAS*, vol. 105, no. 9, pp. 3191–3196, Mar. 2008.
[77] Y.-C. Tan, V. Cristini, and A. P. Lee, “Monodispersed microfluidic droplet generation by shear focusing microfluidic device,” *Sensors and Actuators B: Chemical*, vol. 114, no. 1, pp. 350–356, Mar. 2006.
[78] J. F. Zhong, Y. Chen, J. S. Marcus, A. Scherer, S. R. Quake, C. R. Taylor, and L. P. Weiner, “A microfluidic processor for gene expression profiling of single human embryonic stem cells,” *Lab Chip*, vol. 8, no. 1, pp. 68–74, Jan. 2008.
[79] D. D. Carlo and L. P. Lee, “Dynamic Single-Cell Analysis for Quantitative Biology,” *Anal. Chem.*, vol. 78, no. 23, pp. 7918–7925, 2006.
[80] D. Huh, W. Gu, Y. Kamotani, J. B. Grotberg, and S. Takayama, “Microfluidics for flow cytometric analysis of cells and particles,” *Physiological Measurement*, vol. 26, no. 3, pp. R73–R98, Jun. 2005.
[81] E. D. Pratt, C. Huang, B. G. Hawkins, J. P. Gleghorn, and B. J. Kirby, “Rare cell capture in microfluidic devices,” *Chemical Engineering Science*, vol. 66, no. 7, pp. 1508–1522, Apr. 2011.
[82] S. Billah, J. Stewart, G. Staerkel, S. Chen, Y. Gong, and M. Guo, “EGFR and KRAS mutations in lung carcinoma,” *Cancer Cytopathology*, vol. 119, no. 2, pp. 111–117, Apr. 2011.
[83] A. M. Shah, M. Yu, Z. Nakamura, J. Ciciliano, M. Ulman, K. Kotz, S. L. Stott, S. Maheswaran, D. A. Haber, and M. Toner, “Biopolymer System for Cell Recovery from Microfluidic Cell Capture Devices,” *Analytical Chemistry*, vol. 84, no. 8, pp. 3682–3688, Apr. 2012.
[84] D. R. Gossett, W. M. Weaver, A. J. Mach, S. C. Hur, H. T. K. Tse, W. Lee, H. Amini, and D. Di Carlo, “Label-free cell separation and sorting in microfluidic systems,” *Anal Bioanal Chem*, vol. 397, no. 8, pp. 3249–3267, Apr. 2010.
[85] J. S. Kuo, Y. Zhao, P. G. Schiro, L. Ng, D. S. W. Lim, J. P. Shelby, and D. T. Chiu, “Deformability considerations in filtration of biological cells,” *Lab Chip*, vol. 10, no. 7, pp. 837–842, 2010.
[86] J. C. Dale and S. G. Ruby, “Specimen collection volumes for laboratory tests,” *Arch. Pathol. Lab. Med.*, vol. 127, no. 2, pp. 162–168, Feb. 2003.
[87] R. E. Wells and E. W. Merrill, “INFLUENCE OF FLOW PROPERTIES OF BLOOD UPON VISCOSITY-HEMATOCRIT RELATIONSHIPS,” *J Clin Invest*, vol. 41, no. 8, pp. 1591–1598, Aug. 1962.
[88] E. Hing, M. J. Hall, J. J. Ashman, and J. Xu, “National Hospital Ambulatory Medical Care Survey: 2007 outpatient department summary,” *Natl Health Stat Report*, no. 28, pp. 1–132, Sep. 2010.
[89] J. Prejean, R. Song, A. Hernandez, R. Ziebell, T. Green, F. Walker, L. S. Lin, Q. An, J. Mermin, A. Lansky, H. I. Hall, and for the HIV Incidence Surveillance Group, “Estimated HIV Incidence in the United States, 2006–2009,” *PLoS ONE*, vol. 6, no. 8, p. e17502, Aug. 2011.
[90] L. A. Destarac and E. W. Ely, “Sepsis in Older Patients: An Emerging Concern in Critical Care,” *Advances in Sepsis*, vol. 2, no. 1, pp. 15–22, 2002.
[91] K. C. Halling, W. King, I. A. Sokolova, R. G. Meyer, H. M. Burkhardt, A. C. Halling, J. C. Cheville, T. J. Sebo, S. Ramakumar, C. S. Stewart, S. Pankratz, D. J. O’Kane, S. A. Seelig, M. M. Lieber, and R. B. Jenkins, “A comparison of cytology and fluorescence in situ

hybridization for the detection of urothelial carcinoma," *J. Urol.*, vol. 164, no. 5, pp. 1768–1775, Nov. 2000.
[92] R. Burton-Opitz and R. Dinegar, "The Viscosity of Urine," *Am J Physiol*, vol. 47, no. 2, pp. 220–230, Nov. 1918.
[93] K. F. Fairly and D. F. Birch, "Kidney International - Abstract of article: Hematuria: A simple method for identifying glomerular bleeding," 1982. [Online]. Available: http://www.nature.com/ki/journal/v21/n1/abs/ki198216a.html. [Accessed: 11-Aug-2012].
[94] M. S. Walters, M. C. Lane, P. D. Vigil, S. N. Smith, S. T. Walk, and H. L. T. Mobley, "Kinetics of Uropathogenic Escherichia coli Metapopulation Movement during Urinary Tract Infection," *mBio*, vol. 3, no. 1, Mar. 2012.
[95] T. Zellweger, G. Benz, G. Cathomas, M. J. Mihatsch, T. Sulser, T. C. Gasser, and L. Bubendorf, "Multi-target fluorescence in situ hybridization in bladder washings for prediction of recurrent bladder cancer," *Int. J. Cancer*, vol. 119, no. 7, pp. 1660–1665, Oct. 2006.
[96] D. Schwartz, A. Laplanche, P. Jouannet, and G. David, "Within-subject variability of human semen in regard to sperm count, volume, total number of spermatozoa and length of abstinence," *J Reprod Fertil*, vol. 57, no. 2, pp. 391–395, Nov. 1979.
[97] T. G. Schuster, B. Cho, L. M. Keller, S. Takayama, and G. D. Smith, "Isolation of motile spermatozoa from semen samples using microfluidics," *Reprod. Biomed. Online*, vol. 7, no. 1, pp. 75–81, Aug. 2003.
[98] O. Yetkin, I. Tek, F. Yetkin, and N. Numanoglu, "Role of pleural viscosity in the differential diagnosis of exudative pleural effusion," *Respirology*, vol. 12, no. 2, pp. 267–271, 2007.
[99] D. Feller-Kopman, M. J. Parker, and R. M. Schwartzstein, "Assessment of Pleural Pressure in the Evaluation of Pleural Effusions," *Chest*, vol. 135, no. 1, pp. 201–209, Jan. 2009.
[100] D. E. Ott, "Laparoscopy and Tribology: The Effect of Laparoscopic Gas on Peritoneal Fluid," *The Journal of the American Association of Gynecologic Laparoscopists*, vol. 8, no. 1, pp. 117–123, Feb. 2001.
[101] F. Yetkin, U. Kayabas, Y. Ersoy, Y. Bayindir, S. A. Toplu, and I. Tek, "Cerebrospinal Fluid Viscosity: A Novel Diagnostic Measure for Acute Meningitis," *Southern Medical Journal*, vol. 103, no. 9, pp. 892–895, Sep. 2010.
[102] C. E. Tung, Y. T. So, and M. G. Lansberg, "Cost comparison between the atraumatic and cutting lumbar puncture needles," *Neurology*, vol. 78, no. 2, pp. 109–113, Jan. 2012.
[103] K. C. Meyer, G. Raghu, R. P. Baughman, K. K. Brown, U. Costabel, R. M. du Bois, M. Drent, P. L. Haslam, D. S. Kim, S. Nagai, P. Rottoli, C. Saltini, M. Selman, C. Strange, and B. Wood, "An official American Thoracic Society clinical practice guideline: the clinical utility of bronchoalveolar lavage cellular analysis in interstitial lung disease," *Am. J. Respir. Crit. Care Med.*, vol. 185, no. 9, pp. 1004–1014, May 2012.
[104] D. A. Culver, S. M. Gordon, and A. C. Mehta, "Infection Control in the Bronchoscopy Suite A Review of Outbreaks and Guidelines for Prevention," *Am. J. Respir. Crit. Care Med.*, vol. 167, no. 8, pp. 1050–1056, Apr. 2003.
[105] E. A. Warner, K. T. Kotz, R. F. Ungaro, A. S. Abouhamze, M. C. Lopez, A. G. Cuenca, K. M. Kelly-Scumpia, C. Moreno, K. A. O'Malley, J. D. Lanz, H. V. Baker, L. C. Martin, M. Toner, R. G. Tompkins, P. A. Efron, and L. L. Moldawer, "Microfluidics-based capture of human neutrophils for expression analysis in blood and bronchoalveolar lavage," *Laboratory Investigation*, vol. 91, no. 12, pp. 1787–1795, Sep. 2011.

[106] C. M. Gosden, “Amniotic fluid cell types and culture,” *British medical bulletin*, vol. 39, no. 4, pp. 348–354.
[107] J. G. Larkin, G. D. Lowe, R. D. Sturrock, and C. D. Forbes, “The correlation of clinical assessment of synovial fluid with its measured viscosity,” *Br. J. Rheumatol.*, vol. 23, no. 3, pp. 195–197, Aug. 1984.
[108] U. Gurkan and O. Akkus, “The Mechanical Environment of Bone Marrow: A Review,” *Annals of Biomedical Engineering*, vol. 36, no. 12, pp. 1978–1991, 2008.

Chapter 2

Particle Trapping in Confined Laminar Microvortices

2.1 Introduction

There has been considerable interest in developing deterministic methods of particle ordering, clustering, and separation in microscale flow. In these confined microsystems, shear-gradient lift is dominant for particle manipulation such as particle focusing [1]. However, confined micrvortices consist of a complex system, where the shape of the vortex is not circular or elliptical and the shear gradient changes with the position along the vortex [2]. These complexities, coupled with the presence of a particle, make the understanding of particle behavior in fluid vortices a significant challenge.

In this chapter, we describe a phenomenon where particles above a critical size passively entered fluid vortices to become 'trapped' and maintained a stable orbit within the vortex. To systematically understand particle behavior in vortices, there are two aspects of particle interaction with laminar microvortices that are important to investigate: (i) under what conditions do particles migrate across streamlines to enter vortices, and (ii) what leads to maintenance of particles within vortices once they have entered. We uncover the forces involved in particle

trapping using various particle sizes and densities while trapped in fluid vortices. We investigated the complex velocity profiles in this system, compared empirical evidence with numerical results, and evaluated various fluidic forces that may be relevant to the trapping mechanics. Admittedly, the presented model is a simplification of the problem and assumptions of a circular path and constant pressure gradients across particles should be modified to better describe the phenomenon. Ultimately, an understanding of particle trapping mechanics allows us to build deterministic and predictable vortex trapping systems for practical biological applications.

2.2 Particle Manipulation in Inertial Microfluidics

2.2.1 Inertial Microfluidics

Fluid flow at the microscale is assumed to occupy low Reynolds number, where Reynolds number

$$\mathrm{Re} = \frac{\rho U H}{\mu} \qquad (1)$$

is a dimensionless parameter describing the ratio between inertial and viscous forces. This has always been a safe assumption mainly because channel dimensions have a characteristic length <1 mm. A quick calculation of a common microchannel flow with water density, $\rho \sim 1000$ kg/m3, water viscosity of $\mu \sim 0.001$ Pa s, channel diameter H of 100 μm, and fluid velocity U of ~0.01 m/s, shows that $\mathrm{Re} < 1$. As a result, traditional thinking has often perceived microfluidics as having neglible inertia with the viscous force dominating. However, recent reports demonstrate the important use of inertial effects in microfluidic systems, such as secondary flows in curved channels and inertial migration of particles [1].

2.2.2 Inertial Migration of Particles

Particle and cell manipulation can be achieved using inertial lift forces in confined channel flow. The first reported migration of particles in 1960 was in macroscale flow through a cylindrical pipe (Segre and Silberberg 1961). Segre and Silberberg demonstrated the formation of a ring annulus of particles from a randomly distributed particle solution. Recently, similar observations were observed at the microscale. Inertial effects that lead to particle migration transverse to fluid streamlines have recently been identified as useful in microfluidic systems for focusing [4], [5], separation [1], [4], [6], [7], [8] and filtration [6], [9–12] applications. These systems based on curving or straight channels have been used to perform separations on blood cells, polystyrene & PDMS beads, and oil droplets [6]. During operation, randomly distributed particles are observed to localize at particular equilibrium positions within the channel cross-section that depends on channel geometry, particle size, and flow properties. In straight, high aspect ratio channels (i.e. height > width), equilibrium positions are largely centered to two positions along channel faces and close to the wall [9], [10].

Equilibrium positions occur because of a balance between shear-gradient lift and "wall effect" lift (Di Carlo et al. 2007). The parabolic velocity profile and its associated gradient in shear rate leads to a lift force on flowing particles away from the channel centerline down the gradient in shear rate and toward the channel walls. As particles migrate closer to the walls, a counteracting inertial lift directed away from the stationary wall as a result of inertia of the fluid around the particle balances with the shear-gradient lift creating a stable equilibrium position for particles that is about halfway between the channel centerline and wall. Recent work suggested that when the ratio of particle size to channel dimension (a/W) becomes of order 1, shear-gradient lift would scale as Eq 1. [1]:

$$F_L = \frac{f_L \rho U^2 a^3}{W} \quad (2)$$

where a is the particle diameter, U is the maximum fluid velocity, W is the channel dimension in direction of migration, and ρ is the fluid density. The non-dimensional lift coefficient (f_L), is dependent on the particle's position within the channel (x), the channel aspect ratio (H/W), and the channel Reynolds number. Assuming that the inertial lift force is balanced with Stokes drag on a sphere

$$F_d = 3\pi\mu a U_p \quad (3)$$

where μ is the viscosity of the fluid, the lateral particle migration velocity (U_p) is found to be:

$$U_p = \frac{\rho U^2 a^2}{3\pi\mu W} f_L(R_c, x_c) \quad (4)$$

Note that this equation describes lateral particle migration velocities away from the channel centerline (where shear-gradient lift dominates). Separations based on inertial migration in straight high-aspect ratio channels are inherently limited in the amount of enrichment possible due to the relative location of the particle equilibrium position (x_{eq}) in these systems away from the wall. As discussed above, the equilibrium position in these systems is often between 0.5-0.6 the distance between the centerline and channel wall.

2.3 Laminar Microscale Vortices

2.3.1 Confined Laminar Microvortices

Microscale vortices are less well-known, mainly since flow in microchannels has been regarded to lack appreciable fluid inertia. Microvortices can arise when a microchannel is quickly expanded in width leading to jetting of the narrow entering stream of fluid, detachment of the

boundary layer, and recirculation in the expansion region. Vortex formation relies on fluid inertia: that is increasing Reynolds number of the flow leads to increasing vortex size until the full expansion region is occupied. It is important to note that the microvortices created in this system are different from vortices created in the streamwise direction such as Dean vortices created in curved channel flows with inertia [4], [13] or vortices created due to asymmetrically structured microchannels [14]. Key external parameters to control these flows include the channel dimensions (height, width, chamber width, chamber length) and flow rate.

2.3.2 Particle and Cell Behavior in Microvortices

There has been considerable interest in understanding particle and cell behavior in microvortices. In particular, microvortices have been used for studying cell manipulation [15–19], plasma extraction [20], particle focusing [5], cell docking [21] and fluid mixing [22]. Microvortices have been studied in blood flow where it was observe large cellular aggregates would occupy long residence times inside the vortex [23], [24]. This trapping behavior lead to much work in experimental and computational analysis of particle behavior in vortices [25]. Similar particle trapping and orbiting behaviors have been observed using external forces such as microactuators [26], hydrodynamic tweezers [27], [28], and electrokinetic fields [29]. Microvortices have been used for biological applications such as understanding cell orbiting and rotation but there is little empirical evidence in explaining the behavior of particle trapping [15] [17][19][30][31]. This phenomenon indicates an unknown mechanics of particles in microvortices.

2.4 Experimental Methods

2.4.1 Materials and Methods

Polydisperse PDMS (Polydimethylsiloxane) beads were prepared using an emulsion polymerization process. PDMS was mixed at the standard 10:1 ratio of resin to crosslinker (Dow Corning; Sylgard 184), degassed, and added to deionized water containing 0.1% Tween 20 at 10% w/v PDMS. The uncured solution was mixed vigorously with a vortexer and placed in an oven overnight at 65^{o}C to allow hardening into solid PDMS beads. After curing, PDMS beads smaller than 50 μm were extracted from the bead solution via centrifugation. Any remaining beads larger than 50 μm were removed via filtration through a filter upstream of the trapping arrays in the device.

Polydisperse PDMS particles with sizes (a/W=0.1-0.7 and particle diameter ranging from ~1 to ~35-50 μm) were injected (average velocity = 2.8 m/s) into two different vortex trapping chips with 70 μm channel height (Figure 2.1). One device had a 50 μm channel width and a vortex chamber of 600 μm width by 720 μm length, while the other device had a 40 μm channel width and a chamber of 480 μm width by 560 μm length. Using high-speed video microscopy, we tracked the trajectories of single PDMS particles as they migrated and stabilized in the fluid vortices. Individual particle trajectories were visualized and recorded with Phantom v7.3 high-speed camera (Vision Research, Inc.) conducted with 60-100 μs times between frames.

The particle trajectories were mapped using a custom MATLAB program that determined the PDMS particle center automatically (Figure 2.2). The automated program converted each raw image to a binary image where channel walls and PDMS particles form defined intensity peaks. Each image frame was subtracted from a background image, which contains only the

channel walls, leaving a defined intensity peak representative of the particle. The program measured the particle diameter and located the particle center position, which was then normalized to the channel center and orifice of the expansion-contraction chamber. This process was repeated for each frame until all images were analyzed. Each video consisted of ~1000 frames, which was long enough to observe the particles migrating into and become stably trapped within a fluid vortex. Particles were recognized to be stably trapped when the orbiting trajectory within the vortex remained constant. Particles that were not trapped in fluid vortices contained <10 frames for image analysis. Figures demonstrating particle migration trajectories and particle orbits within the vortex included data binned according to particle size. Each particle range (n = 3 or more samples) contained particle positions that were averaged, mapped, and overlaid onto fluid streamlines computed using finite element modeling. To determine the magnitude of shear gradient lift force, F_L, that each particle experiences, the inertial lift was assumed to balance Stokes drag on a sphere $F_L = 3\pi\mu a v_t$ where the force is dependent on the particle diameter a and transverse velocity v_t. This transverse velocity is derived from the mismatch in particle and fluid element trajectories as the particle migrates across streamlines.

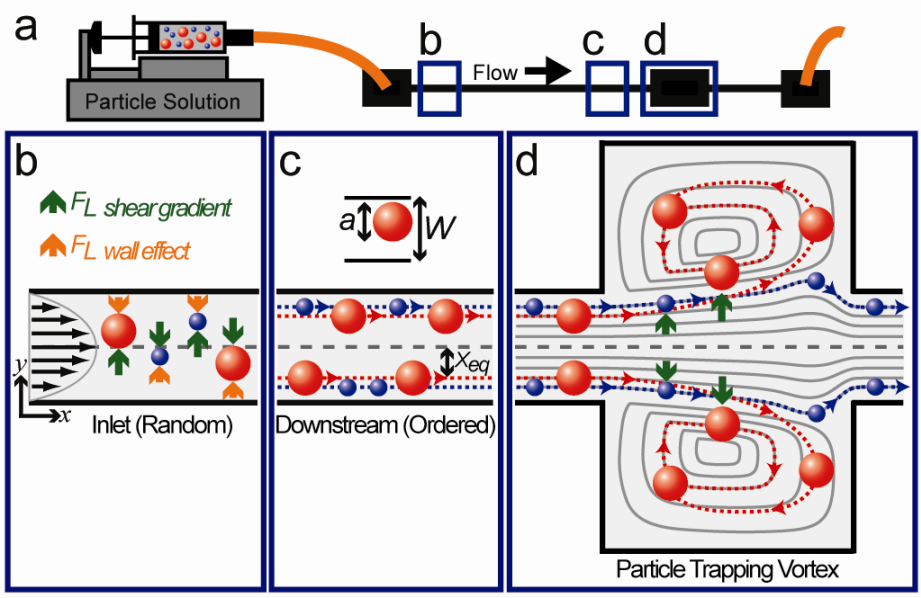

Figure 2.1 Particle entry mechanism in laminar microvortices. (A) For a polydisperse particle solution injected into a device with a straight high-aspect ratio channel leading into an expansion-contraction chamber we expect size-dependent entry into the laminar vortices created. (B,C) Particles are subjected to a shear gradient lift force, which directs particles toward the channel wall, and a wall effect lift force, directed toward the channel center, which leads to entrainment of particles at dynamic equilibrium positions, X_{eq}. (D) As focused particles enter the vortex chamber, the lift forces are decoupled due to the absence of a nearby wall, resulting in a dominate shear gradient lift force. Larger particles (red) experience larger lift forces and are able to migrate across fluid streamlines into the vortices while smaller particles (blue) follow fluid streamlines and flow out of the system.

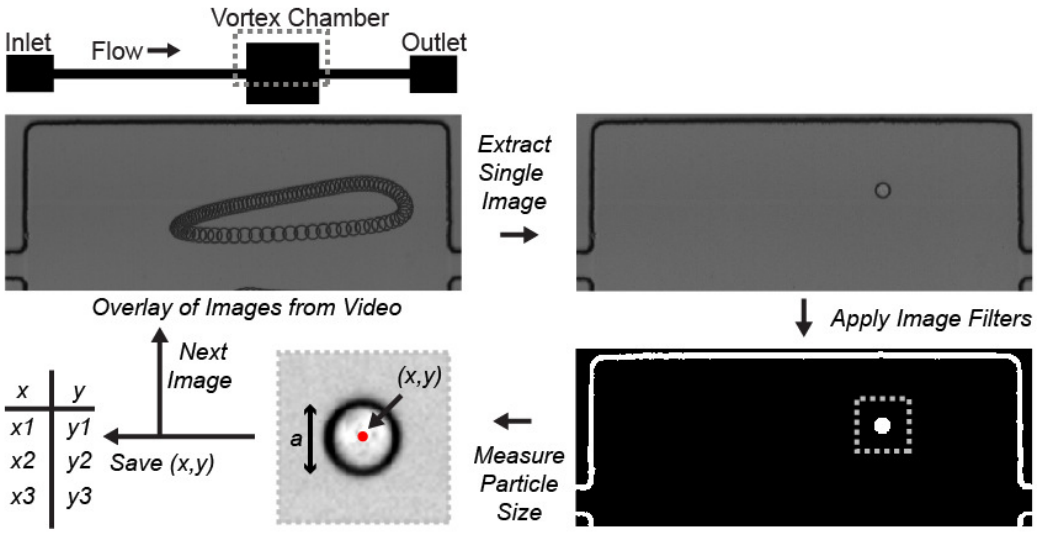

Figure 2.2 Using Phantom v7.3 high-speed camera (Vision Research, Inc.), we tracked the orbital trajectories of single particles in the fluid vortices. The positions of the particle were mapped using a custom MATLAB program that measured the particle diameter and center position. The automated program converted each raw image to a binary image where channel walls and PDMS particles form defined intensity peaks (white). The images were magnified at the particle position to measure the particle diameter (dotted box). This process was repeated for each frame until all images were analyzed. Each video consisted of ~200 frames.

2.4.2 Capture Efficiency of Particle Trapping

The efficiency of trapping depends in a complex fashion on system parameters (Figure 2.3). Capture efficiency is defined as the number of collected beads over the number of beads introduced into the system. We found that optimal trapping was observed for particles above 15μm, a channel height of H=54μm, reservoir width ratio of 15 and reservoir length of 720μm (Figure 2.3A-D). More importantly, we found that the vortex trapping depended on system parameters non-linearly. For example, trapping did not monotonically increase with reservoir

width ratio, displaying a local minimum in trapping at a ratio of 20. These observations require further understanding of particle behavior in the entrance and maintenance in microvortices.

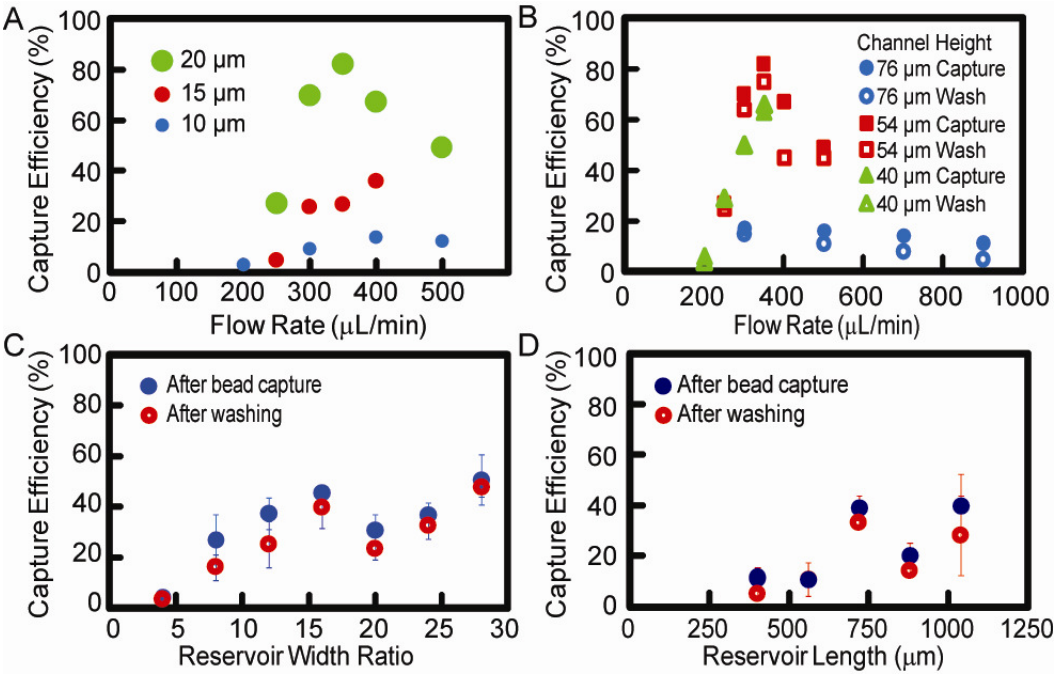

Figure 2.3 Dependence of Capture Efficiency on Geometrical Parameters and Flow Conditions. (A) Size-dependence of particle trapping with H=54µm. Effective trapping observed above 15µm and flow rates of 300µL/min. (B) Effect of H and Q on particle trapping. Effective trapping observed at H≤54µm. Stability of trapping increases with lower heights (C,D) Effect of reservoir width ratio over main channel width and reservoir length on particle trapping. Effective trapping observed at reservoir ratio of 15 and length of 720µm. These experiments completed by E. Sollier.

2.5 Mechanics of Particle Entrance

2.5.1 Particle Focusing Leads to Better Trapping

We first explored the mechanism of particle migration and entry into two symmetric vortices created in a microfluidic chip consisting of a single microchannel with an expansion-contraction chamber. When a polydisperse solution of particles is introduced into the system, the particles begin randomly distributed throughout the channel cross-section at the inlet (Figure 2.1A). As particles travel downstream, they are subjected to a shear gradient lift force, directing particles toward the channel wall, and an opposing wall effect lift force, that is due to the presence of the wall, leading to migration of particles toward the channel centerline. A combination of these forces leads to entrainment of particles at dynamic equilibrium positions about halfway between the channel centerline and wall, X_{eq} (Figure 2.1C) [1], [4], [32]. For the high-aspect ratio microchannels used (70 μm height, 50 μm width), this leads to two focusing positions along the long face of the channel as previously reported [1], [33–35]. There is also a slight particle size-dependence to focusing position, where larger particles are focused closer to the channel center.

2.5.2 Particle Migration Across Fluid Streamlines into Fluid Vortex

When a focused particle reaches the expansion region (Figure 2.1D) the neighboring microchannel wall is no longer within its vicinity. Therefore, the hydrodynamic interaction with the wall disappears leading to a loss of a significant wall-effect lift to balance the remaining shear-gradient lift directed down the shear gradient towards the vortex center. The gradient in shear rate responsible for shear gradient lift decays only slowly as the particle moves downstream through the expansion. The end result of these effects is that transverse particle

migration due to shear gradient lift controls entry of particles into vortices. In previous work [1] we demonstrated that when the ratio of the particle diameter to channel width approaches one, the shear gradient lift (F_L) in a straight channel would scale as Equation 2. For small *a/W*, however, F_L was analytically determined to scale with a^4 [36]. Taking these two possible scalings into account, and assuming that the velocity profile remains similar upon entering the expansion, we can determine a transverse migration velocity, v_t, into the vortex by balancing shear gradient lift with Stokes drag $F_{stk} = 3\pi\mu a v_t$. We find that the transverse migration velocity, v_t, will be a function of particle diameter - between a^2 to a^3. Following this scaling, larger particles (red) are expected to migrate laterally through fluid streamlines and into the vortex while smaller particles (blue) below a critical size will not migrate fast enough to cross into the vortex before passing out of the expansion region (Figure 2.1D).

It should be noted that entry into the vortex is controlled solely by shear gradient lift forces in the case of a dilute solution neglecting particle-particle interactions. In the case of highly concentrated particle solutions, like biofluids used in Chapters 3 and 4, interparticle hydrodynamic interactions are common, and cross-stream migration and entry can be assisted by particle collisions or disturbance flows from neighboring particles[37]. Although we have not explored it in detail, it is apparent that trapping is robust to changes in the vortex chamber geometry – as long as the shear gradient lift is present - including whether vortex chambers expand in one or both directions simultaneously during an expansion. This design flexibility can aid in developing parallel arrays with a small footprint for higher throughput operation.

With increasing particle size, migration occurred over a shorter downstream distance and resulted in final positions closer to the vortex center (Figure 2.4). In agreement with predictions, this is a result of larger particles experiencing higher shear gradient lift forces leading to faster

migration. Note that in the region in which particles enter the vortex the fluid does not change direction appreciably, minimizing local centrifugal effects that might push these particles outwards. Therefore, measured particle trajectories and dynamics calculated from these trajectories (Figure 2.5) are expected to yield a scaling similar to shear gradient lift force alone. In fact, the maximum lift force in this entry region for individual particles over a range of sizes was found to scale with a best fit of $a^{3.2}$, which closely matches previously reported predictions of between a^3 [1] to a^4 [36] (Figure 2.5).

Particles above a critical size migrated into the vortex and maintained a stable orbital position within the vortex (Figure 2.6). Particle trapping was observed for a range of particle sizes between a/W=0.3-0.4 for W=50 μm and a/W=0.4-0.45 μm for W=40 μm, where a is the particle diameter and W is the channel width. Particles smaller than the critical size range were never observed to be trapped and flowed past the trapping chamber and out of the system. The two datasets from Figure 2.6 together suggest that the critical size leading to entry into the vortex does not depend strongly on the inlet channel width and should be robust to small variations in this value.

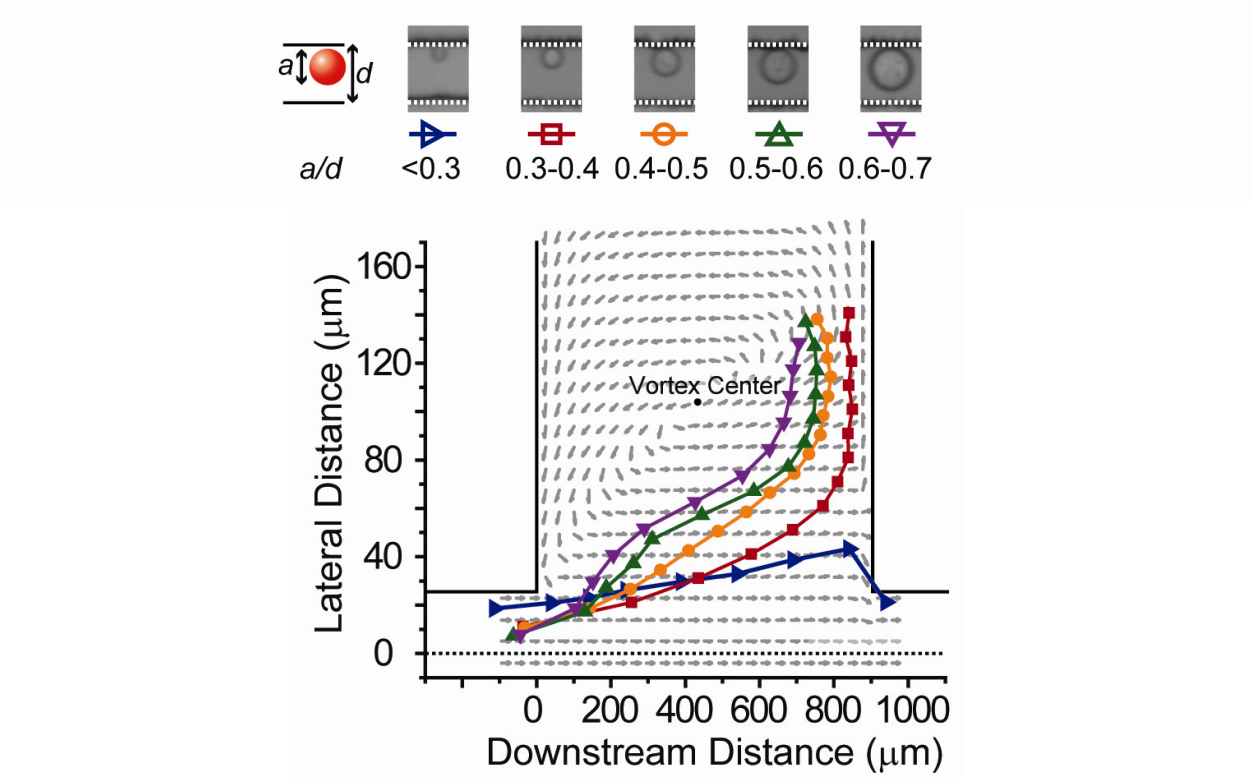

Figure 2.4 Average trajectories of polydisperse PDMS particles overlaid on fluid direction vectors obtained from a COMSOL model. Particle sizes larger than the ratio of particle diameter to channel width of 0.3 entered in vortex traps. As the particle size increases, the particle migrates closer to the vortex center.

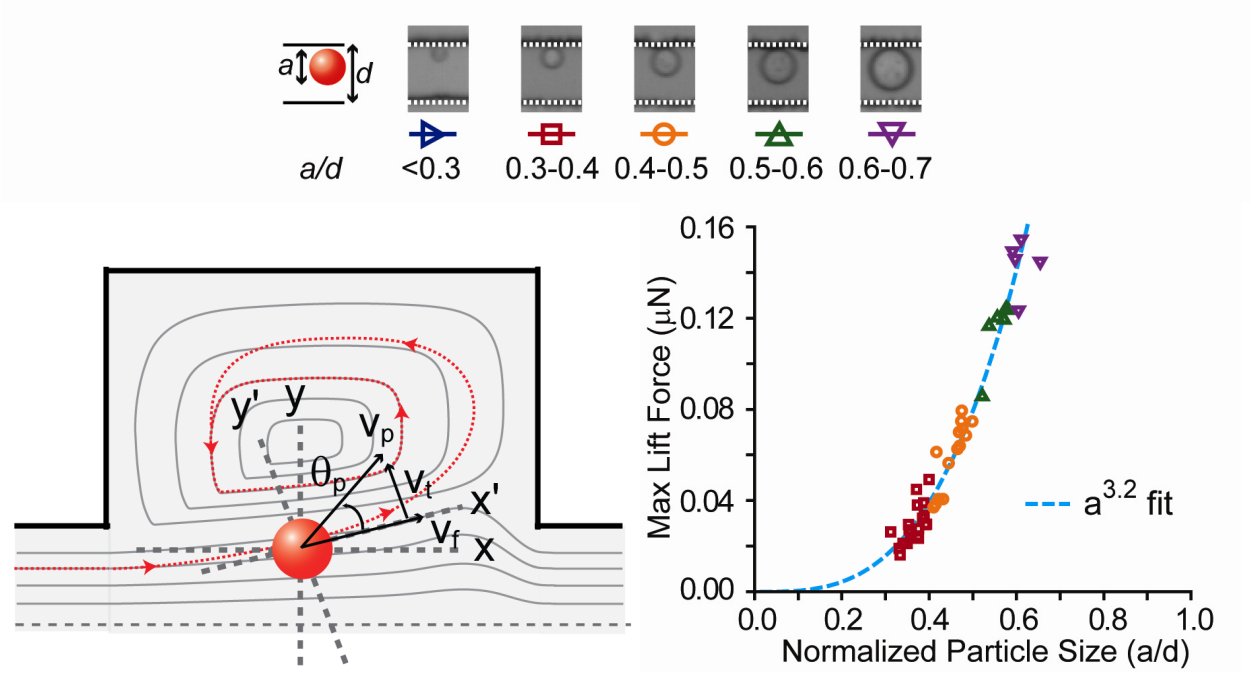

Figure 2.5 Calculation of the shear-gradient lift force. With the absence of the wall, the particle experiences a dominant shear gradient lift force that drives the particle through fluid streamlines into the vortex. This lift force can be measured by calculating the cross-streamline velocity of the particle, v_t. The instantaneous cross-stream velocity is accompanied by a Stokes drag that is equal in magnitude but opposite in direction of the lift force at steady state $F_L = 3\pi\mu a v_t$, where μ is the fluid viscosity, a is the particle diameter, and v_t is the transverse velocity which is calculated based on the mismatch in particle velocity and fluid velocity at each time point. The maximum lift force upon entry into a vortex was found to scale with the particle diameter to the 3.2 power.

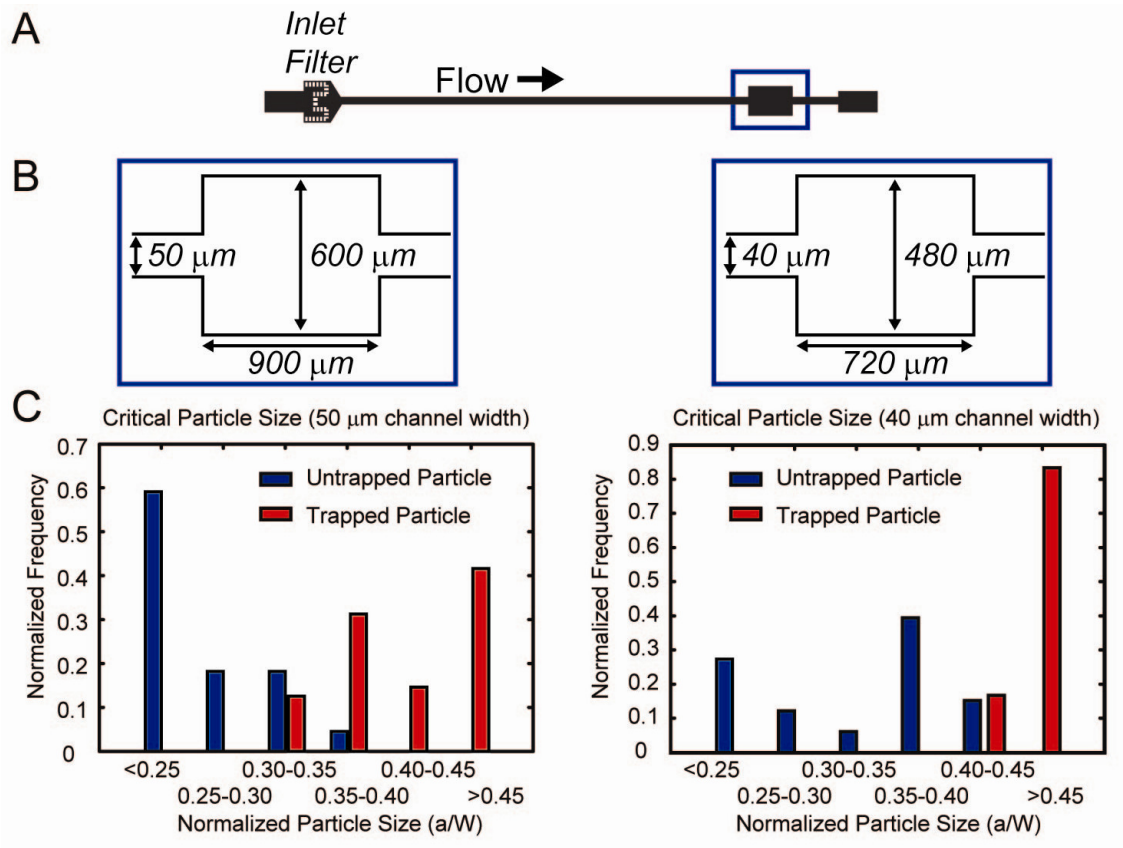

Figure 2.6 Critical particle size for trapping. Particle trapping was observed for a range of particle diameters between *a/W*=0.3-0.4 for a 50 μm channel width and 0.4-0.45 for a 40 μm channel width. Particles smaller than the critical size were incapable of being trapped and flowed past the trapping chamber and out of the system. Interestingly, these results suggest that the critical size leading to entry into the vortex does not depend strongly on the inlet channel width.

2.6 Mechanics of Particle Maintenance

Once particle entry into a microvortex has occurred, the problem of maintaining particles in vortices becomes important. Particles occupy stable and repeatable orbits within the fluid vortices (Figure 2.7). In one orbit trajectory, particles experienced changes in velocities and accelerations based on the surrounding fluid velocity (Figure 2.8). For instance, a particle orbiting closer to the channel center experiences higher velocity and rapid acceleration changes while the same particle orbiting closer to the channel wall experiences slower velocities and acceleration. Particles can experience velocity and acceleration measurements up to 0.5m/s and 1000m/s^2, respectively. We also found that larger particles occupied the inner orbits closer to the vortex center while smaller particles traveled in outer orbits (Figure 2.7). We observed a similar phenomenon with multiple particles in the vortex traps, where larger particles orbited closer to the vortex center (Figure 2.7).

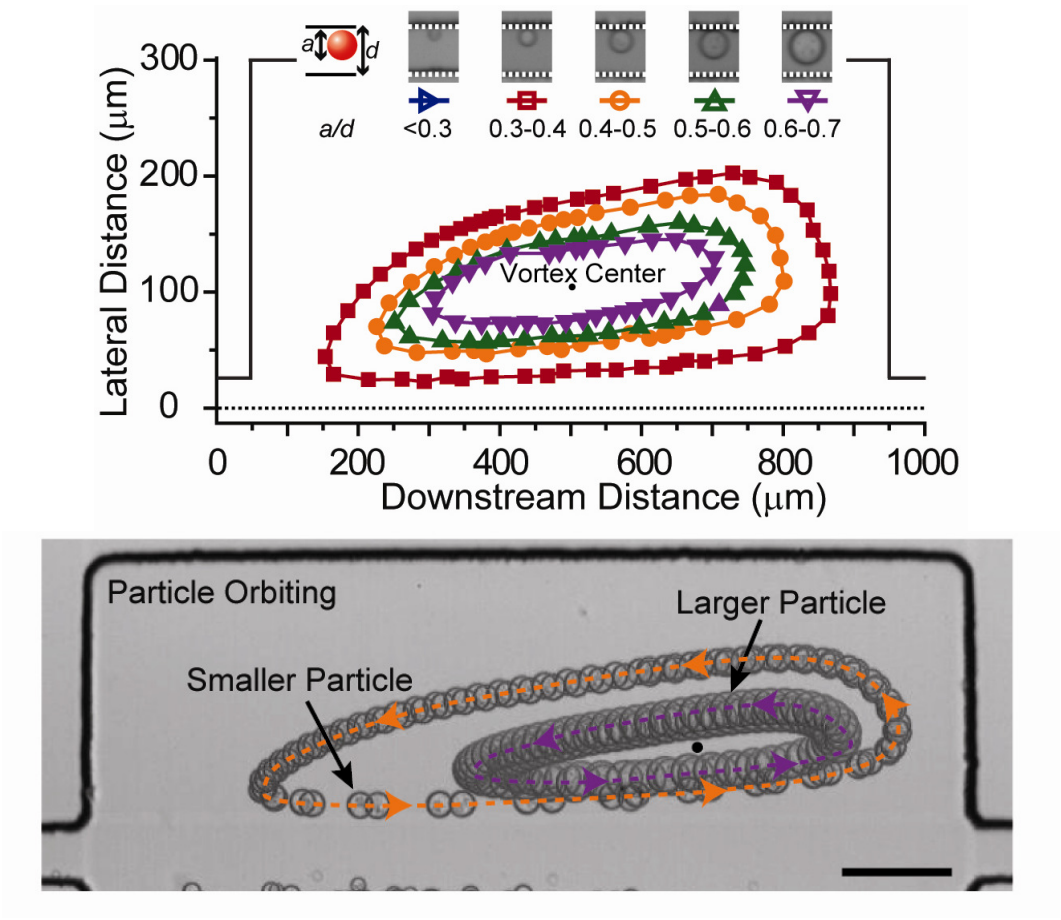

Figure 2.7 Once the particle migrates into the vortex, it occupies an orbit around the vortex center that is dependent on its size. Time-lapse high-speed image of two PDMS particles interacting and traveling in two separate orbits inside a vortex. The larger particle occupies an orbit closer to the vortex center. Elapsed time is ~7 ms.

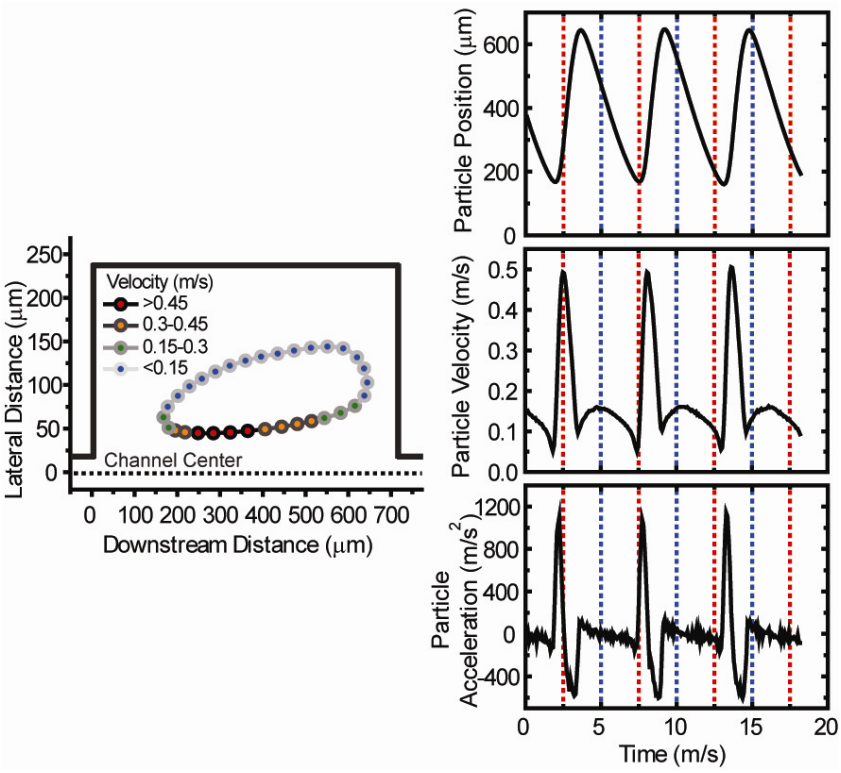

Figure 2.8 Velocity Dependence on Particle Orbit. Particles experienced changes in velocities and accelerations based on the surrounding fluid velocity. Particles can experience velocity and acceleration measurements up to 0.5m/s and 1000m/s^2, respectively.

2.6.1 Balancing Forces Responsible for Particle Trapping

Particle maintenance within the fluid vortex suggests a net balance of forces acting on the particle. Here, we investigate the role of the centrifugal, Saffman, shear gradient lift, and viscous drag forces. The centrifugal force takes place when a particle changes its velocity direction while orbiting. It is defined as:

$$F_{centrifuge} = \frac{(\rho_p - \rho)\pi a^3 v_p^{\ 2}}{6r} \qquad (5)$$

where v_p is the tangential particle velocity, ρ_p is the particle density, a is the particle diameter and r is the radius of the orbit. The Saffman force occurs when there is a mismatch between the particle velocity and the fluid velocity. Theoretically, denser particles should travel at slower speeds and require large forces to catch up with the fluid, while a less dense particle like oil would have little difficulty in maintaining fluid velocity. The shear gradient lift force is defined as Equation 2. The viscous drag force occurs when the particle follows fluid streamlines. The centrifugal and Saffman forces are related to effects of particle inertia, while the shear gradient lift and viscous drag forces are purely determined by the flow velocity profile.

To determine the fluidic forces responsible for particle maintenance, particles of different sizes and densities were individually introduced into the fluid vortex. All three particle materials, both more dense and less dense than the suspending fluid, follow similar orbital trajectories and velocities (Figure 2.9A,B), suggesting particle orbiting is not affected by relative particle density. This was an unexpected behavior as it is well known that particles heavier than the surrounding fluid are ejected out of fluid vortices due to centrifugal force [38]. Furthermore, the maximum velocities of all three particle densities with different particle diameters were plotted with lateral distance from the channel center (Figure 3.9C). The maximum velocity is significant for comparison because it provides information to whether the particle is lagging behind the fluid. The lateral position of interest near the channel center (Figure 2.10C) is important because this region has rapid changes in fluid velocity, providing a fair comparison between particles of different size and density at the same lateral position. Particles do not appear to lag behind the fluid flow since all particle densities have a similar velocity, suggesting that the Saffman force is not a dominant factor in particle maintenance. The centrifugal force is also not responsible for particle maintenance. A simple analysis using the centrifugal and shear gradient

lift equations indicates that a glass particle would experience 30 times larger centrifugal force than a PDMS particle of the same size suggesting that glass particle would occupy an outer orbit compared to the PDMS particle. Particles of similar diameter with different densities occupied a similar orbital pattern with a similar perimeter (Figure 2.9D). Since the denser glass particles do not possess a larger orbit as predicted, this suggests that the centrifugal force is not a dominate force in particle orbiting. Thus, we conclude that the particles orbital pattern is not dependent on particle inertial effects and can only be caused by fluidic velocity profile. Additionally, the viscous drag force can be neglected since particles can self-assemble in different orbits within the fluid vortex based on particle size where larger partticle occupy inner orbites (Figure 2.7). Our unexpected results on how particle density plays a minor role in particle maintenance lead us to logically eliminate potential contributions from particle inertia and Saffman's lift force, suggesting that there remains other factors that can control particle dynamics within the fluid vortex system, such as the dominant shear-gradient lift force seen in other confined systems.

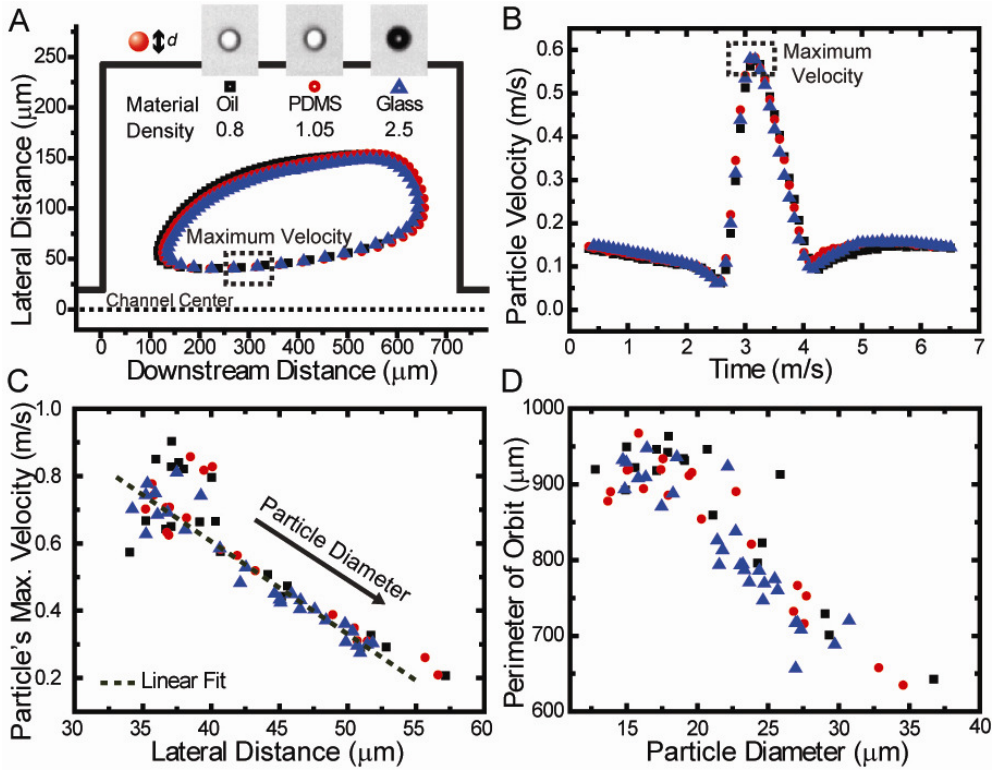

Figure 2.9 Orbit Characteristics are Independent of Particle Density. Using same-sized particles of different densities, oil droplets (0.8g/cm^3), PDMS beads (1.03g/cm^3) and glass beads (2.6g/cm^3), no significant difference was found between (A) orbit size, (B,C) maximum velocity, or (D) orbit perimeter. These results demonstrate that the centrifugal force is not a dominant factor in particle maintenance.

2.6.2 Velocity Curvature Controls Particle Maintenance

The shear-gradient lift force is the dominant force responsible for particle maintenance. The shear gradient lift force is determined by the fluid velocity profile and the particle geometry. In the fluid, particles experience a shear force perpendicular to flow, where the direction of the force is determined by the shear gradient, defined as the second derivative of the velocity. To characterize the behavior of the shear gradient forces on the particle, the fluid velocity line

profile that spans from the channel center through the vortex center to the channel wall were extracted from numerical simulations (Figure 2.10A,B). Admittedly, the simulated velocity profile is not identical to experimental conditions since the simulation models a rigid channel and does not take into account the PDMS deformations found in the vortex chamber [39]. The particle velocities, using similar lateral positions of the numerical line profile, were overlaid with the fluid velocity profiles of two heights at the line profile crossing the vortex center (Figure 2.10C). When a particle orbits closer to the vortex center, it travels at a higher velocity and travels closer to the channel top wall with a particle velocity that matches closer with the fluid velocity at the 13 μm channel height. On the other hand, particles orbiting closer to the channel wall travel slower and experience velocities that match fluid velocities at the 27 μm channel height (Figure 2.10C Inset).

To understand the shear gradient forces involved in particle trapping, we decoupled two regions that experience different shear gradient lift forces. One region, Region I, spans from the channel center to the vortex center (vortex center defined as the position where the fluid velocity is zero/minimum) while the other region, Region II, spans the vortex center to the channel wall. In Region II, particles remain stable in their orbit and follow fluid streamlines, which indicates that the shear gradient force is small compared to the viscous drag force. Region I consists of an inflection point, dividing two velocity profile regions of positive curvature and negative curvature. The positive curvature has the shear gradient force pointing towards the vortex center [32] and is responsible for particle entrance into the fluid vortex. For particles to maintain stability, the negative curvature with the negative shear gradient force should provide the antithesis force acting towards the channel center (Figure 2.10). These two opposing shear

gradient forces are responsible for particle maintenance inside the fluid vortex, suggesting that the velocity profile alone can control particle behavior

To confirm this theory of the negative shear gradient, it is possible to simulate the effects of a particle undergoing negative curvature. This can be created using a straight U-shaped channel to remove the complexities of a fluid vortex system. It is predicted that particles in the negative curvature would move up the shear gradient. This creates an equilibrium position where the particle cannot escape the vortex and prevents the particle from migrating towards the vortex center. Most of the particles lie in the negative curvature region with larger particles closer to the vortex center. This behavior may be a result of the larger shear rate pointing towards the vortex center compared to the smaller opposing force. Additionally, increased flow rate conditions pushes larger particles to outer orbit trajectories [31]. To understand this effect, we mapped the shear rate ratio between region IA and IB where the ratio decreased significantly with higher flow rates. This decrease suggests that particles experience a larger outward force with a shift in the overall equilibrium position. However, smaller particles do not have this similar shift in orbital patterns with increased flow rate as the particle already occupies the stable equilibrium between region IA and IB.

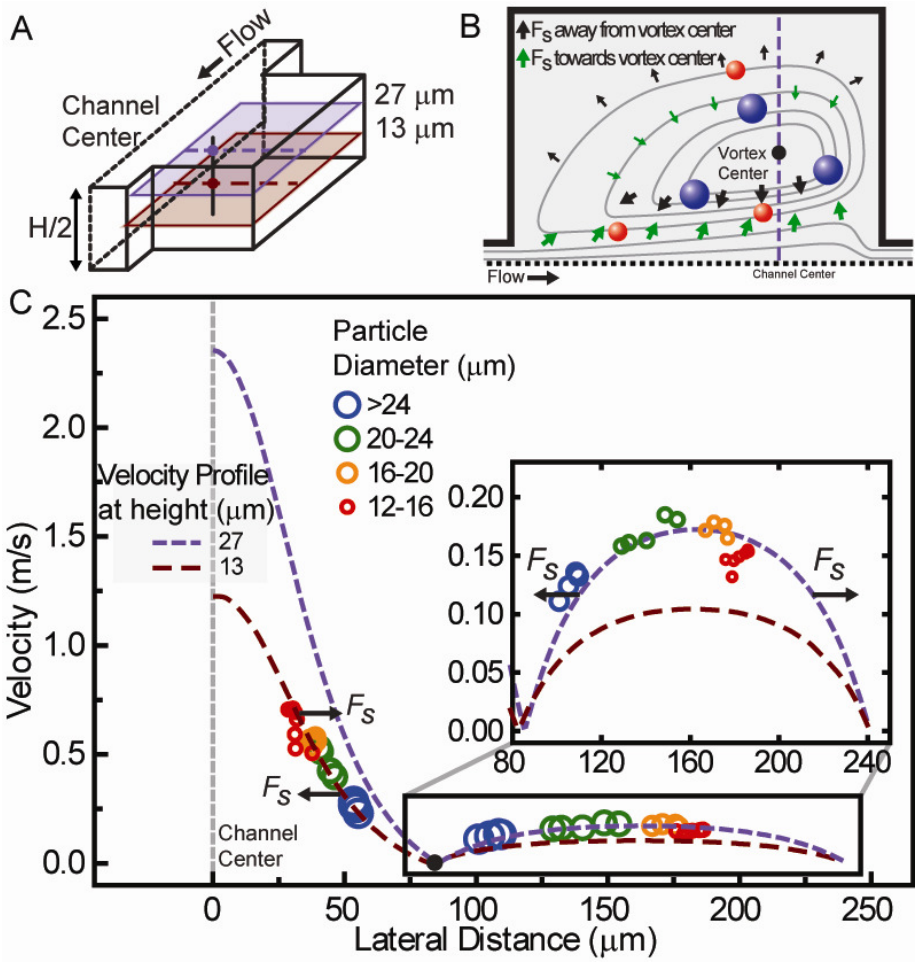

Figure 2.10 Shear Gradient Lift Force (F_S) Alone Can Result in Stable Orbits of Particles in Vortices. (A,B) Schematics of microvortex chamber used in numerical simulation where the velocity line profile (dashed-line) was extracted at H=27μm, 13μm. (B) Schematic showing direction of F_s pointing away and towards the vortex center. (C) Particle velocities (experimental) plotted over fluid velocity line profiles. Particles closer to the channel center experience higher velocity and occupy equilibrium positions closer to the wall (H=13μm) while particles closer to the channel wall are slower with equilibrium position at H=27 μm.

2.7 On-Demand Particle Release

Trapped orbiting particles could be released by changing the flow conditions such that the vortex dissipated (Figure 2.11). This was accomplished by decreasing the input flow rate, which simultaneously reduced the vortex size, allowing particles to escape the vortices into the main channel flow. Thus, particles can be released from the vortex traps on-demand. This serves to be useful for capture and release of target particle and cell populations from a heterogeneous solution (See Chapters 3 and 4). Particle exiting is an interesting phenomenon as it may provide clues on creating more predictable vortex traps. Particle leaving was observed in situations where large quantities of particles crowded the vortex chamber. These particle-particle interactions may induce particles to be bumped out of its stable orbit and trajectory and thereby potentially knock particles into outer orbit or out of the vortex.

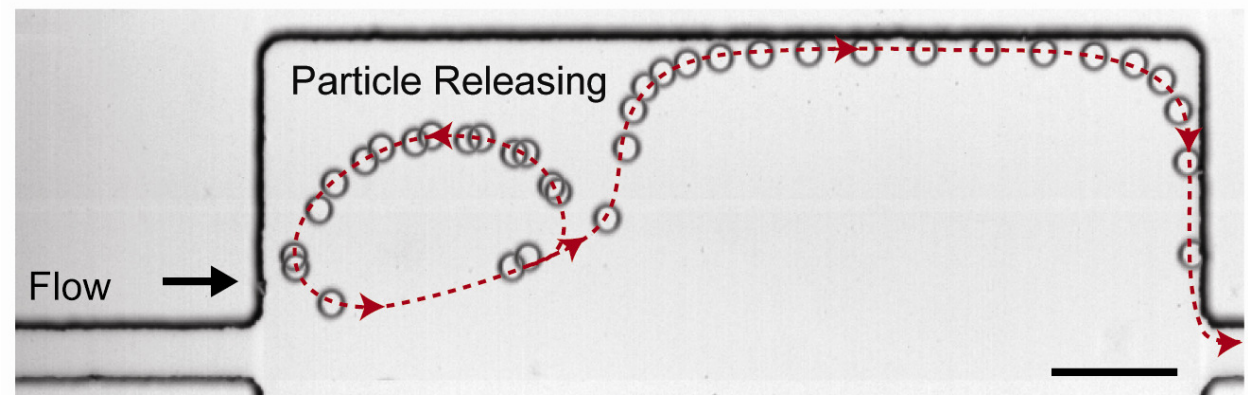

Figure 2.11 On-Demand Particle Release from Vortex Traps. This was accomplished by decreasing the input flow rate, which simultaneously reduced the vortex size, allowing particles to escape the vortices into the main channel flow.

2.8 Designing Deterministic Particle Traps with Microvortices

In order to improve our understanding of particle trapping in microvortices, we developed a model of the capture process which takes into account two critical steps: i) selective particle entry into microvortices from the main flow and ii) particle maintenance within microvortices following entry. Upon investigating particle maintenance, we unexpectedly identified that shear-gradient lift alone can create defined orbits for particles within microvortices, suggesting it is a key component responsible for stable trapping. This insight gives improved intuition for developing far-ranging particle trapping applications by modifying the shape of the velocity field for more predictable vortex trapping systems. For example, building more predictable vortex trapping systems can enable trapping of smaller particles in solution such as bacteria and fungi as a method of water purification. Interestingly, we can also use this information to understand how particles behave in curvature-induced flow even in straight channels [40]. By manipulating the channel dimensions alone, we can engineer velocity flow profiles for precision control of particle dynamics for a variety of applications.

2.9 Acknowledgements

Part of this chapter has been reprinted with minor adaptations with permission from (AJ Mach, JH Kim, A Arshi, SC Hur and D Di Carlo, Automated cellular sample preparation using a Centrifuge-on-a-Chip. *Lab Chip*, 2011, 11, 2827-2834) The Royal Society of Chemistry Copyright 2011. Another part of this chapter is a version of work in preparation for publication. Authors include Elodie Sollier, Xu Yi, Hamed Amini, Derek Go, and Dino Di Carlo.

2.10 References

[1] D. Di Carlo, J. F. Edd, K. J. Humphry, H. A. Stone, and M. Toner, "Particle Segregation and Dynamics in Confined Flows," *Phys. Rev. Lett.*, vol. 102, no. 9, pp. 094503–1 – 094503–4, Mar. 2009.

[2] H. K. Moffatt, "Viscous and Resistive Eddies Near a Sharp Corner," *Journal of Fluid Mechanics*, vol. 18, no. 01, pp. 1–18, 1964.

[3] G. Segre and A. Silberberg, "Radial Particle Displacements in Poiseuille Flow of Suspensions," *Nature*, vol. 189, no. 4760, pp. 209–210, Jan. 1961.

[4] D. Di Carlo, D. Irimia, R. G. Tompkins, and M. Toner, "Continuous inertial focusing, ordering, and separation of particles in microchannels," *Proceedings of the National Academy of Sciences*, vol. 104, no. 48, pp. 18892–18897, Nov. 2007.

[5] J.-S. Park, S.-H. Song, and H.-I. Jung, "Continuous focusing of microparticles using inertial lift force and vorticity via multi-orifice microfluidic channels," *Lab Chip*, vol. 9, no. 7, pp. 939–948, 2009.

[6] D. Di Carlo, J. F. Edd, D. Irimia, R. G. Tompkins, and M. Toner, "Equilibrium Separation and Filtration of Particles Using Differential Inertial Focusing," *Analytical Chemistry*, vol. 80, no. 6, pp. 2204–2211, Mar. 2008.

[7] S. S. Kuntaegowdanahalli, A. A. S. Bhagat, G. Kumar, and I. Papautsky, "Inertial microfluidics for continuous particle separation in spiral microchannels," *Lab Chip*, vol. 9, no. 20, pp. 2973–2980, 2009.

[8] A. A. S. Bhagat, S. S. Kuntaegowdanahalli, and I. Papautsky, "Continuous particle separation in spiral microchannels using dean flows and differential migration," *Lab Chip*, vol. 8, no. 11, pp. 1906–1914, 2008.

[9] A. A. S. Bhagat, S. S. Kuntaegowdanahalli, and I. Papautsky, "Enhanced particle filtration in straight microchannels using shear-modulated inertial migration," *Phys. Fluids*, vol. 20, no. 10, pp. 101702–4, Oct. 2008.

[10] A. A. S. Bhagat, S. S. Kuntaegowdanahalli, and I. Papautsky, "Inertial microfluidics for continuous particle filtration and extraction," *Microfluidics and Nanofluidics*, vol. 7, pp. 217–226, 2009.

[11] J. Seo, M. H. Lean, and A. Kole, "Membrane-free microfiltration by asymmetric inertial migration," *Appl. Phys. Lett.*, vol. 91, no. 3, pp. 033901–3, Jul. 2007.

[12] J. Seo, M. H. Lean, and A. Kole, "Membraneless microseparation by asymmetry in curvilinear laminar flows," *Journal of Chromatography A*, vol. 1162, no. 2, pp. 126–131, Aug. 2007.

[13] J. Wang, Y. Zhan, V. M. Ugaz, and C. Lu, "Vortex-assisted DNA delivery," *Lab Chip*, vol. 10, no. 16, pp. 2057–2061, Aug. 2010.

[14] S. L. Stott, C.-H. Hsu, D. I. Tsukrov, M. Yu, D. T. Miyamoto, B. A. Waltman, S. M. Rothenberg, A. M. Shah, M. E. Smas, G. K. Korir, F. P. Floyd, A. J. Gilman, J. B. Lord, D. Winokur, S. Springer, D. Irimia, S. Nagrath, L. V. Sequist, R. J. Lee, K. J. Isselbacher, S. Maheswaran, D. A. Haber, and M. Toner, "Isolation of circulating tumor cells using a microvortex-generating herringbone-chip," *Proceedings of the National Academy of Sciences*, vol. 107, no. 43, pp. 18392 –18397, Oct. 2010.

[15] Marcos and R. Stocker, "Microorganisms in vortices: a microfluidic setup," *Limnol Oceanogr Meth*, vol. 4, pp. 392–398, 2006.

[16] D. Chiu, "Cellular manipulations in microvortices," *Analytical and Bioanalytical Chemistry*, vol. 387, no. 1, pp. 17–20, Jan. 2007.
[17] J. P. Shelby and D. T. Chiu, "Controlled rotation of biological micro- and nano-particles in microvortices," *Lab Chip*, vol. 4, no. 3, pp. 168–170, 2004.
[18] J. P. Shelby, S. A. Mutch, and D. T. Chiu, "Direct Manipulation and Observation of the Rotational Motion of Single Optically Trapped Microparticles and Biological Cells in Microvortices," *Analytical Chemistry*, vol. 76, no. 9, pp. 2492–2497, May 2004.
[19] J. P. Shelby, D. S. W. Lim, J. S. Kuo, and D. T. Chiu, "Microfluidic systems: High radial acceleration in microvortices," *Nature*, vol. 425, no. 6953, p. 38, 2003.
[20] E. Sollier, M. Cubizolles, Y. Fouillet, and J.-L. Achard, "Fast and continuous plasma extraction from whole human blood based on expanding cell-free layer devices," *Biomed Microdevices*, vol. 12, no. 3, pp. 485–497, Mar. 2010.
[21] M. Khabiry, B. G. Chung, M. J. Hancock, H. C. Soundararajan, Y. Du, D. Cropek, W. G. Lee, and A. Khademhosseini, "Cell Docking in Double Grooves in a Microfluidic Channel," *Small.*, vol. 5, no. 10, pp. 1186–1194, May 2009.
[22] A. P. Sudarsan and V. M. Ugaz, "Multivortex micromixing," vol. 103, no. 19, pp. 7228–7233, May 2006.
[23] T. Karino and H. L. Goldsmith, "Flow Behaviour of Blood Cells and Rigid Spheres in an Annular Vortex," *Philosophical Transactions of the Royal Society of London. Series B, Biological Sciences*, vol. 279, no. 967, pp. 413–445, Jun. 1977.
[24] T. Karino and H. L. Goldsmith, "Aggregation of human platelets in an annular vortex distal to a tubular expansion," *Microvascular Research*, vol. 17, no. 3, pp. 217–237, May 1979.
[25] E. O. Macagno and T.-K. Hung, "Computational and Experimental Study of a Captive Annular Eddy," *Journal of Fluid Mechanics Digital Archive*, vol. 28, no. 01, pp. 43–64, 1967.
[26] T. Petit, L. Zhang, K. E. Peyer, B. E. Kratochvil, and B. J. Nelson, "Selective Trapping and Manipulation of Microscale Objects Using Mobile Microvortices," *Nano Lett.*, 2011.
[27] V. H.-M. Lieu, T. A. House, and D. T. Schwartz, "Hydrodynamic Tweezers: Impact of Design Geometry on Flow and Microparticle Trapping," *Anal. Chem.*, 2012.
[28] B. R. Lutz, J. Chen, and D. T. Schwartz, "Hydrodynamic Tweezers: 1. Noncontact Trapping of Single Cells Using Steady Streaming Microeddies," *Analytical Chemistry*, vol. 78, no. 15, pp. 5429–5435, 2006.
[29] D. Hou and H.-C. Chang, "Electrokinetic particle aggregation patterns in microvortices due to particle-field interaction," *Physics of Fluids*, vol. 18, no. 7, pp. 071702–071702–4, Jul. 2006.
[30] C. M. Lin, Y. S. Lai, H. P. Liu, C. Y. Chen, and A. M. Wo, "Trapping of Bioparticles via Microvortices in a Microfluidic Device for Bioassay Applications," *Analytical Chemistry*, vol. 80, no. 23, pp. 8937–8945, Dec. 2008.
[31] D. S. W. Lim, J. P. Shelby, J. S. Kuo, and D. T. Chiu, "Dynamic formation of ring-shaped patterns of colloidal particles in microfluidic systems," *Appl. Phys. Lett.*, vol. 83, no. 6, pp. 1145–1147, 2003.
[32] D. Di Carlo, "Inertial microfluidics," *Lab Chip*, vol. 9, no. 21, pp. 3038–3046, 2009.
[33] S. C. Hur, H. T. K. Tse, and D. D. Carlo, "Sheathless inertial cell ordering for extreme throughput flow cytometry," *Lab Chip*, vol. 10, no. 3, pp. 274–280, 2010.

[34] J. F. Edd, D. Di Carlo, K. J. Humphry, S. Koster, D. Irimia, D. A. Weitz, and M. Toner, "Controlled encapsulation of single-cells into monodisperse picolitre drops," *Lab Chip*, vol. 8, no. 8, pp. 1262–1264, 2008.
[35] K. J. Humphry, P. M. Kulkarni, D. A. Weitz, J. F. Morris, and H. A. Stone, "Axial and lateral particle ordering in finite Reynolds number channel flows," *Phys. Fluids*, vol. 22, no. 8, p. 081703, 2010.
[36] E. S. Asmolov, "The inertial lift on a spherical particle in a plane Poiseuille flow at large channel Reynolds number," *Journal of Fluid Mechanics*, vol. 381, pp. 63–87, Feb. 1999.
[37] W. Lee, H. Amini, H. A. Stone, and D. Di Carlo, "Dynamic self-assembly and control of microfluidic particle crystals," *Proceedings of the National Academy of Sciences*, vol. 107, no. 52, pp. 22413 –22418, Dec. 2010.
[38] S. I. Green, *Fluid Vortices*. Springer, 1995.
[39] E. Sollier, C. Murray, P. Maoddi, and D. Di Carlo, "Rapid prototyping polymers for microfluidic devices and high pressure injections," *in-revision*.
[40] D. R. Gossett, H. T. K. Tse, J. S. Dudani, K. Goda, T. A. Woods, S. W. Graves, and D. Di Carlo, "Inertial Manipulation and Transfer of Microparticles Across Laminar Fluid Streams," *Small*, p. n/a–n/a, 2012.

Chapter 3

Isolation of Circulating Tumor Cells Using Microscale Vortices

3.1 Introduction

A blood-based, low cost alternative to radiation intensive CT and PET imaging is critically needed for detection of cancer and for management of its treatment. A non-invasive diagnostic that can be repeated regularly to provide up to date molecular information about the cancer would open up key opportunities for personalized therapies. For example, regular blood-based "biopsies" of the cancer after resection/chemotherapy can indicate if the residual cancer is relapsing, or more importantly, is susceptible or has become resistant to specific chemotherapeutics. In effect, if these clinical needs are met, cancer could become a managed disease similar to HIV, in which drugs regimens are started or modified only when viral loads or CD4+ T cell counts reach critical levels. Additionally, if sensitivity and specificity is high enough a blood-based diagnostic might make it possible to detect cancer early in pre-symptomatic patients besides those who are at risk for relapse with a simple noninvasive blood test, leading to a decrease in cancer deaths.

An approach for cost-effective enrichment, enumeration and molecular analysis of circulating tumor cells (CTCs) from large volumes of blood may address these unmet needs. CTCs are thought to play a role in metastasis where cells shed from a solid tumor, enter the bloodstream, and land in secondary sites to form metastases. CTC number has been shown to be predictive of cancer prognosis and may suggest more or less aggressive treatment regimes [1]. However, isolating viable CTCs from blood in a quick, effective and label-free approach remains a significant technical challenge – CTCs are rare events at rates as low as one cell per one billion blood cells [1], [2]. Studies have shown that patients have poor prognosis with 5 or more CTCs per 7.5 mL of blood [1]. While the gold standard and emerging technologies focus on enumeration of CTCs for diagnostics [3], there is a critical need for gathering larger sample sizes of viable CTCs for research purposes [4]. This requires processing large blood volumes with higher throughputs and enriching target cells without the attachment to modified substrates or magnetic beads, providing an advantage for individually selecting captured cells for further analysis or culture.

3.1.1 Gold Standard in CTC Isolation

The gold-standard in CTC enumeration technology is the CellSearch system from Veridex. This system requires that cells are first immuno-magnetically separated from the rest of the blood using anti-EpCAM (Epithelial Cell Adhesion Molecule) conjugated magnetic nanoparticles that bind to EpCAM that is presumed to be present on carcinomas (which are of epithelial origin). Captured cells are then fixed and labeled with fluorescent antibodies a second time to increase the specificity of the assay. Cancer cells are positively identified if they stain positive for a cytokeratin stain (CK) and negative for CD45 (a leukocyte marker). Automated imaging of a

smear of these captured cells is time intensive and cells cannot be further analyzed for molecular markers or growth. Still, this test is very reliable for enumerating CTCs from blood and is FDA-approved for prognostic applications, where increased CTC number is correlated with a poor prognosis.

3.1.2 Emerging technologies in CTC Isolation

A variety of alternative technologies have emerged to isolate and enumerate CTCs. These technologies take advantage of cellular biomarkers for capturing CTCs such as surface markers or cell size [5]. The following CTC isolation technologies are mentioned for their advanced research stage of using clinical samples.

Chief amongst these, now in clinical studies, is the CTC-chip technology from Mass. General Hospital [6–8]. These chips operate on the principles of affinity chromatography, such that cells with EpCAM coated surfaces preferentially adhere to the high device surface area. Anti-EpCAM is immobilized on the chip surfaces and blood is flowed through the device at a controlled rate to maximize specific binding. A major challenge is that currently cells cannot be easily removed from the non-transparent microchannel surfaces once attached, limiting the quality of immunofluorescent images and not ideal for cytopathology examination.

The FAST (Fiber Array Scanning Technology) approach from the Palo Alto Research Center (PARC) and the Kuhn group at Scripps addresses this by imaging stained CTCs amongst all other nucleated cells on a smeared slide [9–14]. The approach uses arrayed fibers to collect more optical data per unit time than conventional automated microscopy used to image the CTC-chips. However, because of the large background of leukocytes, specificity can be an issue and pure cancer cells cannot be obtained for molecular analysis.

The MagSweeper technology uses immunomagnetic capture similar to the CellSearch system, however, the capture technology has been optimized to work on larger volumes and to increase sensitivity. Still the approach results in cells attached to beads and those are not viable and must be imaged separately. Again the costs for the multiple antibodies used are high.

Finally, size-based filtration of CTCs is perhaps the simplest technique and has been successfully demonstrated by two groups [15], [16], [17]. Because CTCs are larger than normal blood cells they can be filtered from blood with a microfabricated filter with precisely controlled and uniform pore size and eluted from the filter after processing. However, because of the large deformability of these cells, Cote has described that it is necessary to fix (i.e. crosslink proteins within) cells prior to filtration. Thus cells that are recovered are not viable. Additionally, cells are not easily recovered from the membranes or imaged on the membranes.

3.2 Centrifuge Chip

3.2.1 Advantages

We improve the operational criteria for CTC isolation by using cutting-edge inertial hydrodynamic separation technology that can isolate larger CTCs from mixed blood populations. This reagentless approach functions by enriching CTCs from blood at high throughput using a massively parallel filtration technique that uses laminar vortices combined with inertial focusing [18–20]. The technology, called the Centrifuge Chip, is tailored to gently and reversibly trap larger CTCs based on size. We branded the Centrifuge Chip name since it can perform all the operations of a standard bench top centrifuge, such as solution exchange, cell concentration, and cell separation, but accomplished on a lab-on-a-chip (Figure 3.1).

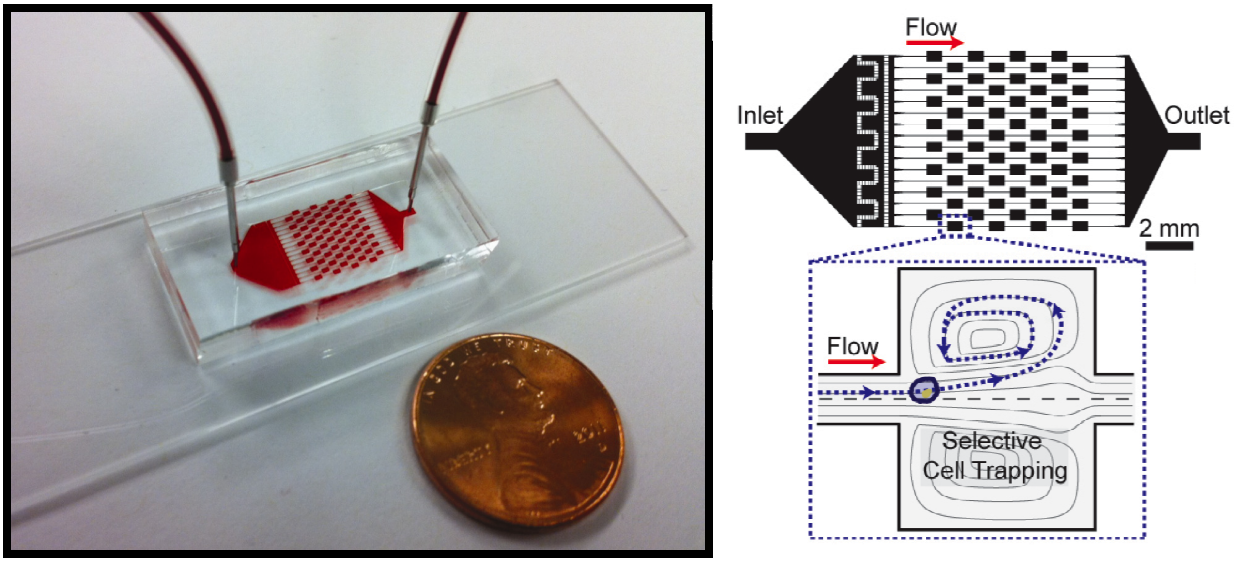

Figure 3.1 A photograph demonstrating the small footprint of the Centrifuge Chip and a schematic of the massively parallel device that employs microscale fluid vortices in each reservoir for selectively trapping cancer cells from whole human blood.

A critical feature of the technology is the ability to size-selectively isolate CTCs in the vortices while smaller RBCs and WBCs pass un-trapped through and flow downstream to a waste reservoir. This is because CTCs have been shown to be 2-3X larger than normal blood cells (Figure 4.2). Circulating lung cancer cells for example were found to be >2X larger than WBCs [21], while circulating malignant breast cancer cells were observed to be >3X larger than WBCs [22]. This allows for the concentration of cells of interest into a smaller volume of fluid (without an overwhelming background of RBCs and WBCs) such that they can be directly analyzed using standard cytological staining techniques that pathologists are familiar with (thus more likely to be adopted by this important stakeholder). Size-selective operation is due to differences in inertial lift forces for different sized particles such that shear-gradient lift scaling

with particle diameter cubed [18] leads to differences in cross-stream migration and entry into laminar vortices. Another key aspect of the system is that it can be easily parallelized to operate at high throughputs and process blood at rates up to 6 mL/min in the current design. A third key feature is that since cells are not attached to surfaces or magnetic beads, or chemically fixed, cells can be simply released for further analysis or culture. In order to remove uncaptured RBCs and WBCs within reservoirs and other dead-spaces we have developed a unique flushing procedure with phosphate buffered saline solution, which operates at the flow rates necessary to maintain vortices. Notably, this flushing procedure that is implemented after capture of cancer cells in the vortices does not lead to appreciable loss of cells

3.2.2 Device Design and Fabrication

The Centrifuge Chip device is designed to handle large liquid volumes and rapid processing times. This was accomplished by arraying the vortex traps in series and parallel and yet maintained the fundamental mechanics of cell trapping in the fluid vortices. In the original design, the Centrifuge Chip was composed of 64 chambers with 8 channels and 8 chambers in each channel. This design was used for collecting data with the syringe pump setup and collecting data with spiked blood samples. To handle large liquid volumes of up to 500 mL, we developed a fluidic pressure system that drives fluid with compressed air and controlled with Labview software. We also designed an improved device that was able to withstand high fluidic pressures from this new setup. In this new design, we significantly shortened the total channel length upstream of the vortex chambers to reduce fluidic resistance. Notably, shortening of the channel did not affect cell trapping in the fluid vortices which demonstrates that inertial focusing

may not be important. This may be a result of cell-cell interactions that disturb the flow dynamics preventing cells to reach equilibrium positions within the channel.

Centrifuge Chip device is connected to a custom-made pressure system that delivers biofluid samples or saline wash from pressurized glass bottles through the Centrifuge Chip. The Labview-controlled system contains a pair of air regulators, air valves and liquid valves that brings compressed air into the bottles and drives fluid through the microchip device. Effusion samples are placed into the pressurized glass bottle and introduced through the device at a flow rate of ~6 mL/min. Once the vortex traps were filled with cells, PBS was introduced into the device to wash out untrapped blood cells in the main flow and the vortex traps. Cells trapped in the fluid vortex were removed by reducing the input air pressure and subsequently released in a collection tube. We implement a 'trap-and-release' program that can continuously introduce sample through the Centrifuge Chip, wash, and release the captured cells into a microtiter plate.

Devices were fabricated using standard lithography techniques. Briefly, KMPR 1050 (Microchem) was spun at 1800 rpm for 30 s to create a 70 μm-thick layer on a 10-cm silicon wafer. The pattern was photolithographically defined in this layer by using a Mylar mask printed at 40,000 dpi. After development, polydimethylsiloxane (PDMS) (Sylgard 184 Dow Corning Corp.) was poured onto the photoresist master at a 10:1 ratio of base to crosslinker, degassed in a vacuum chamber, and cured at 65^{o}C overnight. The devices were then cut from the mold, ports were punched with a punch kit (Technical Innovations), and the devices were bonded to glass slides using oxygen plasma for 30 s (Harrick Plasma). After plasma treatment and placement onto the glass substrate, the devices were maintained at 65^{o}C in an oven for 15 min to increase bonding. PDMS microchip devices were mounted onto the stage of an inverted fluorescent microscope (Nikon TE2000-U).

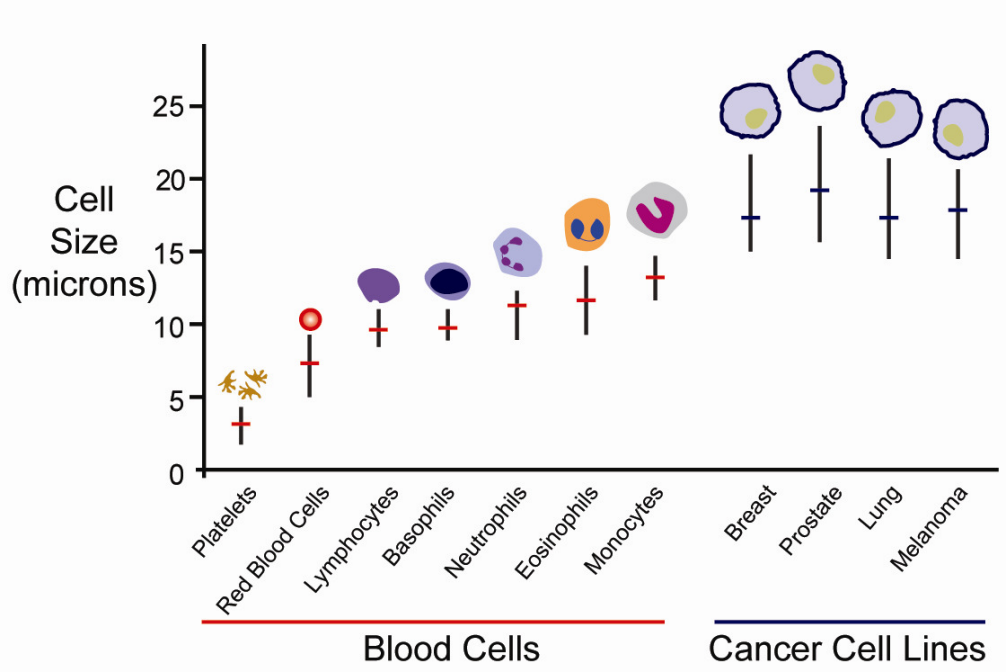

Figure 3.2 Size-Based Isolation of Cancer Cells from Blood Cells. Breast, lung, prostate, and melanoma cancer cells (>15 μm) cultured in the laboratory were measured to be larger than blood cells (2-15 μm). Circulating lung cancer cells were reported to be >2X larger than WBCs [21].

3.3 Experimental Methods

3.3.3 Cell Culturing, Labeling, Imaging and Analysis

Cells were imaged after collection into the smaller volume on the well plate to collect information about capture efficiency, enrichment, and purity. Each well of a 96-well plate was used to collect captured cells from one blood sample and contained ~200 μL liquid volume. To determine the cell population, leukocyte, epithelial and nuclear stains were used. After centrifuging the cells to the bottom of the well with a plate centrifuge (Refer to Dan's machine), the supernatant was aspirated. Cells were treated with 4% v/v formaldehyde for 15 min, permeabilized with 0.4% v/v Triton X-100 (Sigma-Aldrich) for 7 min, and incubated with CK-PE, DAPI, CD45-FITC (Invitrogen). in 2% w/v BSA. Between each step, cells were sedimented with the centrifuge and washed with PBS. After staining, the cells were imaged using a Photometrics CoolSNAP HQ2 CCD camera mounted on a Nikon Eclipse Ti microscope. The whole well was automatically imaged in a few minutes (100X) using an ASI motorized stage operated with Nikon NIS-Elements AR 3.2 software. Captured images were automatically obtained for four configurations: brightfield, FITC, TRITC and DAPI filter sets. Collected images were automatically stitched together using the NIS-Elements Software. Images were analyzed by enumerating the number of cells present in the well.

MCF7 breast cancer cells (ATCC) were cultured in media containing DMEM supplemented with 10% FBS, 1% bovine insulin, and 1% penicillin/streptomycin (Invitrogen). Cells were typically passaged every 4 days. Single and clustered cells were made by incubation for less time with trypsin, 1-2 minutes, in room temperature before neutralizing trypsin with media and resuspending cells in PBS. Blood samples were obtained by venous puncture of

healthy human volunteers by a trained physician. Blood was collected in EDTA tubes and used within 48 h.

Experiments involving rare cell isolation required diluting blood with PBS to 5% to 20% v/v followed by spiking of known amounts of cancer cells. Cancer cell number and concentration was determined by transferring a 100 μL volume of cell solution using a micropipette into a 96-well microtiter plate. After waiting for10 min for the cells to sediment, three wells were imaged using fluorescence microscopy to count the number of cells. The average value was taken as the cell spiking concentration. 100 μL of cell solution was spiked into each blood sample for cell capture efficiency, enrichment and purity experiments described below. Typically, there were about ~500 cells spiked in each 0.5 mL of whole human blood diluted with 9.5 mL PBS. Capture efficiency, enrichment and purity experiments required pre-labeling cancer cells with fluorescent dye (CellTracker Blue, Invitrogen). Blood samples were incubated with CD45-FITC (Invitrogen).

3.3.4 Implementation of the Centrifuge Chip

The Centrifuge-on-a-Chip was applied to separating and concentrating cancer cells (diameter of 20 μm) from normal human blood cells (diameters range from 2 to 15 μm) to demonstrate utility for size-based enrichment and concentration in a high-throughput manner (Figure 3.2). Fluorescently-labeled breast cancer cells (MCF-7) spiked into diluted human blood was injected into the Centrifuge-on-a-Chip device at 4.4 mL/min. At these high flow rates channel deformation is observed in the upstream vortex reservoirs [23], however trapping is not significantly impacted given that downstream vortex chambers operating closer to ambient pressure remain undeformed. Higher operational flow rates are instead limited by bond strength.

Spiked MCF-7 cells included single cells and 2-4 cell clusters, as clustered cells have been shown to be present at significant levels in clinical samples [7]. Blood and cancer cells were observed to enter and orbit in the vortices during the injection step (Figure 3.3). Red blood cells were observed to enter vortices even though particles of similar size did not migrate into vortices in experiments with dilute samples. Likely, the high cell concentration induces collisions and hydrodynamic disturbances between cells that lead to cross-stream migration and entrance into vortices. Additionally, there is a maximum capacity of cells each vortex chamber can maintain. After the vortex occupies the entire reservoir a maximum of ~40 single MCF7 cells can be maintained over a range of higher flow rates. For most spiking experiments we operated at conditions well below this maximum. Once the solution was completely processed, the vortex-trapped cells were "washed" with PBS without disrupting the vortices. Interestingly, we observed that blood cells that initially entered the vortex were not stably trapped and quickly exited from the traps and out of the system leaving only the larger stably trapped cancer cells orbiting. In agreement with our model, red and white blood cells have both higher density and/or smaller size, and therefore cannot form stable orbits. Washed cells were released into one well of a 96-well-plate for characterization and enumeration.

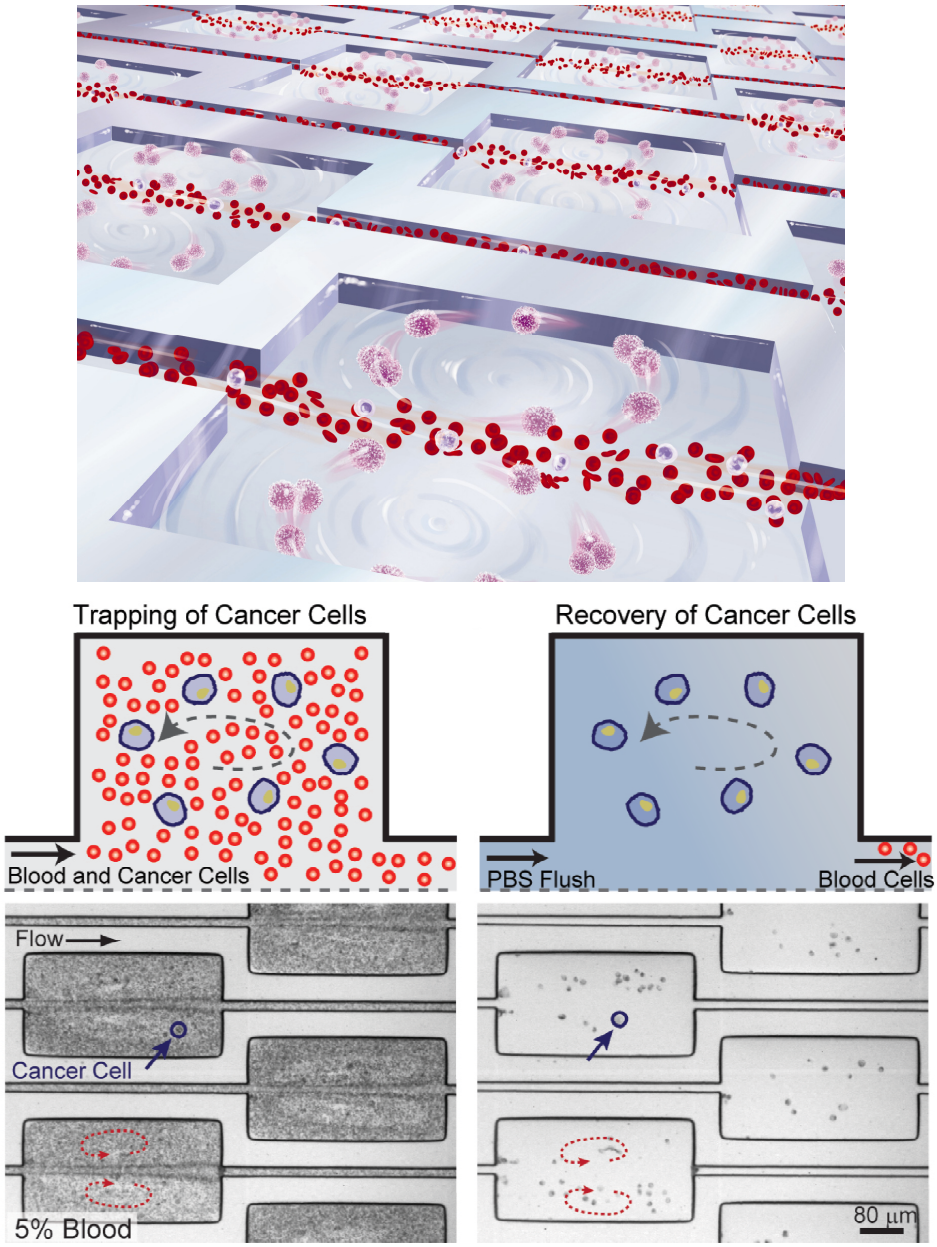

Figure 3.3 Mechanism of Cancer Cell Trapping in the Centrifuge Chip. An artist rendering of the Centrifuge Chip that employs microscale vortices for selective trapping of cancer cells from human blood. A schematic of the operations of the Centrifuge Chip where (i) a spiked blood sample is injected into the microchip causing blood and cancer cells to enter the fluid vortices,

and (ii) once the blood solution has been flowed through, a wash step is performed to remove smaller and denser blood cells while maintaining the vortices and trapped cancer cells.

3.4 Cancer Cell Isolation from Spiked Blood Samples

The Centrifuge Chip system performs well when quantifying key metrics for target cell concentration, enrichment, and purity. 10 mL volume blood samples ($n \geq 6$ samples) of 5% v/v blood (i.e. 0.5 mL whole blood or ~2.5 billion blood cells) spiked with ~500 cancer cells were concentrated to a final volume of less than 200 μL (20-fold volumetric concentration) with relatively little blood cell contamination in <3 min (Figure 3.4, Table 3.1). This corresponds to an enrichment ratio (the ratio of target cancer cells to contaminant blood cells in the output divided by the same ratio in the input solution) of 3.4 million (Figure 3.5). This high level of enrichment leads to high purity of the cancer cells in the 200 μL final volume: ~40% (Figure 3.5, an average of 102 ± 21 cancer cells, and 221 ± 155 blood cells). Blood samples without spiked cancer cells ($n = 3$) that were processed with Centrifuge-on-a-Chip and collected in the well were found to have 772 ± 283 red blood cells and 4 ± 1 CD45+ white blood cells, which is similar to the amount of blood cell contaminants found in the microwells using spiked blood samples. The level of enrichment achieved is comparable to molecular affinity-based and filter-based approaches for target cell separation which have reported enrichments from 1 million [6] to 10 million [16]. The purity of our processed sample is high when compared to affinity-based approaches which report purities of spiked cancer cells of 9.2-14.0% [7]. Reducing the dilution of blood in processed samples leads to increases in cell-processing throughput, but also results in reduced capture efficiency of spiked cells. We recovered 10-20% of the spiked cancer cells, with

decreasing capture efficiency with increasing blood concentrations (Figure 3.5). Higher blood concentrations lead to higher fluid viscosities which modify the fluid vortex size and position, resulting in lower trapping efficiency. This relatively low capture efficiency suggests that in order for this technique to be useful in isolating ultra-rare cells occurring at 1-10 cells/mL, a large volume of blood must be processed (10 mL or more). However, the high throughput of our approach (~5 mL/min of diluted blood for a 2 cm^2 chip) indicates that operation on large volumes in a reasonable time period (< 30 minutes) is achievable.

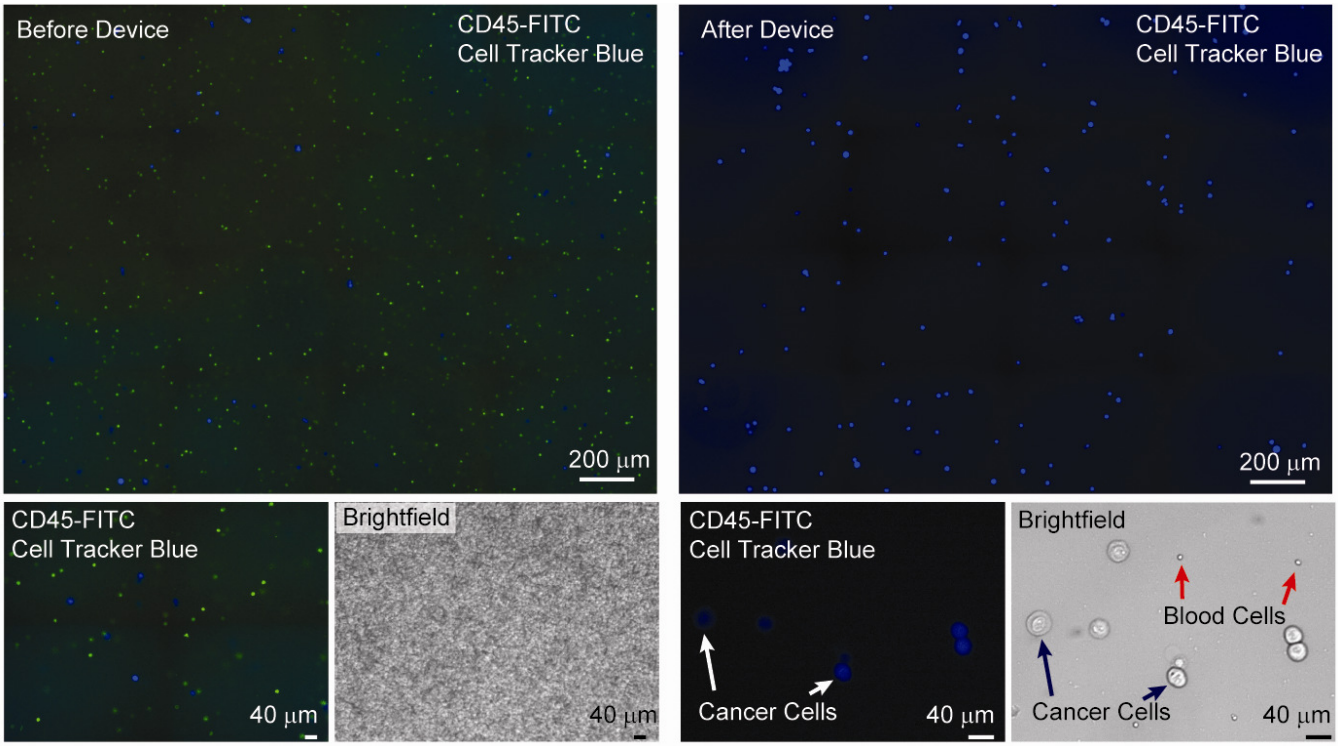

Figure 3.4 Centrifuge Chip Offers High Enrichment and Purity. Wide-field fluorescent and brightfield images of cancer cells (labeled with Cell Tracker Blue), red blood cells and white blood cells (labeled with CD45-FITC) shown before and after processing of blood through the Centrifuge Chip.

Spiked (Input)		Recovered (Output)			Metrics		
Cancer cell	**RBC & CD45+**	**Cancer cell**	**RBC**	**CD45+**	**Efficiency (%)**	**Enrichment**	**Purity (%)**
146	~2,500,000,000	31	-	-	21.2	-	-
146	~2,500,000,000	25	-	-	17.1	-	-
146	~2,500,000,000	27	-	-	18.5	-	-
423	~2,500,000,000	93	-	-	22.0	-	-
423	~2,500,000,000	88	-	-	20.8	-	-
423	~2,500,000,000	93	-	-	22.0	-	-
972	~2,500,000,000	119	39	-	12.2	7851178	75.3
972	~2,500,000,000	189	197	-	19.5	2468594	48.9
972	~2,500,000,000	157	231	-	16.2	1748800	40.4
342	~2,500,000,000	89	498	3	28.7	1431563	16.4
342	~2,500,000,000	72	203	5	21.0	2533327	25.7
342	~2,500,000,000	84	137	4	24.6	4359958	37.3
				AVG	***20.3***	***3398902***	***40.7***
				STDEV	***4.17***	***2406423***	***20.5***

Table 3.1 Counts for spiked and recovered cancer and blood cells. Calculated metrics include efficiency, enrichment, and purity.

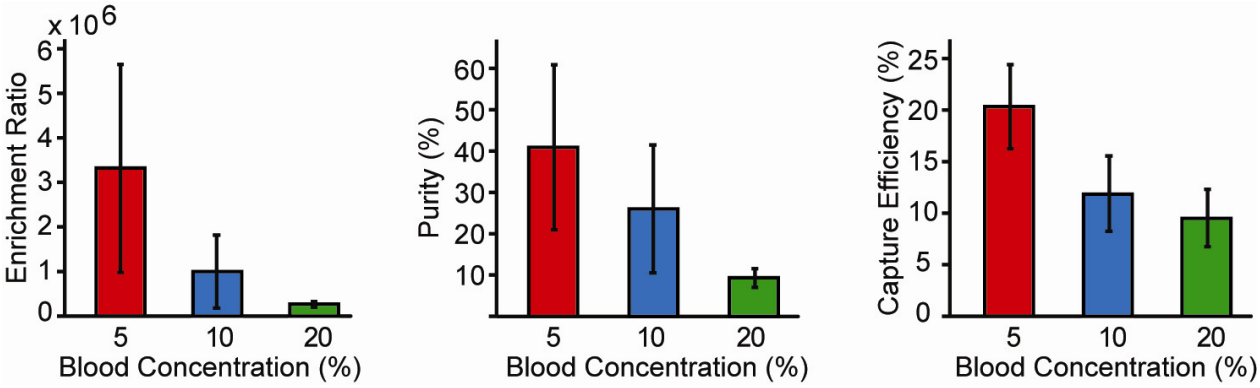

Figure 3.5 Centrifuge Chip Metrics. Capture efficiency, enrichment, and purity data for MCF7 cells spiked into 5-20% diluted blood (~500 cells/mL whole blood) and processed on the Centrifuge Chip indicates the ability to concentrate cancer cells while rejecting other blood cells at clinically useful levels.

Cells captured in the device maintained high levels of viability. We observed no significant changes in cell viability (90.1% vs. 90.3% initial) after injecting cells through the Centrifuge-on-a-Chip as determined by a fluorescent live/dead assay. Cells exposed to similar flow in a microfluidic device were also not shown to have significant changes in gene expression. Viable cells may be important for some sample preparation applications of the Centrifuge Chip [7]. Cells captured and released from the Centrifuge-on-a-Chip system are available for standard molecular assays such as immunostaining. As a proof of concept, unlabeled spiked blood samples were enriched with the chip. Cancer cells were then released and labeled in a microwell. Cancer cells stained positive for Cytokeratin-PE and DAPI and negative for CD45. This ability to enrich on one platform but transfer cells in a small volume for further processing offers significant advantages for rare single cell analysis.

While the Centrifuge Chip offers relatively low capture efficiency compared to other emerging technologies, reprocessing of the blood sample enables harvest larger quantities of cancer cells. Performing serial runs is possible since the Centrifuge Chip system can process 10 mL whole human blood diluted to 5% v/v (total volume of 200 mL) with a flow rate of 6 mL/min for a total processing time of 33 min. Blood samples were spiked with breast, lung, and prostate cancer cells at clinically relevant cell concentrations into dilute human blood and processed three times (Figure 3.6, Figure 3.7). Additional cancer cells were captured with each additional run, demonstrating that large quantities can be captured from one sample. Interestingly, a spiking concentration of 10 cells/mL had the highest capture efficiency, suggesting that the Centrifuge Chip is specialized for rare cell capture. To ensure vortex trapping, a total of 100 20 μm beads was introduced into each sample as a control. Typically, 30% the beads were recovered.

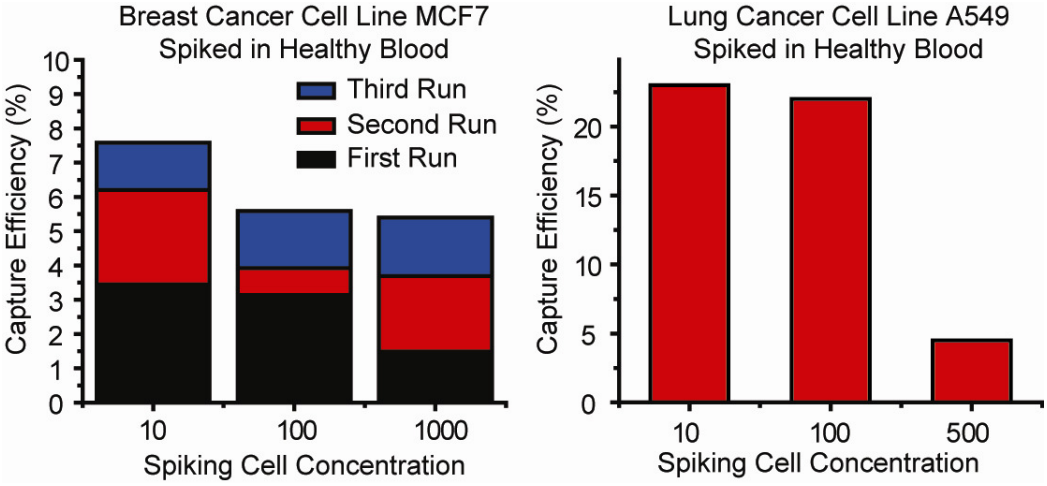

Figure 3.6 Capture Efficiency of Blood Samples Spiked with Lung and Breast Cancer Cell Lines.

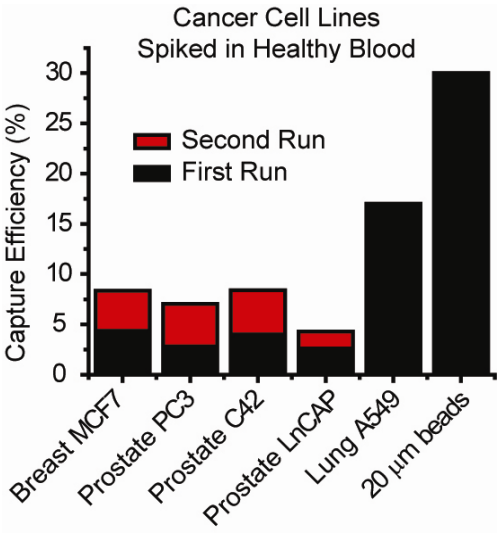

Figure 3.7 Capture Efficiency of Spiked Blood Samples. Breast, prostate, and lung cancer cell lines were spiked into healthy human blood at 100 cells/mL and processed twice with the Centrifuge Chip. The 'waste' of the first run was introduced through the device as the second run. To ensure vortex trapping, a total of 100 20 µm beads was introduced into each sample as a control.

3.5 CTC Isolation from Clinical Patient Blood Samples

To further validate the Centrifuge Chip, we obtained clinical patient blood samples from the Department of Radiation Oncology and the Department of Hematolgy and Oncology of the Geffen School of Medicine at UCLA. Up to 10 mL of blood was harvested from nine Stage IV clinical patients diagnosed with various cancers and processed with the Centrifuge Chip system. After blood processing, isolated cells were stained with anti-Cytokeratin PE, anti-CD45 FITC, and DAPI. The captured cells were imaged and analyzed with fluorescence microscopy. Putative CTCs were captured in 4 of the 9 patient samples (44%) (Figure 3.8). Two of the four positive patient samples were diagnosed with prostate cancer, demonstrating that future studies

should target prostate cancer patients. In patient 1, putative CTCs were stained positive for anti-PSA (Figure 3.9). A clumped cell was captured with the Centrifuge Chip in patient #6 diagnosed with thyroid cancer.

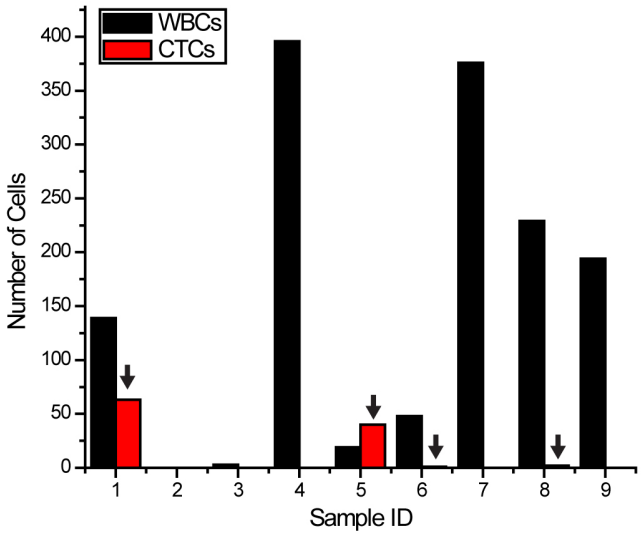

Patient ID	Diagnosis	CTC	WBC
1	Prostate	63	139
2	Lung	0	0
3	Bladder	0	3
4	Rhabdomyosarcoma	0	396
5	Neck of Bladder	40	19
6	Thyroid	1	48
7	Thymus	0	376
8	Prostate	2	229
9	Head & Neck Squamous	0	194

Figure 3.8 Isolation of CTCs from Stage IV Clinical Patient Blood Samples. Putative CTCs were collected and analyzed in 4 of 9 patient samples (44%). Two positive samples were from patients diagnosed with Prostate, one from Neck of Bladder patient, and one from Thyroid patient.

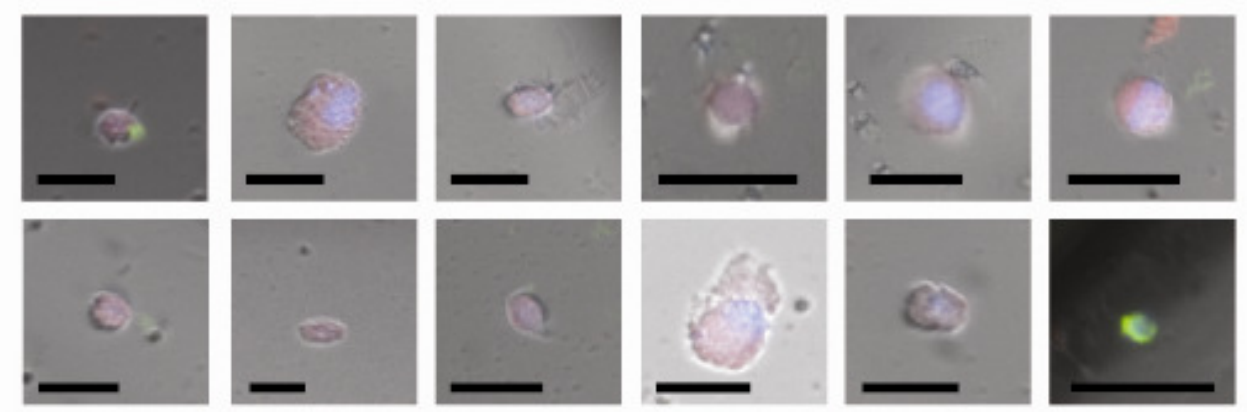

Figure 3.9 Gallery of Putative Circulating Tumor Cells from Patient Blood Samples. CTCs were harvested from a Stage IV patient diagnosed with prosate cancer. CTCs are labeled with PSA (red) and DAPI (blue) and negative for CD45 (green).

3.6 Conclusions

The Centrifuge Chip has potential to be a revolutionary tool for translational research and diagnostics. It has advantages in 1) processing large volumes beyond the standard 7.5 mL of blood to be able to harvest larger quantities of CTCs, 2) screening one sample in 30 min compared to gold standard of 4-6 hrs, 3) and providing CTCs freely available in solution in a concentrated volume for molecular analysis.

3.7 Acknowledgements

We acknowledge Rajan Kulkarni MD PhD of the Department of Dermatology, Julie Jung Kang MD PhD, Nicholas Nickols MD PhD, and Niraj Mehta MD of the Department of Radiation Oncology, and Jonathan Goldman PhD of the Department of Hematology and Oncology, for obtaining patient samples. This work was supported by IRB# 11-001798. We also thank the

Coulter Foundation for funding. This chapter is a version of work in preparation for publication.

Authors include Derek Go, Ish Talati, Rajan Kulkarni, and Dino Di Carlo.

3.8 References

[1] M. Cristofanilli, G. T. Budd, M. J. Ellis, A. Stopeck, J. Matera, M. C. Miller, J. M. Reuben, G. V. Doyle, W. J. Allard, L. W. M. M. Terstappen, and D. F. Hayes, "Circulating Tumor Cells, Disease Progression, and Survival in Metastatic Breast Cancer," *N Engl J Med*, vol. 351, no. 8, pp. 781–791, Aug. 2004.
[2] J.-M. Hou, M. Krebs, T. Ward, K. Morris, R. Sloane, F. Blackhall, and C. Dive, "Circulating Tumor Cells, Enumeration and Beyond," *Cancers*, vol. 2, no. 2, pp. 1236–1250, Jun. 2010.
[3] B. Mostert, S. Sleijfer, J. A. Foekens, and J. W. Gratama, "Circulating tumor cells (CTCs): Detection methods and their clinical relevance in breast cancer," *Cancer Treatment Reviews*, vol. 35, no. 5, pp. 463–474, Aug. 2009.
[4] Z. S. Lalmahomed, J. Kraan, J. W. Gratama, B. Mostert, S. Sleijfer, and C. Verhoef, "Circulating Tumor Cells and Sample Size: The More, the Better," *Journal of Clinical Oncology*, vol. 28, no. 17, pp. e288 –e289, Jun. 2010.
[5] J. Chen, J. Li, and Y. Sun, "Microfluidic approaches for cancer cell detection, characterization, and separation," *Lab on a Chip*, vol. 12, no. 10, p. 1753, 2012.
[6] S. Nagrath, L. V. Sequist, S. Maheswaran, D. W. Bell, D. Irimia, L. Ulkus, M. R. Smith, E. L. Kwak, S. Digumarthy, A. Muzikansky, P. Ryan, U. J. Balis, R. G. Tompkins, D. A. Haber, and M. Toner, "Isolation of rare circulating tumour cells in cancer patients by microchip technology," *Nature*, vol. 450, no. 7173, pp. 1235–1239, Dec. 2007.
[7] S. L. Stott, C.-H. Hsu, D. I. Tsukrov, M. Yu, D. T. Miyamoto, B. A. Waltman, S. M. Rothenberg, A. M. Shah, M. E. Smas, G. K. Korir, F. P. Floyd, A. J. Gilman, J. B. Lord, D. Winokur, S. Springer, D. Irimia, S. Nagrath, L. V. Sequist, R. J. Lee, K. J. Isselbacher, S. Maheswaran, D. A. Haber, and M. Toner, "Isolation of circulating tumor cells using a microvortex-generating herringbone-chip," *Proceedings of the National Academy of Sciences*, vol. 107, no. 43, pp. 18392 –18397, Oct. 2010.
[8] S. Maheswaran, L. V. Sequist, S. Nagrath, L. Ulkus, B. Brannigan, C. V. Collura, E. Inserra, S. Diederichs, A. J. Iafrate, D. W. Bell, S. Digumarthy, A. Muzikansky, D. Irimia, J. Settleman, R. G. Tompkins, T. J. Lynch, M. Toner, and D. A. Haber, "<title> Detection of Mutations in *EGFR* in Circulating Lung-Cancer Cells </title>," *N Engl J Med*, vol. 359, no. 4, pp. 366–377, Jul. 2008.
[9] E. H. Cho, M. Wendel, M. Luttgen, C. Yoshioka, D. Marrinucci, D. Lazar, E. Schram, J. Nieva, L. Bazhenova, A. Morgan, A. H. Ko, W. M. Korn, A. Kolatkar, K. Bethel, and P. Kuhn, "Characterization of circulating tumor cell aggregates identified in patients with epithelial tumors," *Physical Biology*, vol. 9, no. 1, p. 016001, Feb. 2012.
[10] P. Kuhn and K. Bethel, "A fluid biopsy as investigating technology for the fluid phase of solid tumors," *Physical Biology*, vol. 9, no. 1, p. 010301, Feb. 2012.
[11] D. C. Lazar, E. H. Cho, M. S. Luttgen, T. J. Metzner, M. L. Uson, M. Torrey, M. E. Gross, and P. Kuhn, "Cytometric comparisons between circulating tumor cells from prostate cancer patients and the prostate-tumor-derived LNCaP cell line," *Physical Biology*, vol. 9, no. 1, p. 016002, Feb. 2012.

[12] D. Marrinucci, K. Bethel, A. Kolatkar, M. S. Luttgen, M. Malchiodi, F. Baehring, K. Voigt, D. Lazar, J. Nieva, L. Bazhenova, A. H. Ko, W. M. Korn, E. Schram, M. Coward, X. Yang, T. Metzner, R. Lamy, M. Honnatti, C. Yoshioka, J. Kunken, Y. Petrova, D. Sok, D. Nelson, and P. Kuhn, "Fluid biopsy in patients with metastatic prostate, pancreatic and breast cancers," *Physical Biology*, vol. 9, no. 1, p. 016003, Feb. 2012.
[13] J. Nieva, M. Wendel, M. S. Luttgen, D. Marrinucci, L. Bazhenova, A. Kolatkar, R. Santala, B. Whittenberger, J. Burke, M. Torrey, K. Bethel, and P. Kuhn, "High-definition imaging of circulating tumor cells and associated cellular events in non-small cell lung cancer patients: a longitudinal analysis," *Physical Biology*, vol. 9, no. 1, p. 016004, Feb. 2012.
[14] M. Wendel, L. Bazhenova, R. Boshuizen, A. Kolatkar, M. Honnatti, E. H. Cho, D. Marrinucci, A. Sandhu, A. Perricone, P. Thistlethwaite, K. Bethel, J. Nieva, M. van den Heuvel, and P. Kuhn, "Fluid biopsy for circulating tumor cell identification in patients with early-and late-stage non-small cell lung cancer: a glimpse into lung cancer biology," *Physical Biology*, vol. 9, no. 1, p. 016005, Feb. 2012.
[15] S. Zheng, H. Lin, J.-Q. Liu, M. Balic, R. Datar, R. J. Cote, and Y.-C. Tai, "Membrane microfilter device for selective capture, electrolysis and genomic analysis of human circulating tumor cells," *Journal of Chromatography A*, vol. 1162, no. 2, pp. 154–161, Aug. 2007.
[16] H. K. Lin, S. Zheng, A. J. Williams, M. Balic, S. Groshen, H. I. Scher, M. Fleisher, W. Stadler, R. H. Datar, Y.-C. Tai, and R. J. Cote, "Portable Filter-Based Microdevice for Detection and Characterization of Circulating Tumor Cells," *Clinical Cancer Research*, vol. 16, no. 20, pp. 5011–5018, Sep. 2010.
[17] S. Zheng, H. K. Lin, B. Lu, A. Williams, R. Datar, R. J. Cote, and Y.-C. Tai, "3D microfilter device for viable circulating tumor cell (CTC) enrichment from blood," *Biomed Microdevices*, Oct. 2010.
[18] D. Di Carlo, "Inertial microfluidics," *Lab Chip*, vol. 9, no. 21, pp. 3038–3046, 2009.
[19] D. Di Carlo, D. Irimia, R. G. Tompkins, and M. Toner, "Continuous inertial focusing, ordering, and separation of particles in microchannels," *Proceedings of the National Academy of Sciences*, vol. 104, no. 48, pp. 18892–18897, Nov. 2007.
[20] D. Di Carlo, J. F. Edd, K. J. Humphry, H. A. Stone, and M. Toner, "Particle Segregation and Dynamics in Confined Flows," *Phys. Rev. Lett.*, vol. 102, no. 9, pp. 094503–1 – 094503–4, Mar. 2009.
[21] D. Marrinucci, K. Bethel, M. Luttgen, R. H. Bruce, J. Nieva, and P. Kuhn, "Circulating tumor cells from well-differentiated lung adenocarcinoma retain cytomorphologic features of primary tumor type," *Arch. Pathol. Lab. Med*, vol. 133, no. 9, pp. 1468–1471, Sep. 2009.
[22] D. Marrinucci, K. Bethel, R. H. Bruce, D. N. Curry, B. Hsieh, M. Humphrey, R. T. Krivacic, J. Kroener, L. Kroener, A. Ladanyi, N. H. Lazarus, J. Nieva, and P. Kuhn, "Case study of the morphologic variation of circulating tumor cells," *Human Pathology*, vol. 38, no. 3, pp. 514–519, Mar. 2007.
[23] E. Sollier, C. Murray, P. Maoddi, and D. Di Carlo, "Rapid prototyping polymers for microfluidic devices and high pressure injections," *in-revision*.

Chapter 4

Sample Preparation of Pleural and Peritoneal Effusions for Diagnostic Cytopathology

4.1 Introduction

Pleural and peritoneal effusions – fluid that builds up surrounding the lung and abdominal cavities, respectively - can harbor malignant cells which are important to identify for the diagnosis of cancer. This fluid is drained via needle injection in the clinic during a procedure called thoracentesis with over 1.5 million cases per year [1]. Once collected, the fluid is routinely processed to form cell smears and cell blocks for cytopathological analysis [2]. Disseminated cancer cells originating from the lung, breast, ovaries, gastrointestinal tract can be identified in malignant effusions. However, sensitivity of cytologic examinations can have failures in 40% of effusions [3]. This can be a result of scant cellularity of malignant cells or too much handling of technicians. Additionally, these samples often originate from patients with previous cancer history and may be the only source of tumor cells following relapse in which the original tumor mass was removed. Harvesting large quantities of tumor cells in high purity could improve cytology-based diagnoses. Applications of harvested malignant cells include probing cellular properties like cell deformability [4][5], identifying specific genetic mutations [6],

evaluation of effusion microenvironments [7], and identifying cell metastases such as adhesion, migration, and proliferation [8]. Previous studies have indicated that only a subset of pleural effusions is suitable for mutational analysis because of contaminating cells. Pleural fluids are almost always bloody, with a large population of leukocytes and/or erythrocytes [9]. These large populations of leukocytes contain wild type DNA that interferes with the detection of the genetic lesions of interest [10].

There are several possible approaches to harvest cancer cells from pleural effusions. The gold standard is a technology called laser capture microdissection (LCM), a technique used to isolate pure population from cytology slides, live cells culture and heterogeneous tissue sections [11–15]. However, the technique requires drying out of cells during capture, can lead to cell damage, and may not be capable of extracting large quantities of cells for analysis. Flow cytometry and fluorescence activated cell sorting (FACS) are also common methods for cell separation and sorting. While FACS offers throughputs of 30 mL/hr, the sorted cells are not suitable for further analysis as a result of the initial fixing and staining for the sorting process. Notably, these methods neglect many patients, are slow, manually intensive, and cannot be performed on the whole large volume samples of pleural fluid. Ideally, sample preparation of pleural effusions should be performed in an automated, repeatable fashion to enable clinicians and cytopathologists to perform molecular assays on the purified cancer cells with the highest possible sensitivity and specificity, a combination of operate in the macroscale like a standard centrifuge or flow cytometer with the capability of microscale dissection like the LCM. Rapid sampling of fluids requires mL/min processing rates and separation using a label-free marker such as cell size [16].

We have previously demonstrated a miniaturized microfluidic system that recapitulates the high-throughput operations of enrichment and concentration of a standard laboratory centrifuge [17]. Here, we use the "Centrifuge Chip" for the isolation of larger cancer cells and mesothelial cells at high purity from complex biological fluids such as pleural effusions and peritoneal fluids as a preparation step for analysis by traditional cytology (Figure 4.1A). By processing a large volume of fluid and selectively enriching larger cells over a background of red and white blood cells we replace the traditional centrifugation step in the clinical lab while also potentially enabling more sensitive analysis of pure preparations originating from a larger volume. Briefly, the approach employs unique inertial fluid physics to selectively collect larger cells in laminar fluid microvortices at high rates without clog-prone filters (See Chapter 2 and 3) (Figure 4.1B,C). Smaller leukocytes and erythrocytes are not stably trapped in vortices and are significantly reduced in the collected concentrated sample (Figure 4.1D). We have also implemented fluid plumbing automation to process samples and release isolated cells back into a small volume, under the control of a software program (Figure 1C, Figure 4.2). The Centrifuge Chip processes effusions at a flow rate of 6 mL/min from up to 50 mL liquid volume and concentrates larger cells (mesothelial and epithelial). Purified cells are released and made readily available in a collection vial or micro-titer plate for cytology analysis and identifying gene mutations.

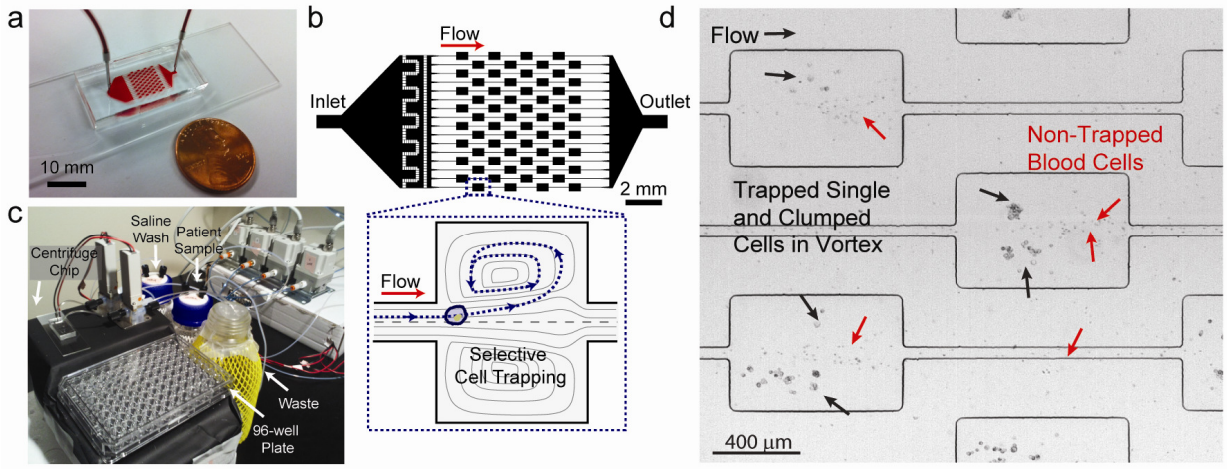

Figure 4.1 Principles of Centrifuge Chip. (A) A photograph of the Centrifuge Chip device. Only a single inlet and outlet is required. (B) A schematic of the massively parallel microfluidic device that selectivelv traps cells in individuals microscale vortices. (C) A photograph of the device connected to an automated fluidic instrument to deliver patient pleural samples and saline wash through the Centrifuge Chip into the waste bottle or collection vial. Trapped epithelial cells are made readily available 1) into a collection tube for further cytology slide comparisons with the original and/or 2) a well-plate for immunolabeling, imaging and analysis. (D) Snapshot high-speed microscopic image of trapping of single and clumped cells while smaller red and white blood cells are washed out.

4.2 Experimental Methods

4.2.1 Microfluidic device fabrication and setup

Devices were fabricated using standard photolithography and polydimethylsiloxane replica molding techniques. The devices were designed in AutoCAD (Autodesk) and printed on a transparency photomask at 20,000 dots per inch (CAD/Art Service, Inc.). The mold was photolithographically defined using this mask in the UCLA Nanoelectronics Research Facility.

Negative photoresist, KMPR 1050 (MicroChem), was spun at 2400 rpm for 30 s on a 10-cm silicon wafer. The wafer was soft-baked at 100C for 15 min, exposed under near UV for 30 s, post-baked at 100C for 4 min, and developed in SU-8 Developer (MicroChem). The height of the resulting feature was measured to be 50 μm using a profilometer. Polydimethylsiloxane (PDMS) (Sylgard 184 Dow Corning Corp.) was poured onto the photoresist master at a 10:1 ratio of base to crosslinker, degassed in a vacuum chamber, and cured at 65^{o}C overnight. The devices were then cut from the mold, ports were punched with a punch kit (Technical Innovations), and the devices were bonded to glass slides using oxygen plasma for 30 s (Harrick Plasma). After plasma treatment and placement onto the glass substrate, the devices were maintained at 65^{o}C in an oven for 15 min to increase bonding.

The Centrifuge Chip device contains 16 parallel channels with 4 chambers in each channel for a total for 128 cell trapping reservoirs. The device is connected to a custom-made pressure system that delivers effusion samples or saline wash from pressurized glass bottles through the Centrifuge Chip. The Labview-controlled system contains a pair of air regulators, air valves and liquid valves that brings compressed air into the bottles and drives fluid through the microchip device. Effusion samples are placed into the pressurized glass bottle and introduced through the device at a flow rate of ~6 mL/min. Once the vortex traps were filled with cells, PBS was introduced into the device to wash out untrapped blood cells in the main flow and the vortex traps. Cells trapped in the fluid vortex were removed by reducing the input air pressure and subsequently released in a collection tube. We implement a ‘trap-and-release’ program that can continuously introduce sample through the Centrifuge Chip, wash, and release the captured cells into a microtiter plate or collection vial.

4.2.2 Cell Trapping Mechanism

The mechanism of operation is based on size-dependent inertial lift which leads to selective entry and stable orbits for larger cells within vortices created in an expansion reservoir (Figure 3B) (See Chapter 2 and 3). Smaller cells do not experience sufficient lift force and therefore either do not enter the vortex, or do not have enough restoring lift force to remain stable within the vortices in the presence of de-stabilizing disturbances from other orbiting particles. In our previous work we identified reservoir geometries and flow conditions to selectively collect cells and particles above ~15 μm. We made several device modifications including 1) the integration with a custom-made pressure system that operates using a simple 'plug-and-play' option in which an operator does not need to be present at all times, 2) the shortening of the device channel length to reduce fluidic resistance, and 3) the increase of the number of parallel channels to 16 to process samples at a flow rate of 6 mL/min with one patient sample taking <10 minutes to operate. These changes make a complete automated system that can potentially revolutionize sample preparation of bloody pleural effusions with high purity.

4.2.3 Sample Collection and Preparation

The material studied comprised of 112 samples from 110 patients (95 pleural and 17 peritoneal) obtained from Ronald Reagan UCLA Medical Center, Santa Monica UCLA Medical Center, and Northridge Hospital Medical Center. From all specimens, up to 50 mL of sample were processed with the Centrifuge Chip. Effusions were passed through a 40 μm cell strainer before introducing through the centrifuge chip system.

4.2.4 Cell Smear Preparation and Imaging

Each sample submitted for cytologic evaluation was made into cell smear using traditional cytological methods. Briefly, fresh samples are aliquoted into 50 mL conical tubes and centrifuged down with a standard benchtop centrifuge. After centrifugation, the supernatant is aspirated, the cells resuspended in a buffer solution and placed into a cytocentrifuge to make a cell smear. The cell slides are air dried or fixed and stained with Papanicolou (Pap), May-Grunwald-Giemsa (MGG). In parallel, harvested cells after processing with the Centrifuge Chip were collected in a vial and returned to the cytology laboratory to prepare a cell smear.

4.2.5 Blot Analysis of Harvest Cells

RNA was extracted from lysed HeLa, A549, and white blood cells using PureLink RNA Mini Kit (Ambion, Invitrogen). First-strand synthesis was performed using the SuperScript III First-Strand Synthesis System (Invitrogen), and PCR was performed with *Taq* DNA Polymerase (Invitrogen) in a 100 uL reaction mixture with the following conditions: 1X kit-supplied PCR buffer, 0.2 mM deoxyribonucleotide triphosphate, 1.5 mM $MgCl_2$, 0.5 μM of each primer, 10 uL of cDNA sample, and 2.5 U of *Taq* DNA polymerase. The MasterCycler gradient (Eppendorf) thermal cycler was programmed as follows: 94°C for 45 s, 55°C for 30 s, and 72°C for 45 s for 35 cycles. Electrophoresis was performed on PCR products using a 1.5% agarose gel with 1x SYBR Safe DNA Gel Stain (Invitrogen) and a UV light table.

4.2.6 Fluorescent Staining for Purity Measurements

For each specimen, 300 uL of the original effusion was transferred into one well of a 96-well microtiter plate. To compare the processed sample versus the original sample, up to 10 mL

effusion volume was processed with the Centrifuge Chip and isolated cells were released in a volume of 250 microliters in the microtiter plate. To determine the cell population, leukocyte, epithelial and nuclear stains were used. After centrifuging the cells to the bottom of the well with a plate centrifuge, the supernatant was aspirated. Cells were treated with 4% v/v formaldehyde for 15 min, permeabilized with 0.4% v/v Triton X-100 (Sigma-Aldrich) for 7 min, and incubated with CK-PE, DAPI, CD45-FITC (Invitrogen) in 2% w/v BSA. Between each step, cells were sedimented with the centrifuge and washed with PBS. After staining, the cells were imaged using a Photometrics CoolSNAP HQ2 CCD camera mounted on a Nikon Eclipse Ti microscope. The whole well was automatically imaged in a few minutes (100X) using an ASI motorized stage operated with Nikon NIS-Elements AR 3.2 software. Captured images were automatically obtained for four configurations: brightfield, FITC, TRITC and DAPI filter sets. Collected images were automatically stitched together using the NIS-Elements Software. Images were analyzed by enumerating the number of CK+ and CD45+ cells present in each well. Purity is defined as the ratio of selected target cancer cells captured to the total number of captured cells.

4.3 Identification of Cell Size Distributions in Effusions

To ensure the high enrichment capabilities of our device we recorded detailed information on the number of cells and associated size ranges present in pleural and peritoneal fluids (Figure 4.2). Possible cytolological diagnoses included: positive for malignancy, suspicious for malignancy, and negative for malignancy (Table 4.1). Patient samples diagnosed with negative fluid results oftentimes were diagnosed with acute inflammation - associated with an increased neutrophil population, and chronic inflammation - associated with a larger fraction of lymphocytes and

histiocytes, reactive changes, and lymphocytosis – associated with the increase of lymphocytes. In positive cases, the tissue of origin was often known from patient history. It is commonly known that malignant and mesothelial cells are large compared to the rest of the cell population [18].

With these cell sizes in mind, we modified the original centrifuge chip to target larger cell populations greater than 15 μm [17]. We expect large mesothelial cells to be present, although it would not have a huge effect on trapping of malignant cells. To characterize the Centrifuge Chip, cells larger than 15 μm (size cutoff for device) were counted over the total number of cells and averaged over the number of samples (Table 4.2). Of the patients diagnosed with Positive for Malignancy, 19% of cells are larger than 15 μm. Moreover, patients diagnosed with Negative and Negative with Chronic Inflammation have 15.4% and 10.57% of cells larger than 15 μm, respectively [5]. These large percentages are a result of activated leukocytes that gain cell size as well as the presence of mesothelial cells. Thus, cell size is a potential biomarker for harvesting malignant cells from patients diagnosed with positive for malignancy.

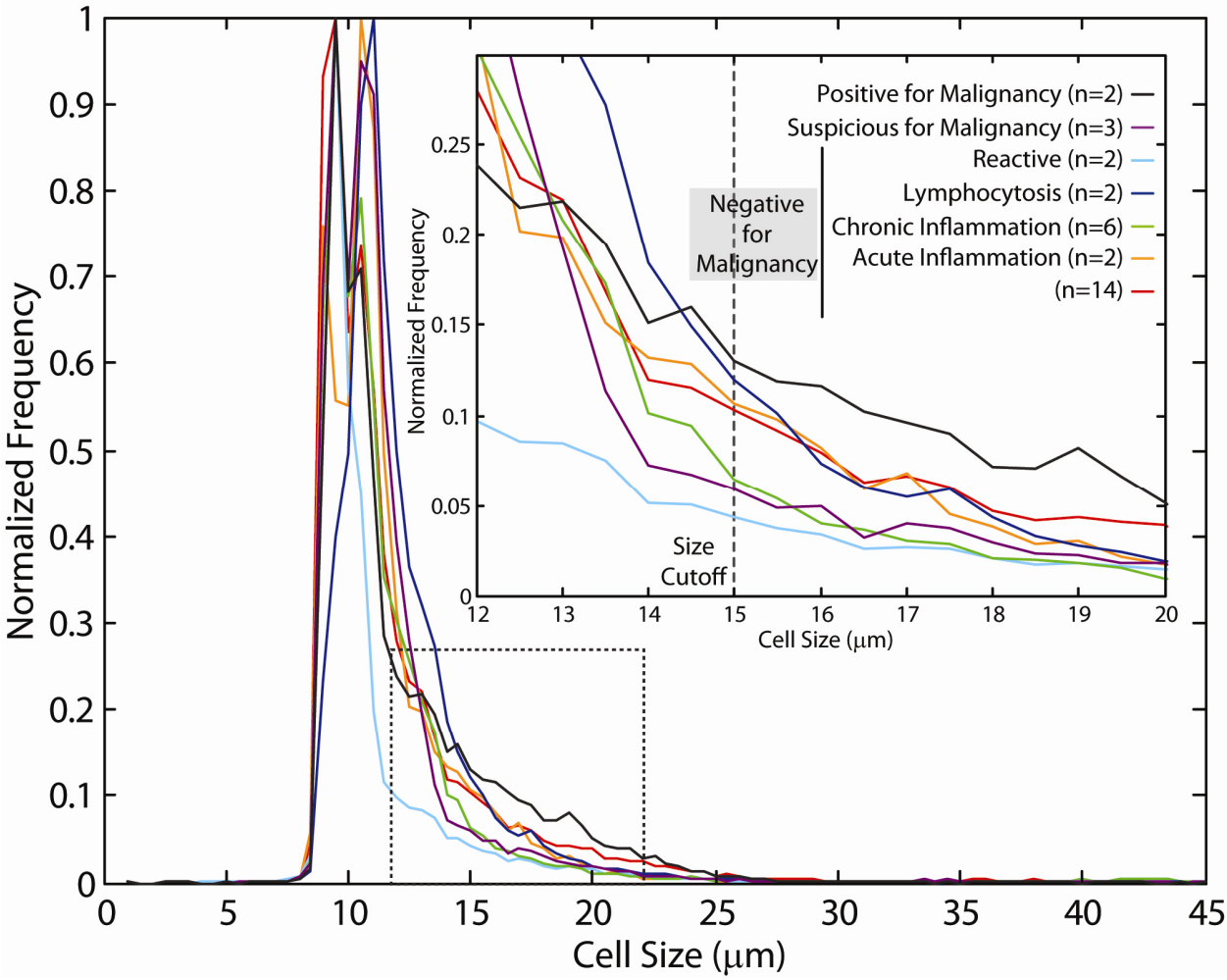

Figure 4.2 Distribution of Cell Size Measurements from Pleural Fluids.

Summary of Cases			
Cytodiagnosis	**Pleural Fluids**	**Peritoneal Fluids**	**Total**
Positive	9	4	13
Lung	5	0	
Gastric	1	3	
Breast	2	0	
Ovarian	0	1	
Esophagus	1	0	
Suspicious	14	0	14
Negative	20	8	28
Lymphocytosis	16	0	16
Acute Inflammation	9	0	9
Chronic Inflammation	18	3	21
Reactive Changes	9	2	11
Total	95	17	112

Table 4.1 Summary of 112 Pleural and Peritoneal Samples and Cytodiagnosis. 13/112 (11.6%) of samples were diagnosed positive for malignancy, 14/112 (12.5%) were diagnosed suspicious for malignancy, 85/112 (75.9%) were diagnosed negative for malignancy.

Cytodiagnosis	**No. of Samples**	**Mean**	**Standard Deviation**	**Min**	**Max**
Negative	14	15.4	12.99	2.14	51.14
Acute Inflammation	2	8.69	2.24	5.97	11.4
Chronic Inflammation	6	10.57	5.15	5.14	23.12
Lymphocytosis	2	7.55	3.1	6.34	8.76
Reactive	2	8.07	5.33	3.86	12.28
Suspicious	3	11.73	5.07	3.3	22.2
Positive	2	19.07	5.44	14.46	23.68

Table 4.2 Analysis of Cell Size Measurements from Pleural Fluids. To characterize the Centrifuge Chip, cells larger than 15 μm (size cutoff for device) were counted over the total number of cells (Mean) and averaged over the number of samples. Of the patients diagnosed with Positive for Malignancy, 19% of cells are larger than 15 μm. Interestingly, patients

diagnosed with Negative and Negative with Chronic Inflammation have 15.4% and 10.57% of cells larger than 15 μm.

4.4 Achieving High Purity with Clinical Samples

High purity samples provided by sample preparation can enable pathologists and clinicians an easily accessed source of cells for exploration. Purity above 40% is needed for cells with genetic lesions to obtain accurate identification of these mutations by PCR [19], [20] or gene sequencing. To quantify purity, fresh and processed samples with the Centrifuge Chip (n=82) were placed in a well-plate, immunostained with Cytokeratin-PE (epithelial cell), CD-45-FITC (leukocyte), and DAPI (nucleus), imaged and analyzed. Purity is defined as the number of epithelial cells over the total number of cells. The Centrifuge Chip delivers a higher purity sample compared to a fresh and centrifuged specimen (Figure 4.3A-C). Reduction in background and concentration from a large sample volume to a small field of view can aid rapid scanning and diagnosis by the cytopathologist (Figure 4.3C).

The Centrifuge Chip increased purity in all 82 cases (100%) (Figure 4.3D, Table S4.1). The malignant cases (n=11) were diagnosed positive from cytological examination for adenocarcinoma, carcinoma, and rhabdomyosarcoma. Suspicious cases (n=6) are typically diagnosed when suspicious cells are present and require further testing for final diagnosis. Most cases (n=65) were diagnosed negative for malignancy in addition to having acute or chronic inflammation, lymphocytosis, or reactive changes. In agreement with our cell size measurements, we observed many cells captured for positive cases and less for negative cases with lymphocytosis, reactive changes, and acute inflammation. Additionally, the amount of purity (purity fold) increased from fresh to Centrifuge Chip processed specimens (Table 4.3).

Purity fold is defined as the purity of a processed sample over the initial fresh sample. As expected, we enriched more than 70 fold for samples diagnosed with positive for malignancy. Interestingly, samples with chronic inflammation had 108.3 fold increase as a result of large leukocyte populations in initial samples with <1% purity. Moreover, some suspicious (3/6) and malignant cases (5/11) demonstrated purity greater than 40% (the threshold for accurate molecular analysis), suggesting it is possible for detecting specific gene mutations such as EGFR or KRAS. While some purity measurements do not exceed the 40%, higher purities can be achieved by increasing the critical size cutoff range of the Centrifuge Chip to eliminate leukocyte capture. High purity samples provided by a simple rapid preparation step described here would enable pathologists and clinicians to explore and better proscribe targeted drug therapies with an easily accessed source of cells compared to solid tumor biopsies.

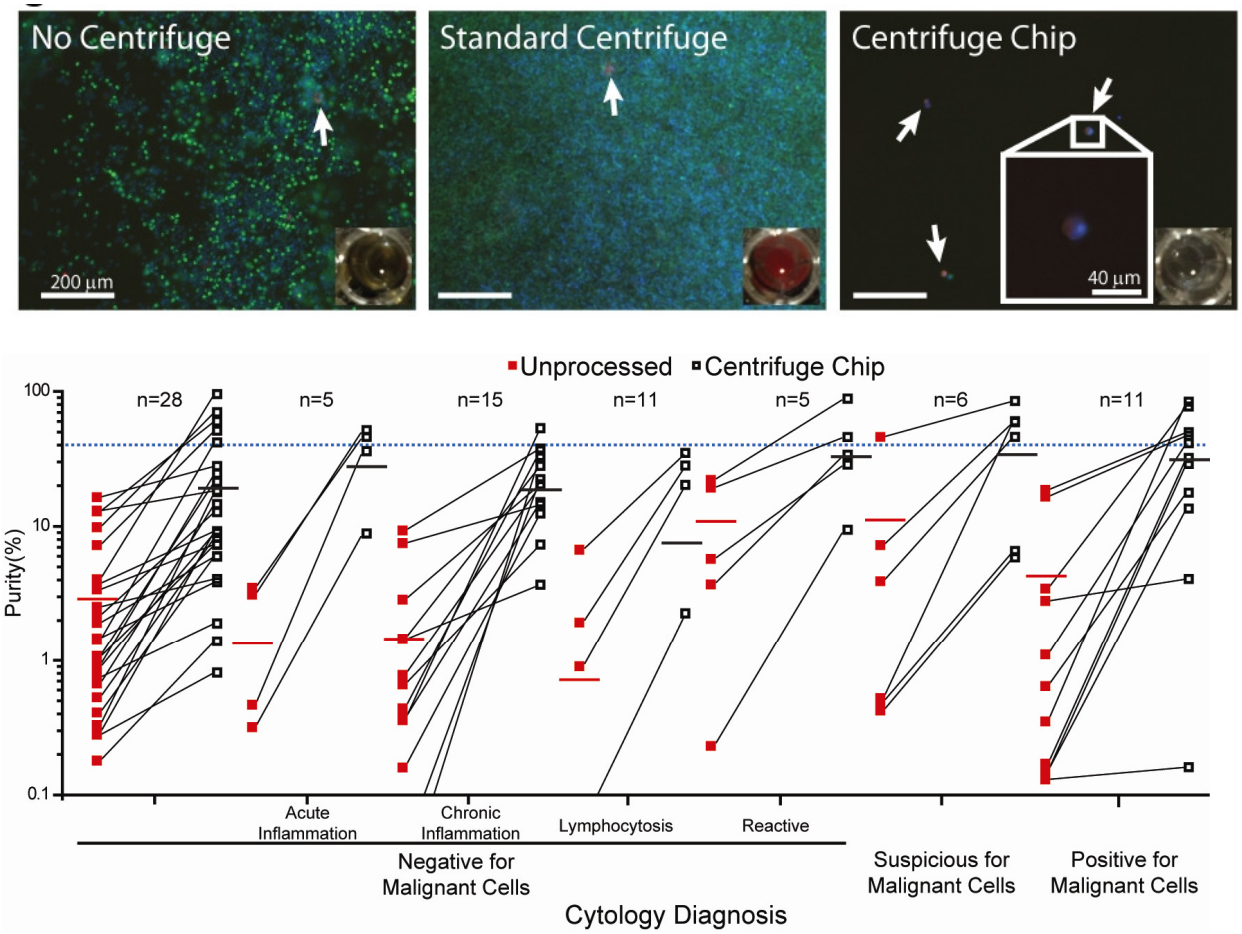

Figure 4.3 Purity Analysis of Patient Pleural and Peritoneal Samples. (A-C) Qualitative comparison of fresh sample, centrifuged sample and sample processed with Centrifuge Chip. Immunofluorescent images of Cytokeratin (red – epithelial cells), CD45 (green - leukocytes), DAPI (blue - nuclear). High purity after Centrifuge Chip processing leads to enhanced sensitivity for mutation or expression analysis. Insets show well-plate color: yellow (fresh specimen), red (indicating bloody) and colorless (after processing with device. Arrows indicate CK+/DAPI+ epithelial cells. (D) Purity increases upon processing with the Centrifuge Chip. Purity is defined as the presence of CK+/DAPI+ (epithelial cells) over the total number of cells. All samples (n=82) demonstrate higher purity after processing with Centrifuge Chip. Solid lines indicate

average of purity for respective diagnosis. Dashed line indicates 40% purity, a threshold previously proposed for accurate molecular analysis.

Purity Fold Increase	
Cytodiagnosis	Pleural and Peritoneal Fluids
Positive	73.3
Suspicious	34.0
Negative	15.4
Lymphocytosis	5.4
Acute Inflammation	23.3
Chronic Inflammation	108.7
Reactive Changes	10.4

Table 4.3 Results of Cytologic and Purity Analysis of Pleural and Peritoneal Fluids. Purity fold is defined as the amount of purity increased from a fresh specimen to a sample processed with Centrifuge Chip.

4.5 Removal of Bloody Background from Cytology Slides

Cytopathologists analyze pleural samples to determine the cause (presence or absence of cancer) by examining stained cell smears on a glass slide. However, there exist a few limitations with the traditional cytological methods. First, bloody samples have blood cell components (leukocytes/erythrocytes) that create a background, making it difficult to locate potentially malignant epithelial cells of interest over a large field of view necessary for diagnostic accuracy. Oftentimes, red blood cell lysis buffer is added to the sample before making a cytology slide as a method to remove erythrocytes. Another method requires manually smearing a bloody sample on multiple slides as to produce a thin single layer of cells for microscopy analysis. Additionally, some samples contain scant cellularity or rare cell populations like malignant cells

and require analyzing large specimen volumes. Consequently, multiple cell smears have to be made and analyzed for this process. Combined, these specimens require technician-intensive sample preparation involving multiple centrifugation steps followed by manual microscopic scanning of cytology slides by the cytopathologist. We address these issues with the Centrifuge Chip where we concentrate the larger cell populations (mesothelial and epithelial) from a large sample volume of up to 50 mL to a smaller volume of 300 μL, the maximum volume used for cytocentrifugation. The device has no volume limitations unlike the standard centrifuge, where it is limited by the volume placed in the largest 50 mL conical centrifuge tube. To characterize the device, harvested cells after processing with the Centrifuge Chip were collected in a vial and returned to the cytology laboratory to create cell smear. This was made in parallel with cell smears produced with traditional cytological methods. In all samples, malignant and mesothelial cells are found amongst a cellular background of red and white blood cells in standard slides while little background is observed in the Centrifuge Chip slide (Figure 4.4A-F). As expected from our cell measurements above, we collected mesothelial and malignant cells in samples diagnosed with positive for malignancy (Figure 4.4A-C). Malignant cells are characterized by large nuclei and high nuclear-cytoplasmic ratio. Malignant cells are often seen as cell aggregates or clumps in effusions [21] and these cell populations were also harvested using the Centrifuge Chip. The ability to isolate single and clumped cells without tampering cellular viability makes it a comparable tool compared to gold standard LCM techniques. In patients diagnosed with negative for malignancy, mesothelial cells were harvested. The Centrifuge Chip may aid pathologists in rapid visualization of rarer malignant cells for clinical diagnosis.

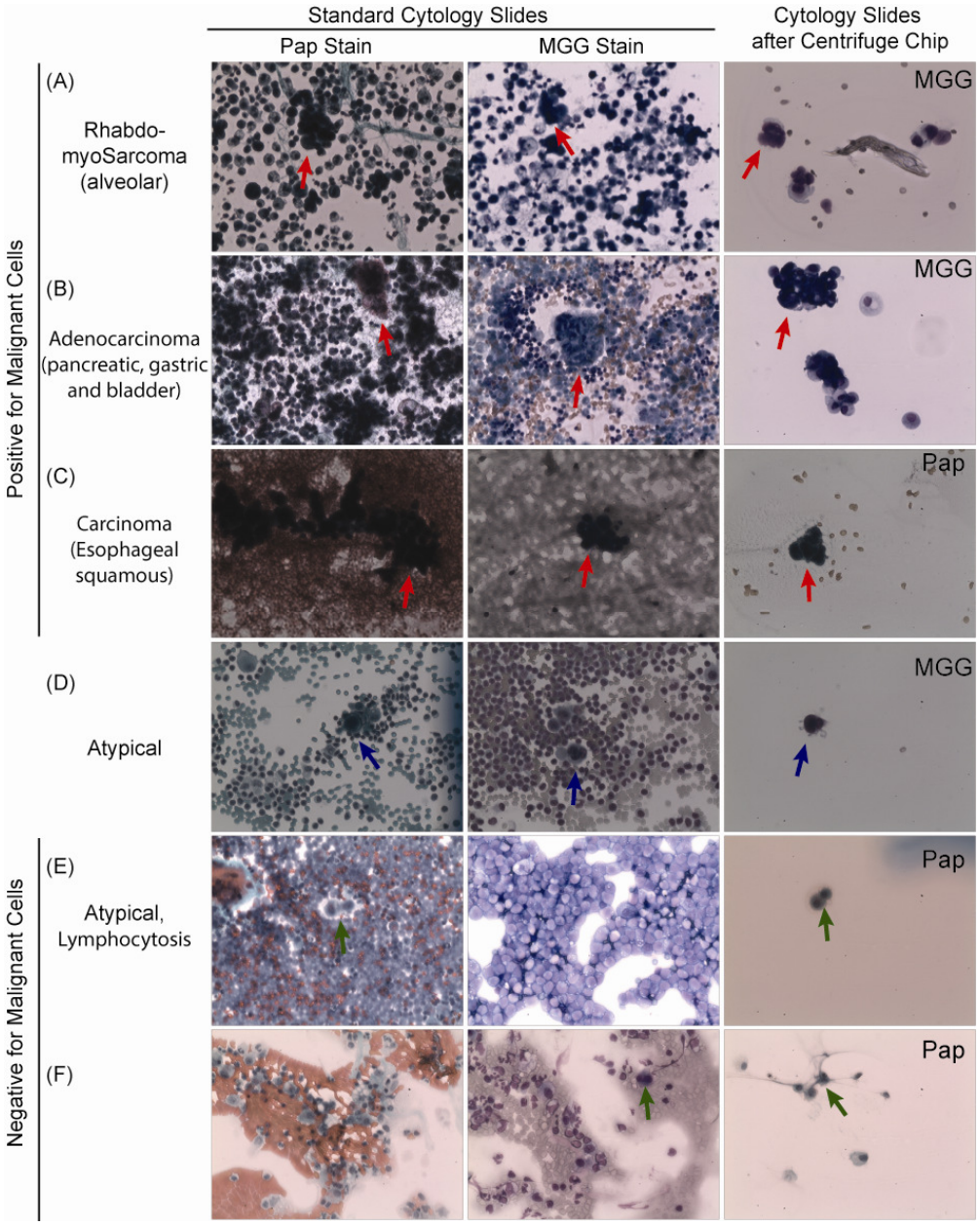

Figure 4.4 Reduced Background Cytology Slides When Prepared Using the Centrifuge Chip. Fresh patient samples are prepared with traditional cytological techniques using Papanicolaou (Pap) and May-Grunwald–Giemsa (MGG) stains. Cells collected from samples processed with Centrifuge Chip are also made into cytology slides. In all samples, malignant and mesothelial cells are found amongst a cellular background of immune cells in standard slides while little

background is observed in the Centrifuge Chip slide. In patients diagnosed with 'positive for malignancy', single and clumped malignant cells (red arrows) are retrieved after the Centrifuge Chip. In patients diagnosed with 'negative for malignancy', single mesothelial cells (green arrows) found amongst a background of red and white blood cells in standard slides compared to Centrifuge Chip slide with no cellular background. Images obtained at 200x magnification.

4.6 Detecting KRAS Gene Mutation in Spiked Bloody Samples

Increasing the purity of the sample enables molecular diagnostics for targeted cancer therapies. This can be achieved by removing a large population of leukocytes that contain interfering wild-type DNA, which aid with the detection of genetic lesions that contribute to sensitivity or resistance to specific chemotherapies. Previously, a threshold of 40% purity was reported for high accuracy [12]. We evaluated the performance of the Centrifuge Chip by extract molecular information from enriched cancer cells to determine the potential improvement provided by high purity capture for PCR. A549 lung cancer cells were evaluated for known activating mutation in KRAS, which can provide resistance to targeted therapies [11] (Figure 4.5). Specifically, we looked at the 34 G>A substitution in KRAS as identified by the Sanger Cosmic database [22]. We used primers with terminal base pair substitutions (amplification refractory mutation system, ARMS) [23]. Primers encode the mutation (KRAS*: 5'-ACTTGTGGTAGTTGGAGCTA-3' (KRAS 34G>A)) and wild-type gene (KRAS: 5'-ACTTGTGGTAGTTGGAGCTG-3' (KRAS wild-type)). As controls we assayed blood without spiked cells and pure cell lines, respectively (Figure 5). Additionally, we evaluated the presence of H2B, a histone housekeeping gene responsible for chromatin structure. We also demonstrated successful amplification and agarose gel electrophoresis readout of genes from as few as 5 cells.

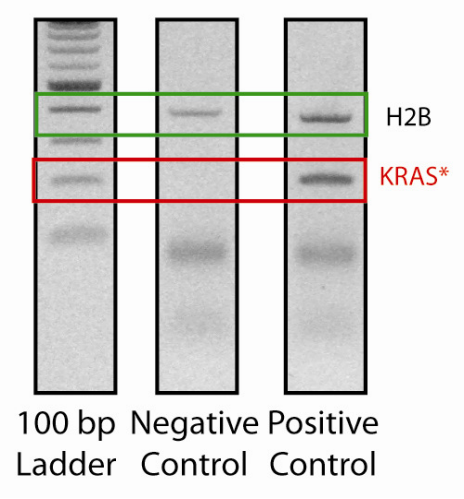

Figure 4.5 Identifying KRAS Mutations in Spiked Samples. Agarose gel electrophoresis of amplification refractory mutation system (ARMS) products reveals a 34 G>A mutation in A549 cells. Bands appear in A549 lung cancer cells for primers encoding the mutation (KRAS*: 5'-ACTTGTGGTAGTTGGAGCTA-3' (KRAS 34G>A)), whereas no bands for the wild-type gene (KRAS: 5'-ACTTGTGGTAGTTGGAGCTG-3' (KRAS wild-type)) are present in the negative control containing only lysed blood.

4.7 Conclusions

We developed a device called the Centrifuge Chip, containing the macroscale power of a standard centrifuge of assessing large liquid volumes and the precise manipulation of microscale technologies. We use the Centrifuge Chip for the selective harvesting of malignant and mesothelial cells from pleural and peritoneal effusions in a high purity, label-free and rapid fashion using size as a biomarker. The device prepares a fresh effusion specimen in 10 min compared to the gold standard of laser capture microdissection, which requires trained technicians and >1.5 hrs of micromanipulation. The Centrifuge Chip system makes cells freely

available in solution enabling cytopathologists, clinicians, and researches access to purified cellular material required for preparing background-less cytology slides, detecting gene mutations, mesothelial and malignant cell culturing or even gene sequencing.

4.8 Acknowledgements

We thank Sean O'Byrne, Christopher Johnson, Hwee Ng, Mary Levin, Jin Yu-Sheng, Michael Cutidioc, Gwen Hawkins and Amanda Zopfi-Conklin for preparing samples. We also thank Libo Zhao, Kan Liu, Huijiang Ding, and Hsian-Rong Tseng for technical assistance. This chapter is a version of work in preparation for publication. Authors include James Che, Derek Go, Ish Talati, Yong Ying, Rajan Kulkarni, Jianyu Rao, and Dino Di Carlo.

4.9 Supporting Information

Table S4.1: Complete Results of Cytologic and Purity Analysis of 112 Patient Pleural and Peritoneal Fluids. Pos = positive for malignancy, Sus = suspicious for malignancy, N = negative for malignancy, R = reactive changes, L = lymphocytosis, CI = chronic inflammation, and AI = acute inflammation. Purity is defined as the number of CK+/DAPI+ cells over the total number of cells.

Patient	Fluid	Detail	No. of CK+	Purity
1	N	R		
2	Sus		181	58.96
3	N		21	95.45
4	Sus			
5	Pos	Gastric	1110	46.69

6	Sus			
7	N			
8	N	R	900	28.52
9	N			
10	N		0	0.00
11	Pos	Lung	23	31.94
12	Pos	Breast	4800	4.05
13	N	L		
14	N			
15	N			
16	Sus		31	5.86
17	N	L	13	31.71
18	Pos	Lung		
19	N		52	21.40
20	N		33	5.95
21	N		46	8.20
22	N			
23	N	CI	21	33.33
24	N		75	41.90
25	N	CI	114	53.27
26	N			
27	N	CI	39	28.06
28	Sus			
29	Pos	Lung	194	49.49
30	N		12	17.91
31	N		12	27.91
32	N		6	6.00
33	N	CI	4	20.00
34	N	CI	19	36.54
35	N	AI	2080	36.24
36	N		64	14.61
37	N	AI		
38	N	CI	131	14.46
39	Pos	Gastric	86	17.66
40	N	R	105	12.03

41	N	L	0	0.00
42	N		19	7.28
43	N		22	9.21
44	N	R	3	9.38
45	Sus		6	6.52
46	N	CI	81	7.33
47	N	AI	0	0.00
48	N	R	44	20.18
49	N	L		
50	Sus			
51	N	L	17	2.26
52	N		0	0.00
53	N		1	0.81
54	N		177	6.78
55	N			
56	N			
57	N	CI	32	15.09
58	N	AI	12	8.89
59	N		17	1.90
60	N	CI	38	3.69
61	N	CI	0	0.00
62	N	CI	35	12.46
63	N		12	24.49
64	N	L	5	1.53
65	N		5	1.39
66	N	R	109	45.61
67	Pos	Esophagus	7	13.46
68	N		3	3.85
69	N		0	0.00
70	N			
71	N			
72	N	L	0	0.00
73	N	L	0	0.00
74	Pos	Gastric		
75	N		23	8.91

76	N		15	7.35
77	N	L	97	100.00
78	N		98	4.06
79	N		754	69.94
80	N	L	0	
81	Pos	Breast	15	83.33
82	N		129	60.00
83	N		57	12.75
84	N		253	18.32
85	N	L	0	0.00
86	N	AI		
87	N	CI	0	0.00
88	N			
89	N	CI	53	22.36
90	N	R	1792	33.73
91	Sus		107	59.89
92	N	R	1600	87.72
93	N	CI	256	20.51
94	N		768	51.06
95	Pos	Lung	25	40.98
96	N	AI	576	46.15
97	N	CI	1440	37.82
98	N	L	171	20.25
99	Sus		1024	45.71
100	Pos	Lung	53	76.81
101	N	L	0	0.00
102	N	L	0	0.00
103	N		145	9.15
104	N	AI	101	51.79
105	N	R	5	3.03
106	Pos	Ovarian	19	28.79
107	Sus		44	84.62
108	N	L	36	28.13
109	N	L	15	34.88
110	Sus			

111	Pos	Gastric
112	N	

4.10 References

[1] S. A. Sahn, "The value of pleural fluid analysis," *Am. J. Med. Sci.*, vol. 335, no. 1, pp. 7–15, Jan. 2008.

[2] G.-K. Nguyen, *Essentials of Fluid Cytology*. Library and Archives Canada, 2010.

[3] K. N. Fenton and J. David Richardson, "Diagnosis and management of malignant pleural effusions," *The American Journal of Surgery*, vol. 170, no. 1, pp. 69–74, Jul. 1995.

[4] S. E. Cross, Y.-S. Jin, J. Rao, and J. K. Gimzewski, "Nanomechanical analysis of cells from cancer patients," *Nature Nanotechnology*, vol. 2, no. 12, pp. 780–783, 2007.

[5] D. R. Gossett, H. T. K. Tse, S. A. Lee, Y. Ying, A. G. Lindgren, O. O. Yang, J. Rao, A. T. Clark, and D. Di Carlo, "Hydrodynamic Stretching of Single Cells for Large Population Mechanical Phenotyping," *PNAS*, Apr. 2012.

[6] S. R. Chowdhuri, L. Xi, T. H.-T. Pham, J. Hanson, J. Rodriguez-Canales, A. Berman, A. Rajan, G. Giaccone, M. Emmert-Buck, M. Raffeld, and A. C. Filie, "EGFR and KRAS mutation analysis in cytologic samples of lung adenocarcinoma enabled by laser capture microdissection," *Modern Pathology*, vol. 25, no. 4, pp. 548–555, Dec. 2011.

[7] J. Kassis, J. Klominek, and E. C. Kohn, "Tumor microenvironment: what can effusions teach us?," *Diagn. Cytopathol.*, vol. 33, no. 5, pp. 316–319, Nov. 2005.

[8] D. Hanahan and R. A. Weinberg, "Hallmarks of Cancer: The Next Generation," *Cell*, vol. 144, no. 5, pp. 646–674, Mar. 2011.

[9] V. Villena, A. López-Encuentra, R. García-Luján, J. Echave-Sustaeta, and C. J. Á. Martínez, "Clinical Implications of Appearance of Pleural Fluid at Thoracentesis*," *Chest*, vol. 125, no. 1, pp. 156 –159, Jan. 2004.

[10] N. Papadopoulos, K. W. Kinzler, and B. Vogelstein, "The role of companion diagnostics in the development and use of mutation-targeted cancer therapies," *Nat Biotech*, vol. 24, no. 8, pp. 985–995, 2006.

[11] L. Boldrini, S. Gisfredi, S. Ursino, T. Camacci, E. Baldini, F. Melfi, and G. Fontanini, "Mutational analysis in cytological specimens of advanced lung adenocarcinoma: a sensitive method for molecular diagnosis," *J Thorac Oncol*, vol. 2, no. 12, pp. 1086–1090, Dec. 2007.

[12] U. Malapelle, N. de Rosa, D. Rocco, C. Bellevicine, C. Crispino, A. Illiano, F. V. Piantedosi, O. Nappi, and G. Troncone, "EGFR and KRAS mutations detection on lung cancer liquid-based cytology: a pilot study," *Journal of Clinical Pathology*, 2011.

[13] M. A. Molina-Vila, J. Bertran-Alamillo, N. Reguart, M. Taron, E. Castellà, M. Llatjós, C. Costa, C. Mayo, A. Pradas, C. Queralt, M. Botia, M. Pérez-Cano, E. Carrasco, M. Tomàs, J. L. Mate, T. Moran, and R. Rosell, "A Sensitive Method for Detecting EGFR Mutations in Non-small Cell Lung Cancer Samples with Few Tumor Cells," *Journal of Thoracic Oncology*, vol. 3, no. 11, pp. 1224–1235, Nov. 2008.

[14] M. R. Emmert-Buck, R. F. Bonner, P. D. Smith, R. F. Chuaqui, Z. Zhuang, S. R. Goldstein, R. A. Weiss, and L. A. Liotta, "Laser Capture Microdissection," *Science*, vol. 274, no. 5289, pp. 998–1001, Nov. 1996.

[15] V. Espina, J. D. Wulfkuhle, V. S. Calvert, A. VanMeter, W. Zhou, G. Coukos, D. H. Geho, E. F. Petricoin, and L. A. Liotta, "Laser-capture microdissection," *Nature Protocols*, vol. 1, no. 2, pp. 586–603, 2006.
[16] D. R. Gossett, W. M. Weaver, A. J. Mach, S. C. Hur, H. T. K. Tse, W. Lee, H. Amini, and D. Di Carlo, "Label-free cell separation and sorting in microfluidic systems," *Anal Bioanal Chem*, vol. 397, no. 8, pp. 3249–3267, Apr. 2010.
[17] A. J. Mach, J. H. Kim, A. Arshi, S. C. Hur, and D. Di Carlo, "Automated cellular sample preparation using a Centrifuge-on-a-Chip," *Lab on a Chip*, vol. 11, p. 2827, 2011.
[18] N. Kimura, K. Dota, Y. Araya, T. Ishidate, and M. Ishizaka, "Scoring system for differential diagnosis of malignant mesothelioma and reactive mesothelial cells on cytology specimens," *Diagnostic Cytopathology*, vol. 37, no. 12, pp. 885–890, 2009.
[19] J. H. Smouse, E. S. Cibas, P. A. Jänne, V. A. Joshi, K. H. Zou, and N. I. Lindeman, "EGFR mutations are detected comparably in cytologic and surgical pathology specimens of nonsmall cell lung cancer," *Cancer Cytopathology*, vol. 117, no. 1, pp. 67–72, Feb. 2009.
[20] S. Billah, J. Stewart, G. Staerkel, S. Chen, Y. Gong, and M. Guo, "EGFR and KRAS mutations in lung carcinoma," *Cancer Cytopathology*, vol. 119, no. 2, pp. 111–117, Apr. 2011.
[21] S. A. Sahn, "The Differential Diagnosis of Pleural Effusions," *West J Med*, vol. 137, no. 2, pp. 99–108, Aug. 1982.
[22] T. Kashii, Y. Mizushima, S. Monno, K. Nakagawa, and M. Kobayashi, "Gene analysis of K-, H-ras, p53, and retinoblastoma susceptibility genes in human lung cancer cell lines by the polymerase chain reaction/single-strand conformation polymorphism method," *J. Cancer Res. Clin. Oncol.*, vol. 120, no. 3, pp. 143–148, 1994.
[23] C. R. Newton, A. Graham, L. E. Heptinstall, S. J. Powell, C. Summers, N. Kalsheker, J. C. Smith, and A. F. Markham, "Analysis of any point mutation in DNA. The amplification refractory mutation system (ARMS).," *Nucleic Acids Res*, vol. 17, no. 7, pp. 2503–2516, Apr. 1989.